COMPARISON OF ANALYSIS METHODS OF EMBEDDED RETAINING WALLS

A THESIS SUBMITTED TO
THE GRADUATE SCHOOL OF NATURAL AND APPLIED SCIENCES
OF
MIDDLE EAST TECHNICAL UNIVERSITY

BY

SERKAN HARMANDAR

IN PARTIAL FULFILLMENT OF THE REQUIREMENTS
FOR
THE DEGREE OF MASTER OF SCIENCE IN
CIVIL ENGINEERING

DECEMBER 2006

Approval of the Graduate School of Natural and Applied Science

Prof. Dr. Canan Özgen
Director

I certify that this thesis satisfies all the requirements as a thesis for the degree of Master of Science.

Prof. Dr. Güney Özcebe
Head of Department

This is to certify that we have read this thesis and that in our opinion it is fully adequate, in scope and quality, as a thesis for the degree of Master of Science.

Dr. Oğuz Çalışan
Co-Supervisor

Prof. Dr. Yener Özkan
Supervisor

Examining Committee Members

Prof. Dr. Erdal Çokça (METU, CE) _____

Prof. Dr. Yener Özkan (METU, CE) _____

Dr. Oğuz Çalışan (Çalışan Geoteknik) _____

İnş. Yük. Müh. Gülru Yıldız (DSİ) _____

İnş. Yük. Müh. Hakan Özçelik (EAST İnş.) _____

I hereby declare that all information in this document has been obtained and presented in accordance with academic rules and ethical conduct. I also declare that, as required by these rules and conduct, I have fully cited and referenced all material and results that are not original to this work.

Serkan HARMANDAR

ABSTRACT

COMPARISON OF ANALYSIS METHODS OF
EMBEDDED RETAINING WALLS

HARMANDAR, Serkan
M.S., Department of Civil Engineering
Supervisor : Prof. Dr. Yener Özkan
Co -Supervisor : Dr. Oğuz Çalışan

December 2006, 123 pages

In this study a single-propped embedded retaining wall supporting a cohesionless soil is investigated by four approaches, namely limit equilibrium, subgrade reaction, pseudo-finite element and finite element methods. Structural forces, such as strut loads, wall shear forces, bending moments are calculated by each method and results are compared. The analyses are carried for for three values of internal friction angle of soil; 30^o, 35^o, and 40^o. Effects of modulus of soil elasticity of the backfill and wall stiffness on structural forces are investigated by using different values for these parameters.

It is found that, in those of obtained by, limit equilibrium approach results in embedment depth greater than other methods. Minimum strut loads for the same soil and structure parameters are obtained by limit equilibrium method. An increase of Young's modulus of the soil results in decrease of the strut loads.

Keywords : embedded retaining wall, limit equilibirium, subgrade reaction, pseudo finite, finite element

ÖZ

ZEMİNE GÖMÜLÜ İKSA DUVARLARININ
HESAP YÖNTEMLERİNİN KARŞILAŞTIRILMASI

HARMANDAR, Serkan
Yüksek Lisans, İnşaat Mühendisliği Bölümü
Tez Yöneticisi : Prof. Dr. Yener Özkan
Tez Yönetici Yardımcısı: Dr. Oğuz Çalışan

Aralık 2006, 123 sayfa

Bu tez çalışmasında, kohezyonsuz zemini tutan tek sıra içten destekli zemine gömülü iksa duvarı, dört farklı yöntem (limit denge yöntemi, elastik zemine oturan kiriş yöntemi, pseudo-sonlu elemanlar yöntemi ve sonlu elemanlar yöntemi) ile analiz edilmiştir. Destek sisteminde oluşan kuvvetler, duvarda oluşan kesme kuvveti ve eğilme momenti gibi yapısal kuvvetler her bir yönteme göre hesaplanmış ve karşılaştırılmıştır. Analizler, üç farklı zemin içsel sürtünme açısı (30^o, 35^o ve 40^o) için yapılmıştır. Zemin elastisite modülünün ve duvar rijitliğinin yapısal kuvvetlere olan etkisi, bu parametreler için farklı değerler kullanılarak araştırılmıştır.

Genel olarak limit denge yönteminin, duvar gömülme derinliğini, diğer yöntemlere göre daha fazla hesapladığı tespit edilmiştir. Limit denge yöntemi destek sisteminde oluşan kuvvetleri, diğer yöntemlere göre daha az hesaplamaktadır. Zemin elastisite modülündeki artış, destek sistemindeki kuvvetlerin azalmasına sebep olmaktadır.

Anahtar kelimeler: zemine gömülü iksa duvarı, limit denge, elastik zemine oturan kiriş, pseudo-sonlu elemanlar, sonlu elemanlar

ACKNOWLEDGMENTS

The author wishes to express his deepest gratitude to his supervisor Prof. Dr. Yener Özkan for his guidance, advice, criticism, encouragements, tolerance and great patience throughout the study.

The author would also like to thank his co-supervisor Dr. Oğuz Çalışan for his supports, suggestions and comments.

TABLE OF CONTENTS

LIST OF TABLES

LIST OF FIGURES

LIST OF SYMBOLS

Symbol	Description
B	soldier beam width or pile width
c'	cohesion
c'_m	mobilised cohesion
c_w	wall adhesion
c_{wm}	mobilised wall adhesion
d	embedment depth
δ	soil / wall friction angle
D	effective contact dimension
δ_m	mobilised angle of soil / wall friction
E_{conc}	Young's modulus of concrete
EI_{wall}	wall flexural rigidity per meter
E_{soil}	Young's modulus of soil
ϕ'	soil angle of shearing resistance
F_d	factor on embedment
ϕ'_m	mobilised angle of shearing resistance
F_{np}	factor on net total pressure
F_p	factor on gross pressure
F_r	factor on net available passive resistance
F_S	factor on strength
γ_{conc}	unit weight of concrete
h	soil height
K_0	at rest earth pressure coefficient
K_a	active earth pressure coefficient
k_h	coefficient of horizontal subgrade reaction
k_{ha}	horizontal coefficient of subgrade reaction – at rest to active
k_{hp}	horizontal coefficient of subgrade reaction – at rest to passive

K_P	passive earth pressure coefficient
I_h	subgrade constant for continuous walls
ν	poisson's ratio
N_{60}	SPT blow count at 60% efficiency
n_h	constant of horizontal subgrade reaction for soldier beams
M_{LEQ}	bending moment obtained from the limit equilibrium analysis
M_{SSI}	bending moment obtained from the subgrade reaction, pseudo-finite and finite element methods
N.B.M.	normalised bending moment
N.S.F.	normalised shear force
P	prop (strut) load
P_{LEQ}	prop (strut) load obtained from the limit equilibrium analysis
P_{SSI}	prop (strut) load obtained from the subgrade reaction, pseudo-finite and finite element methods
p	net pressure difference on pile
Q	equivalent force
R_0	at rest stress state for soil spring (at zero deformation)
R_a	active stress state for soil spring
R_P	passive stress state for soil spring
S_u	undrained shear strength
S_{um}	mobilised undrained shear strength
ψ	angle of dilation of soil
V_{LEQ}	shear force obtained from the limit equilibrium analysis
V_{SSI}	shear force obtained from the subgrade reaction, pseudo-finite and finite element methods
y	pile lateral movement
y_a	deflection representing the change from linear elastic to active
y_p	deflection representing the change from linear elastic to passive
z	depth below ground surface
z_p	depth of the pivot point below formation level

CHAPTER 1

INTRODUCTION

1.1 General Considerations

An embedded retaining wall is one that penetrates the ground at its base and obtains some lateral support from it. The wall may also be supported by structural members such as props, berms, ground anchors and slabs.

The need for design and construction of embedded retaining walls increased in the last decades as the need for underground structures, such as deep basements and subway systems, increased. Any embedded wall project must be designed to provide suitable protection against ultimate limit states and serviceability limit states. Ultimate limit states are those associated with collapse or with other similar forms of structural failure. They are concerned with the safety of people and the safety of the structure. Serviceability limit states correspond to conditions beyond which specific service performance requirements are no longer met, for example predefined limits on the amount of water seepage, wall deflections.

The design of the embedded walls include the determination of penetration depth of the wall (wall toe level), structural forces and the effects on adjacent structures or facilities if any.

The wall toe level (or penetration depth of the wall) of any embedded retaining wall should be the deeper of that required to satisfy load bearing capacity, hydraulic cut-off and uplift, global stability and lateral stability.

The wall toe level for overall lateral stability can be determined by limit equilibrium method, subgrade reaction method, pseudo finite element method and finite element&finite difference methods. These various design methods have different capabilities and yield different results which confuse the designers.

1.2 Aim of the Study

The aim of this thesis is to compare the output of these analysis methods and their response (except limit equilibrium method) to Young's modulus of soil and wall flexural rigidity in terms of structural forces.

Chapter 2 represents the brief description of these methods and comparison of the methods theoretically.

Chapter 3 presents the considered wall-soil-strut systems in the analysis. The excavation geometry (excavation width, excavation height), soil properties, wall properties, strut properties and their combinations in the analysis are presented.

The results of the analysis are represented in Chapter 4 and conclusions derived from the analysis are represented in Chapter 5.

CHAPTER 2

ANALYSIS METHODS OF EMBEDDED RETAINING WALLS

2.1 General

Retaining wall problems are treated as plane strain problems, since the wall has a one dimension very large in comparison with the other two dimensions, with non-linear material properties (soil behaviour). As mentioned in the previous chapter, embedded retaining walls can be designed either by, from simple to complex, limit equilibrium, subgrade reaction, pseudo-finite and finite element & finite difference methods. Each method is based on different assumptions and idealisations to represent the actual problem.

In this chapter, the summary and theoretical comparison of these methods are represented.

2.2 Limit Equilibrium Method

Traditional limit equilibrium methods of calculation are based on conditions at collapse, when the full strength of the soil is mobilized uniformly around the retaining wall.

A factor of safety is applied to one or more of the parameters involved in the calculation to give the design geometry. The purpose of a factor of safety is to take account of uncertainties, and the appropriate value for design principally depends on:

- The method by which it is incorporated in the design calculation.
- The soil parameters selected. Variability of soil strata can have a major effect on the design.
- The geometric parameters. The risk of over excavation or a rise in water table are particularly important.
- The values *of* any imposed loading (e.g. surcharges).
- The risk of damage to adjacent buildings by ground movements. (However, ground movements around an excavation are not necessarily significantly reduced by increasing the factor of safety.)
- The construction procedure and programme. The design of temporary works is strongly dependent on the phasing of any prop *or* anchoring systems.

Limit equilibrium calculations are usually based on simple linear lateral stress distributions; in reality the lateral stress distributions are different. They are better developed and more directly applicable for structural forms (eg unpropped cantilever walls) than others (e.g. multi-propped walls and walls propped significantly below the top).

As limit equilibrium calculations are based on the soil strength, they do not in themselves give any indication of wall movements.

2.2.1 Cantilever Walls

Unpropped embedded walls rely entirely for their stability on an adequate depth of embedment: they are not supported in any other way. They will tend to fail by rotation about a pivot point near the toe, above which active conditions are developed in the retained soil and passive conditions in the restraining soil. The idealized stress distribution at failure is shown, together with the corresponding bending moments and implied wall deflections, in Figure 2.1.

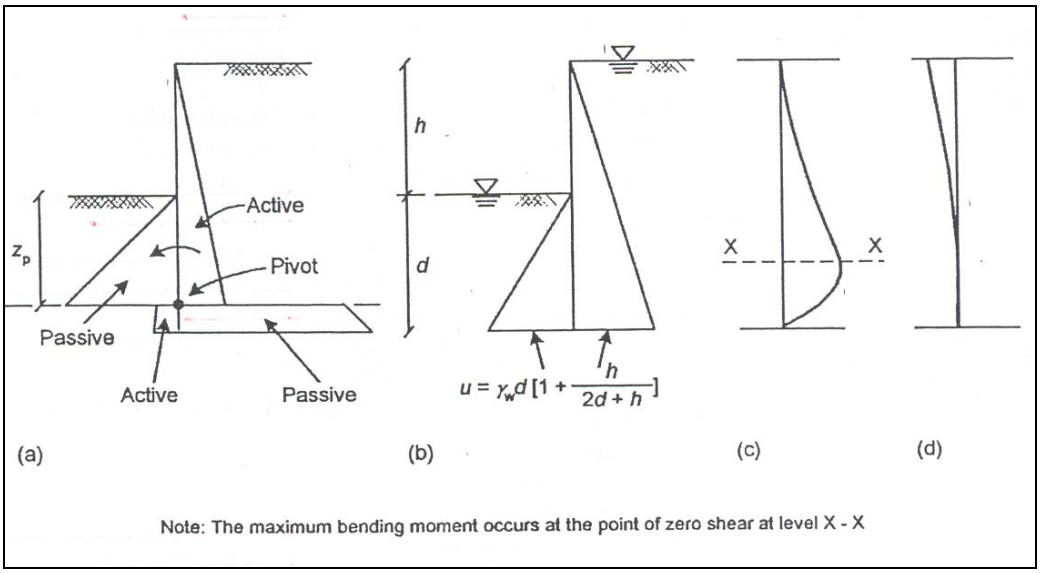

Figure 2.1 Idealised stress distribution for an unpropped cantilever wall at failure : a) effective stress; b) pore water pressures; c) wall bending moment distribution; d) wall deflection (Powrie,2003)

These conditions are known as fixed earth support, because the depth of embedment has to be large enough to prevent translation or rotation of the toe.

Given the soil height h and the angle of shearing resistance,ϕ' , the depth of embedment required just to prevent collapse, d , of a cantilever wall can be determined from the depth of the pivot point (about which the wall can be imagined to rotate) below formation level, z_p. The equations of horizontal and moment equilibrium can be used to find these unknowns, so the system is statically determinate.

If the linear approximation to the steady-state pore water pressure distribution is used, the two equilibrium equations are simultaneous and quartic in the two unknowns, and can be solved either directly or by adopting an iterative solution such as that outlined by Bolton and Powrie (1987).

The inconvenience of the iterative solution in the days before personal computers led to the development of an approximate to the exact solution, in which the resultant of the stresses below the pivot point is replaced by a single point force Q acting at the pivot(Figure 2.2).

The portion of the wall below the pivot point does not feature in the approximate analysis. The two unknowns are now the depth to the pivot point z_p and the equivalent force Q. Solution is simpler in this case , since moments can be taken about the pivot, eliminating Q from the moment equilibrium equation. The value obtained for z_p is multiplied by an empirical factor, historically 1.2, to arrive at the overall depth of embedment, d . This factor of 1.2 is nothing to do with distancing the wall from collapse (i.e. it is not a factor of safety), but is necessary because the calculation is approximate. If the simplified procedure is used, then a check should be carried out to ensure that the added depth is sufficient to mobilize at least the calculated value of Q, Figure 2.2(c).

To determine the design depth of embedment, the calculation indicated in Figure 2.1 should be carried out with the appropriate factors of safety, including any surface surcharges and allowance for overdig. Bending moments and shear forces, either at limiting equilibrium or for the design embedment depth with the specified factors of safety and modifications to geometry and loading applied, may be calculated from the appropriate equilibrium pressure distribution.

Powrie (1996) and Bica and Clayton (1998) argue that the stress distribution illustrated in Figure 2.1 gives a realistic estimate of the geometry of an unpropped cantilever wall at collapse , allowing for likely uncertainties in the soil angle of shearing resistance ϕ' and the direction and magnitude of the soil/wall friction angle δ (Figure 2.3, adapted from Bica and Clayton, 1998, for walls in dry sand).

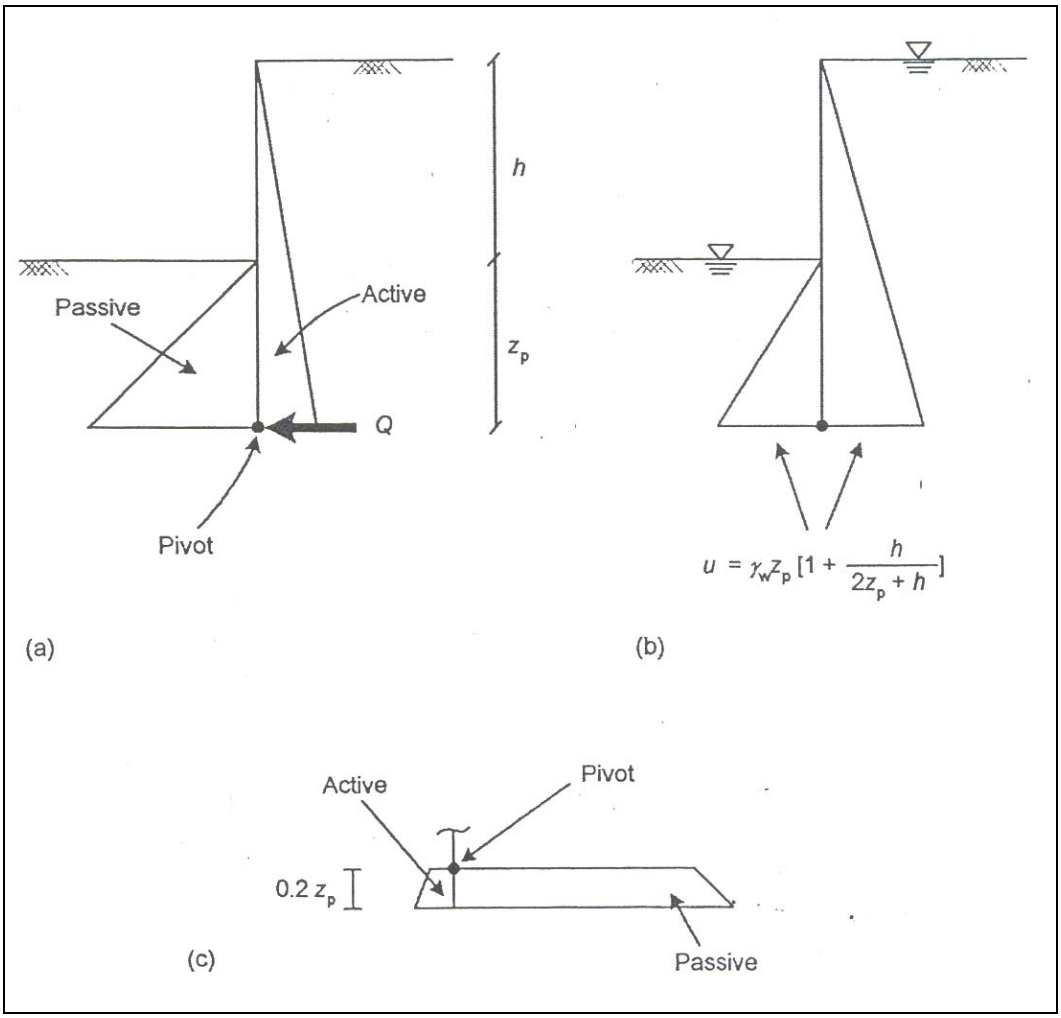

Figure 2.2 Approximate stress analysis for unpropped walls a) effective stresses b)pore water pressures c) check that the added depth can mobilize at least the required force Q (Powrie 2003)

2.2.2 Single Propped Embedded Walls

If the possibility of a structural failure of the wall or excessive movement of the props is discounted, an embedded wall propped at the top can only fail by rotation about the position of the prop. A simple, equilibrium effective stress distribution at failure is shown in Figure 2.4(a), and pore water pressures according to the linear seepage model are shown in Figure.2.4(b).

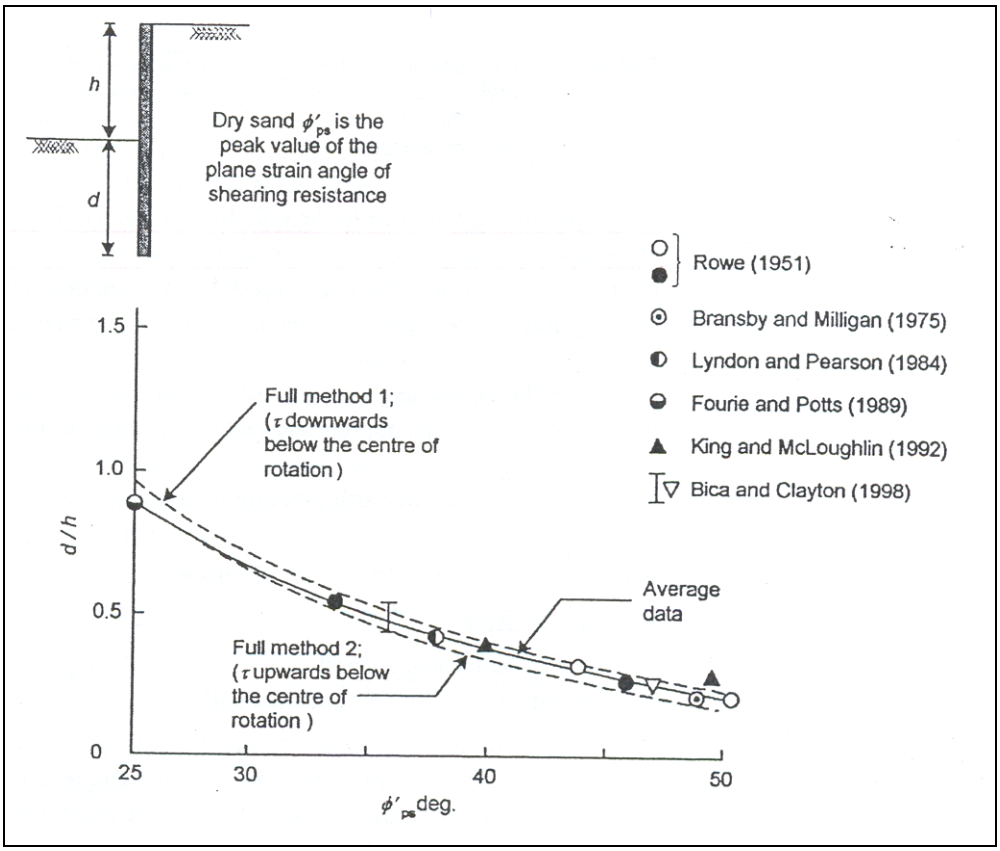

Figure 2.3 Normalised depths of embedment at failure (after Bica and Clayton, 1998)

The conditions giving rise to the effective stress distribution shown in the Figure 2.4 (a) are known as free earth support, because no fixity is developed at the toe. In this case, the two unknowns are the prop force P and the depth of embedment, required just to prevent failure. The depth of embedment d, can be calculated by taking moments about the prop, and P then follows the condition of horizontal force equilibrium. To determine the design depth of embedment, the calculation indicated in Figure 2.4 must be carried out with the appropriate factors of safety.

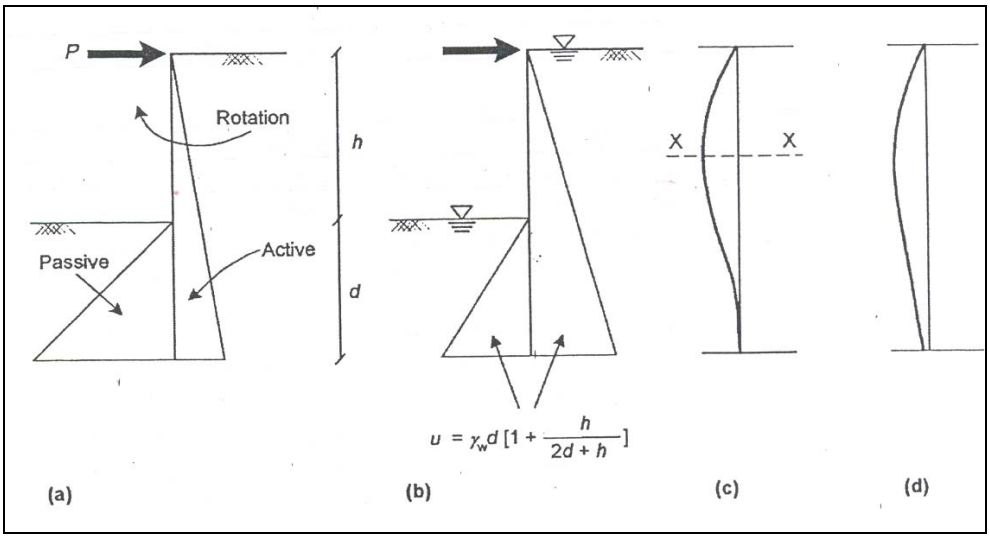

Figure 2.4 Idealised stress distribution at failure for a stiff wall propped rigidly at top a)effective stresses b)steady-state pore water pressures for a wide excavation where the differential water head dissipates uniformly c) wall bending moment distribution d) wall deflection (Powrie,2003)

For several reasons, the earth pressure distribution illustrated in Figure 2.4 may be less representative of what actually happens at collapse than Figure 2.2 for unpropped walls. In particular, real props are :

- of finite depth
- likely to be located a small distance below the top, so that the wall above prop level may rotate back into the retained soil.
- Likely to provide a kinematic restraint may inhibit the development of fully active conditions in the immediate vicinity, and is in any case not taken into account in the derivation of the lateral earth pressure coefficients likely to be used in analysis (Bolton and Powrie,1987).

For these reasons, there may be a local increase in the lateral stress in the vicinity of the prop (compared with Figure 2.4), and a decrease in the lateral stress below it. This redistribution of lateral stress would result in an increase in prop load and a reduction in wall bending moments in

comparison with those obtained using the simple linear lateral stress distribution shown in Figure 2.4. As a result , a reduction in wall depth might be possible.

Some authors (eg Williams and Waite, 1993; British Steel, 1997) describe the use of a fixed earth support calculation for a propped wall. The idealised and simplified effective stress distributions are shown, together with indicative wall bending moments and deflections, in Figure 2.5.

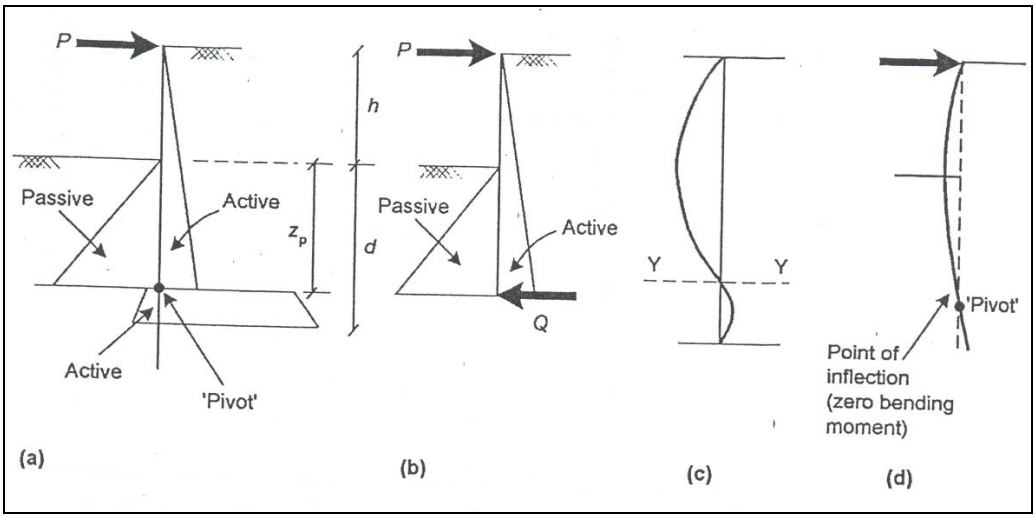

Figure 2.5 Fixed earth support effective stress distributions and deformations for an embedded wall propped at the top
a) idealized stresses b) simplified stresses c) wall bending moment distribution d) wall deflection (Powrie, 2003)

This stress distribution might correspond to a mechanism of failure involving the formation of a plastic hinge at the point of maximum bending moment. The fixed earth support analysis is unlikely to be appropriate for strong walls in clay soils whose embedment depths are governed by considerations of lateral stability. For such walls, the embedment depth calculated assuming fixed earth support conditions for a propped wall will be greater than that in a free earth support analysis. The fixed earth support analysis represents a very conservative bound for wall toe depth. There may be other reasons

why the embedment depth of the wall is taken deeper than that required to satisfy lateral stability, e.g. to provide an effective groundwater cut-off or for adequate vertical load bearing capacity. In such circumstances, fixed earth conditions provide a more realistic basis than Figure 2.4 for the estimation of lateral stresses.

In the absence of a plastic hinge (which would define the wall bending moment at this point), both the idealised and the simplified stress distributions shown in Figure 2.5 are statically indeterminate. To calculate the prop force and the depth of embedment, the designer is free to introduce a further requirement or simplification. Williams and Waite (1993) suggest the designer assumes that the point of contraflexure (i.e. where the bending moment is zero) occurs at the level where the net pressure acting on the wall is zero (Figure 2.5).

The stress distribution shown in Figure 2.5 would correspond to the correct failure mechanism for a propped or anchored wall where the prop or anchor yields at a constant load, which is just sufficient to prevent failure. Such a system is statically determinate, provided that the prop or anchor yield load is known.

2.2.3 Alternative Solution Methods of Limit Equilibrium Approach

In limit equilibrium method, there are five different methods to determine the wall geometry which are:

- embedment factor method
- strength factor method
- gross pressure method
- net total pressure method
- burland-potts method.

Each method may be used for short or long-term stability, and they are applicable to both cantilever and single-propped walls. Each method is

described in the following sections.

2.2.3.1 Embedment Factor Method

The geometry is adjusted to satisfy equilibrium with fully-mobilised strength. It is then readjusted to provide a safety margin.

This method is probably the simplest to use and to understand. It is explained and illustrated in detail in the US Steel Design Manual, also in the BSC Piling Handbook. The only pressure distributions which may be predicted with reasonable certainty are those which occur at collapse of the wall. Full active and full passive pressure distributions are then acting, regardless of the flexibility of the wall, the stiffness of any props or anchors, etc. Consequently, by adjusting the depth of embedment of the wall a geometry can be found to represent moment equilibrium with fully mobilised active and passive soil pressures. The wall is theoretically on the point of collapse. It is then necessary to increase the depth of embedment by an empirically determined factor, F_d. Because of the empirical nature of F_d ,it is incorrect to treat it as a factor of safety against overall rotation of the wall. In view of this, it is recommended that- the method should always be checked against one of the other methods. Particular care may be necessary when softer material exists beneath the calculated depth of embedment.

2.2.3.2 Strength Factor Method

The parameter values are factored to provide a safety margin, and the geometry is adjusted to satisfy equilibrium with the pressures derived from the factored parameters.

This method satisfies the moment equilibrium equation by calculating forces on the basis of factored strength parameters

In an effective stress analysis, there are generally two soil strength parameters, c' and ϕ'. In addition, wall friction and adhesion parameters, δ and c_w are included in the calculation. Because there are different uncertainties associated with each of these parameters, a method of factoring strength potentially involves a factor for each parameter. A simplified approach adopted by some designers is to reduce the strength parameters by a single factor of safety, F_s, such that for an effective stress analysis

$$\tan \phi'_m = \tan \phi' / F_s \qquad (2.1)$$

$$c'_m = c'/ F_s \qquad (2.2)$$

where ϕ'_m and c'_m are the mobilised values of the respective strength parameters ϕ' and c' . Values of ϕ'_m and c'_m are used in the analysis to obtain the active and passive pressures on the wall. To be consistent, the mobilised angle of wall friction δ_m, and adhesion, c_{wm} should be determined by maintaining constant values of the mobilised ratios, $(\delta/\phi')_m$ and $(c_w/c')_m$, equal to the assumed values of δ/ϕ' and c_w/c', respectively.

Similarly, for a total stress analysis:

$$S_{um} = S_u / F_s \qquad (2.3)$$

where is the mobilized value of the undrained shear strength, S_u.

The strength factor method is a consistent, logical and reliable method which factors the parameters representing the greatest uncertainty, leaving bulk forces constant and using the moment equilibrium equation. The result is very sensitive to the value of F_s chosen.

Use of a factor on strength leads to an increase in K_a and decrease in K_p, which not only modifies the magnitude but also the relative distribution of earth pressures. This distorts the predicted values for moment in the wall stem. Factored parameters should therefore only be used for stability calculations. The design moment should, in general, only be calculated for unfactored soil parameters.

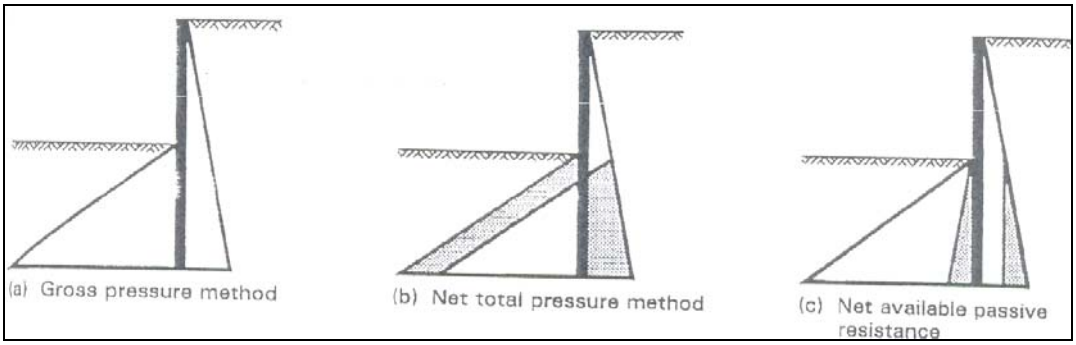

Figure 2.6 Different methods of assessing the ratio of restoring moments to overturning moments (Padfield,1991)

2.2.3.3 Gross Pressure Method

This method is described in CP2, and it consists of only factoring the gross passive pressure diagram. Water pressures are not factored, net water pressures are included in the overturning moments. The factor of safety is as given in equation 2.4.

F_p = factor of safety = restoring moments / overturning moments (2.4)

There is often some mechanical justification in factoring the restoring moments in that the total passive force is only partially mobilised at working load, even though the passive pressure often is fully mobilised for same distance below excavation level (but not over the full depth of the wall). CP2 only considers the design of walls in clays in terms of the gross pressure

method and total stress (i.e. in terms of undrained shear strength). The method may be illogical for soft clay, and it does not appear consistent, because the bulk weight of the soil is in effect being factored. For effective stress analyses, it may be argued for the case when c' = 0, where the method reduces to applying a factor to K_p although K_p is not strictly a parameter value.

When the method is used with effective stress analysis, it is conservative for permanent works design in the case of most clays if the conventional value of $F_p = 2.0$ is adopted.

2.2.3.4 Net Total Pressure Method

Elimination of all balancing loads from the equilibrium equation, leaving only the unbalanced loads, grossly alters the factor of safety obtained from the moment equilibrium relationship. The factor of safety is as given in equation 2.5.

F_{np} = (moments from net passive pressure) / (moments from net active pressure) (2.5)

In other words, as shown in Figure 2.6 (b), the factor of safety is equal to the ratio of the moment of the unshaded area on the passive side of the wall to the moment of the unshaded area on the active side. To obtain a conventionally-satisfactory design consistent with the other design methods, very large values of F_{np} have to be used. This approach diverges so much from accepted practice that dangerous errors are likely to result. The discrepancies between F_{np} values and factors of safety determined by other methods have been well illustrated by Burland and Potts (1981,1983). If a design is produced using the net pressure method with F_{np} of the order of 2,

a marginally safe design should result, but very little margin is built in for error, and strength may be expected to be almost completely mobilised, with correspondingly large ground movements.

In the calculation of factor of safety, the exact formulation of any moment relation is very important, because, whatever grouping of forces is selected for the calculation of restoring moments; the magnitude of restoring moments should exceed that of overturning moments by a factor, and the appropriate value depends on the formulation.

2.2.3.5 Burland – Potts Method

This method has been developed and described by Burland, Potts and Walsh (1981), and a further detailed comparison with the other available methods is given by Potts and Burland (1983). It consists of eliminating some of the balancing loads from the moment equilibrium equation, and it arose out of a search for a consistent method which resulted in the calculation of one single lumped safety factor while avoiding same of the unsatisfactory attributes of the other methods. The method derives from an analogy drawn between the distribution of forces at equilibrium under, and adjacent to, a footing which is on the point of failure, and the distribution of forces which act if strength is fully mobilised on both the active and the passive sides of a stable retaining wall. The resulting safety factor is defined in equation 2.6.

F_r = (moment of net available passive resistance) / (moment activated by retained material (including water)and surcharge) (2.6)

The simplest way of arriving at the safety factor using this method is to draw a vertical line on the active pressure diagram from the level of the

excavation, as shown in Figure 2.6(c). The shaded area is then subtracted from the passive resistance to give the net passive resistance, which is available to resist the net active resistance given by the unshaded area behind the wall.

The analogy forming the basis of this method does not represent more than an illustration which points the way to a particularly fortunate allocation of loads to the top and the bottom of the factor of safety equation. However, it appears that, compared with others, the method leads to a consistent lumped factor of safety throughout the practical range of soils and wall geometries.

2.3 Subgrade Reaction (Winkler) Method

Beam on elastic foundation analysis, or Winkler spring analysis, is a soil structure interaction (SSI) method of analysis that enforces compatibility of deflections, soil pressures, and support forces while accounting for wall and support (strut and anchor) flexibility.

The major approximation is the assumed soil behaviour. The method is based on a one-dimensional (1-D) finite element representation of the wall soil system consisting of linearly elastic, beam column elements for the wall, distributed nonlinear Winkler springs to represent the assumed soil behaviour, and nonlinear preloaded concentrated springs to represent the supports. Cut offs are applied to the springs representing the soil behaviour. These cut offs are obtained from the Rankine or Coulomb earth pressure theories. It is important to appreciate that these cut offs are not a direct result of the beam-spring calculation, but are obtained from separate approximate solutions and then imposed on the beam-spring calculation process.

Only a single structure can be accommodated in the analysis. Consequently, only a single retaining wall can be analyzed. Further

approximations must be introduced if more than one structure (pile, retaining wall or foundation) interact. Solutions from these calculations include forces and movements of the structure. They do not provide information about global stability or movements in the adjacent soil. They do not consider adjacent structures.

It is difficult to select appropriate spring stiffnesses and to simulate some support features. For example, it is difficult to account realistically for the effects of soil berms. Retaining wall programs using interaction factors to represent the soil have problems in dealing with wall friction and often neglect shear stresses on the wall, or make further assumptions to do with them. In the analysis of retaining walls a single wall is considered in isolation and structural supports are represented by simple springs fixed at one end (grounded). It is therefore difficult to account for realistic interaction between structural components such as floor slabs and other retaining walls. This particularly so if 'pin-jointed' or 'full moment' connections are appropriate. As only the soil acting on the wall is considered in the analysis, it is difficult to model realistically the behaviour of raking props and ground anchors which rely on resistance from soil remote from the wall.

In embedded wall design and analysis, the Winkler spring analysis can be used to:

- evaluate the lateral resistance of the embedded wall toe for wall loadings based on apparent pressure distributions.
- evaluate actual (rather than apparent) soil pressure distributions, wall forces, support loads, and displacements at final excavation.
- simulate in approximate manner construction sequencing, and actual soil pressure distributions, wall forces, support loads, and displacements at intermediate stages of construction.

The Winkler soil spring system for a tieback wall is illustrated in Figure 2.7. These infinitely closely spaced soil springs can have a stiffness that

increases linearly with depth to approximate the behavior of cohesionless soils, normally consolidated silts, and normally consolidated clays, or may be constant with depth to represent the approximate behavior of soil types of cohesive soils.

Difficulties in obtaining reasonable results from a Winkler spring analysis often occur because

- The load deformation characteristics of the soil are not linear and may not be suitably represented by ideal elastoplastic behavior.

- The soil stiffness varies with respect to confining pressure and zone of influence.
- The soil stiffness changes with submergence.
- The ultimate resistance of the soil is dependent on different failure mechanisms depending on whether the soil is near the surface or at some depth below the surface.
- The behavior of discrete wall systems (soldier beam systems) is different from continuous wall systems because the earth pressure distribution behind the wall is different (zone of influence is different) and because soil has a tendency to arch between the structural elements of discrete wall systems.

2.3.1 Concept of Soil Spring Stiffness

In the Winkler analysis, springs can be taken as either linear or nonlinear with their response based on curves that relate soil resistance, p, to wall displacement, y. In general p-y curves are nonlinear; however, they can be approximated as ideal elastoplastic systems. An idealized elastoplastic representation of p-y response is the basis for the Winkler springs described herein. The p-y curve concept is illustrated in Figure 2.8 with respect to a secant pile tieback wall system. Before excavation begins, the pressures on the secant pile are in equilibrium and therefore the resultant force, p, is zero.

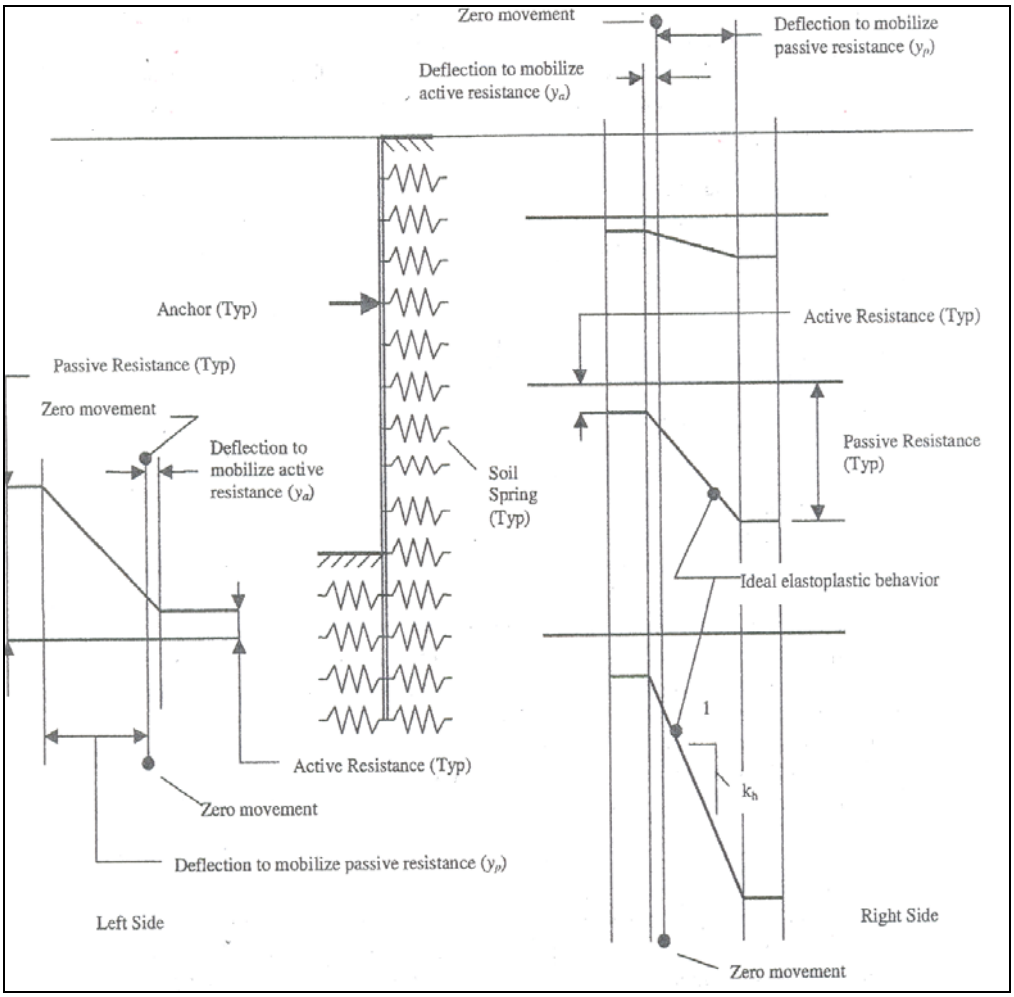

Figure 2.7 Tieback wall soil springs for Winkler analysis (Strom and Ebelling,2001)

The secant pile moves toward the excavation as excavation takes place. This movement causes earth pressures on the unexcavated side of the pile to decrease and those on the excavated side to increase, as indicated in Figure 2.8.

A plot of the net pressure difference (reaction), p, on the pile versus pile lateral movement, y is designated the p-y curve. These curves can be generated for various elevations along the wall height. These p-y curves are the basis for the idealized elastoplastic springs used in the Winkler analysis. Since for the idealized Winkler spring the relationship

between the horizontal reaction p and the displacement y is linear, the ratio p/y is the spring stiffness as given in equation 2.7.

$$p / y = k_h \qquad (2.7)$$

where the spring stiffness, k_h, is termed the coefficient of horizontal subgrade reaction (Terzaghi 1955).

In his treatise on subgrade reaction, Terzaghi (1955) indicates that the coefficient of horizontal subgrade reaction k_h is dependent on the deformation characteristics of the subgrade. For stiff (that is, overconsolidated) clays, the deformation characteristics are more or less independent of depth such that the subgrade reaction p would be uniformly distributed with respect to depth along the face of the soldier beam or continuous wall, as the case might be. Therefore, for stiff clays, the coefficient of subgrade reaction, k_h, would be constant with depth. For cohesionless sands, the pressure required to produce a given horizontal displacement increases in direct proportion to the effective confining pressure, which for uniform soil layers would be in direct proportion to the depth z. Therefore, for cohesionless sands the coefficient of subgrade reaction, k_h , would increase linearly with depth. The assumption used for sand has also been proven valid for normally consolidated silts and normally consolidated clays (Peck and Davisson 1962). The relationships described above are illustrated in Figure 2.9.

For cohesionless soils, normally consolidated silts, and normally consolidated clays, the coefficient of horizontal subgrade reaction is a function of the relative density. For stiff clays, the coefficient of horizontal subgrade reaction is a function of S_u, the undrained unconfined compressive strength.

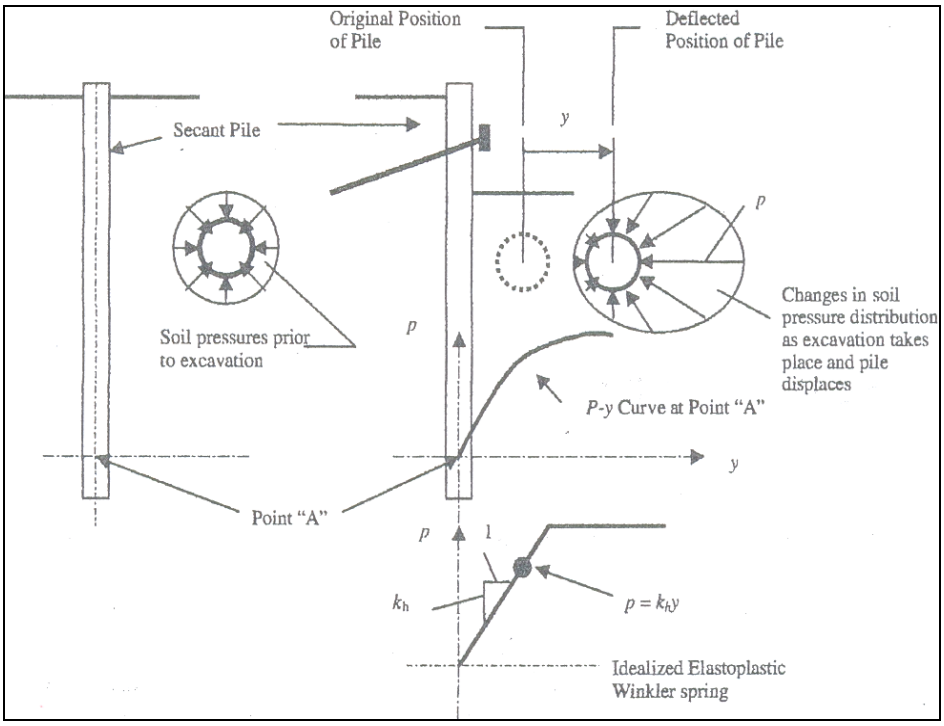

Figure 2.8 Concept of p-y curve (Strom and Ebelling,2001)

Terzaghi (1955) recommends the coefficient of subgrade reaction for different wall systems (discrete wall systems, continuous wall systems) in both cohesive and cohesionless soil types. The mentioned recommendations are summarised below.

For discrete wall systems in stiff clay, Terzaghi (1955) recommends constant value of coefficient of horizontal subgrade reaction along the wall which is defined by the equation 2.8 .

$k_h = 64\ S_u / B$ (2.8)

S_u : undrained strength of the soil

B : pile width

For discrete wall systems in cohesionless soils, Terzaghi (1955) recommends linearly increasing value of coefficient of horizontal subgrade reaction along the wall which is defined by the equation 2.9.

$k_h = n_h z / B$ (2.9)

where

n_h : constant of horizontal subgrade reaction for soldier beams

z : depth below ground surface

B : pile width

Values of n_h for loose medium and dense sands are provided in Table 2.1.

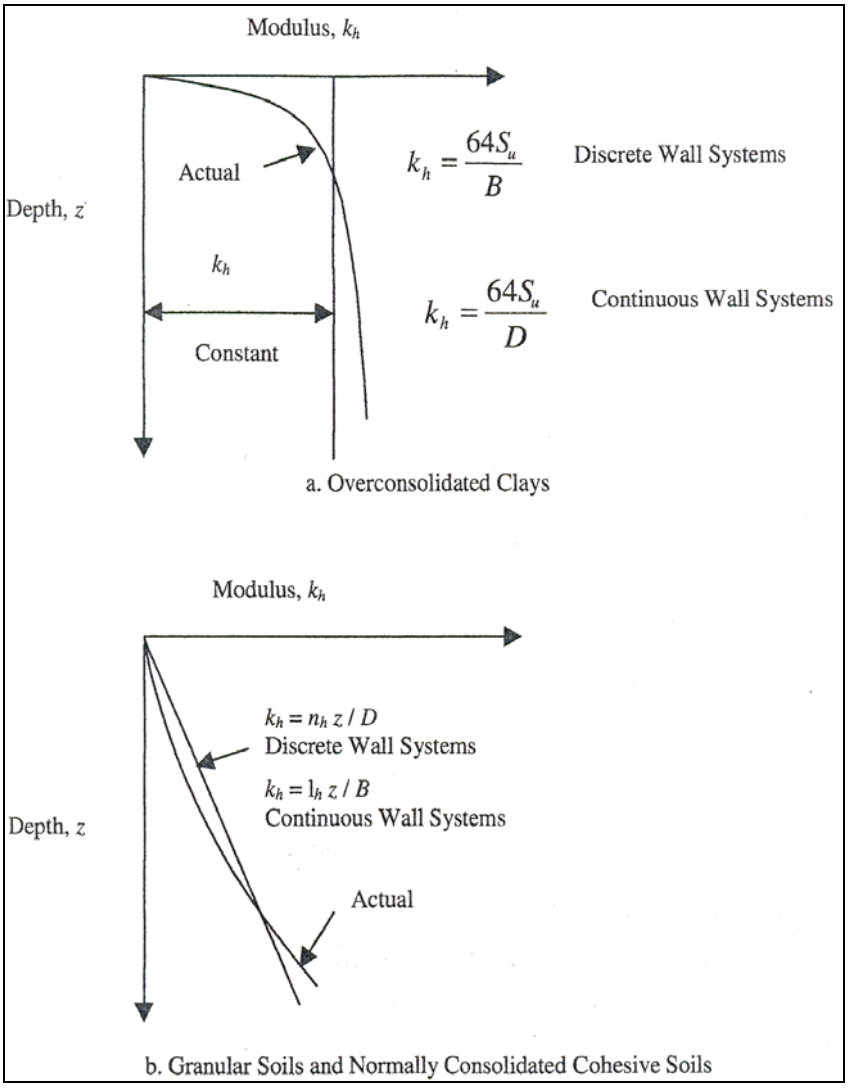

Figure 2.9 Subgrade reaction idealizations (Strom and Ebelling,2001)

Terzaghi (1955) indicated that, for continuous walls (i.e., sheet-pile walls and diaphragm walls) in stiff clay, the subgrade reaction k_h can be assumed to be constant with depth, and taken as given in equation 2.10.

$$k_h = 64\ S_u / D \qquad (2.10)$$

D is the effective contact dimension (Haliburton 1971), or interaction distance. Dawkins (1994a) provided guidance for estimating the interaction distance. These guidelines are illustrated for single-and multiple-tieback anchor walls in Figure 2.10.

Table 2.1 Estimated values of the constant of horizontal subgrade reaction, discrete wall systems in moist and submerged sands (Terzaghi 1955)

Soil Type - Sand	Constant of horizontal subgrade reaction, n_h (kPa)		
Relative density	Loose	Medium	Dense
Dry or moist sand (range)	28 - 90	90 - 296	296 - 593
Dry or moist sand (adopted)	55	172	441
Submerged sand (range)	21 - 55	55 - 186	186 - 372
Submerged sand (adopted)	35	110	276

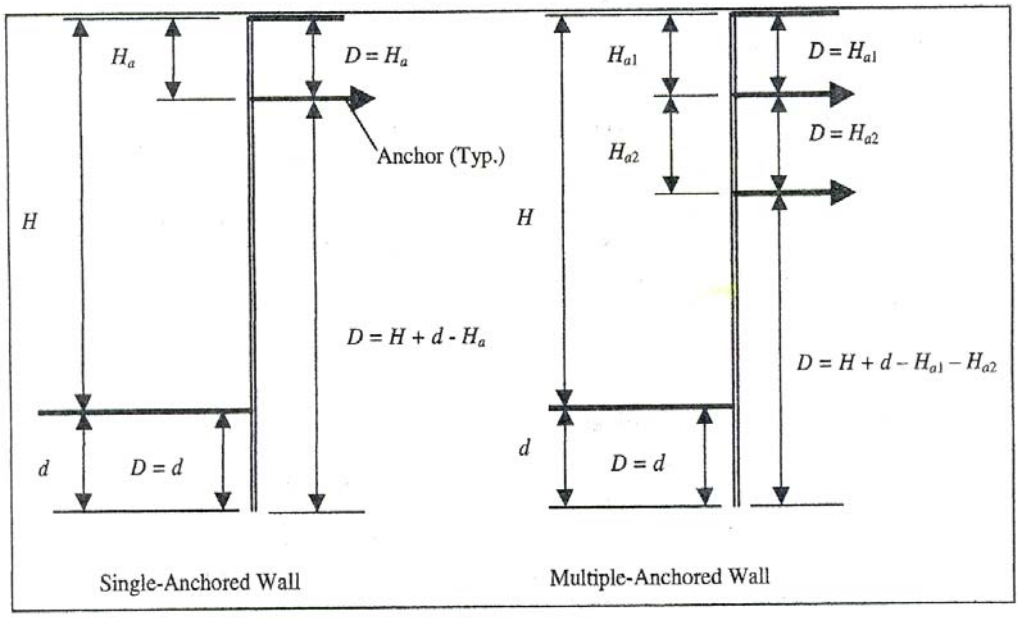

Figure 2.10 Initial estimates of interaction distances, D (adapted from Dawkins 1994a)

For continuous walls in cohesionless soils, or in normally consolidated silts and clays, the coefficient horizontal subgrade reaction k_h can be assumed to increase linearly with depth and taken as given in equation 2.11.

$$k_h = l_h \, z / D \qquad (2.11)$$

where

l_h : subgrade constant for continuous walls

z : depth below ground surface

Values of l_h for loose, medium, and dense sands are provided in Table 2.2.

It should be noted that many computations have indicated that the moments and shears in soldier beams and continuous tieback wall systems are rather insensitive to the constant of horizontal subgrade reaction selected for the Winkler analysis. Upper and lower bound constants should be used to determine the impact on soldier beam and wall moments and shears. However, wall and soldier beam deflections are very sensitive to the

constant of horizontal subgrade reaction used in the Winkler analysis. Therefore, it is difficult to obtain reasonable deflection values using this method of analysis.

Table 2.2 Estimated values of the constant of horizontal subgrade reaction, for continuous wall systems in moist and submerged sands(Terzaghi, 1955)

Soil Type - Sand	Subgrade constant , l_h (kPa)		
Relative density	Loose	Medium	Dense
Dry or moist sand (adopted)	83	249	637
Submerged sand (adopted)	55	166	415

2.3.2 Alternative Procedures for Idealised Elasto-Plastic Earth Response Curve

In general practice, the SSI analysis for embedded wall systems must consider the nonlinear characteristics of the soil springs. This is usually accomplished with springs that use ideal elastoplastic behavior to capture the nonlinear response, although more exact representations of the nonlinear soil response have been developed by the American Petroleum Institute (Murchison and O'Neill1984, O'Neill and Murchison 1983).

A typical elastoplastic soil pressure curve is shown in Figure 2.11. This curve is generally constructed by the Coefficient of Subgrade Reaction Method, the Reference Deflection Method, or the Pfister Method as described below. Earth pressure-deflection springs below the excavation for a discrete wall system are different from those of a continuous wall system. The earth-pressure deflection springs for discrete wall systems must include three-dimensional (3-D) effects, similar to a laterally loaded pile (Weatherby, Chung, Kim, and Briaud 1998).

The elastoplastic soil response curves used for the evaluation of continuous and discrete embedded wall systems will be designated as R-y curves. The active and passive loads defining the R-*y* curve plastic regions for continuous wall systems use active and passive pressures over a unit width of wall. The active and passive loads defining the R-y *c*urve plastic regions of discrete wall systems use active and passive pressures multiplied by the pile spacing.

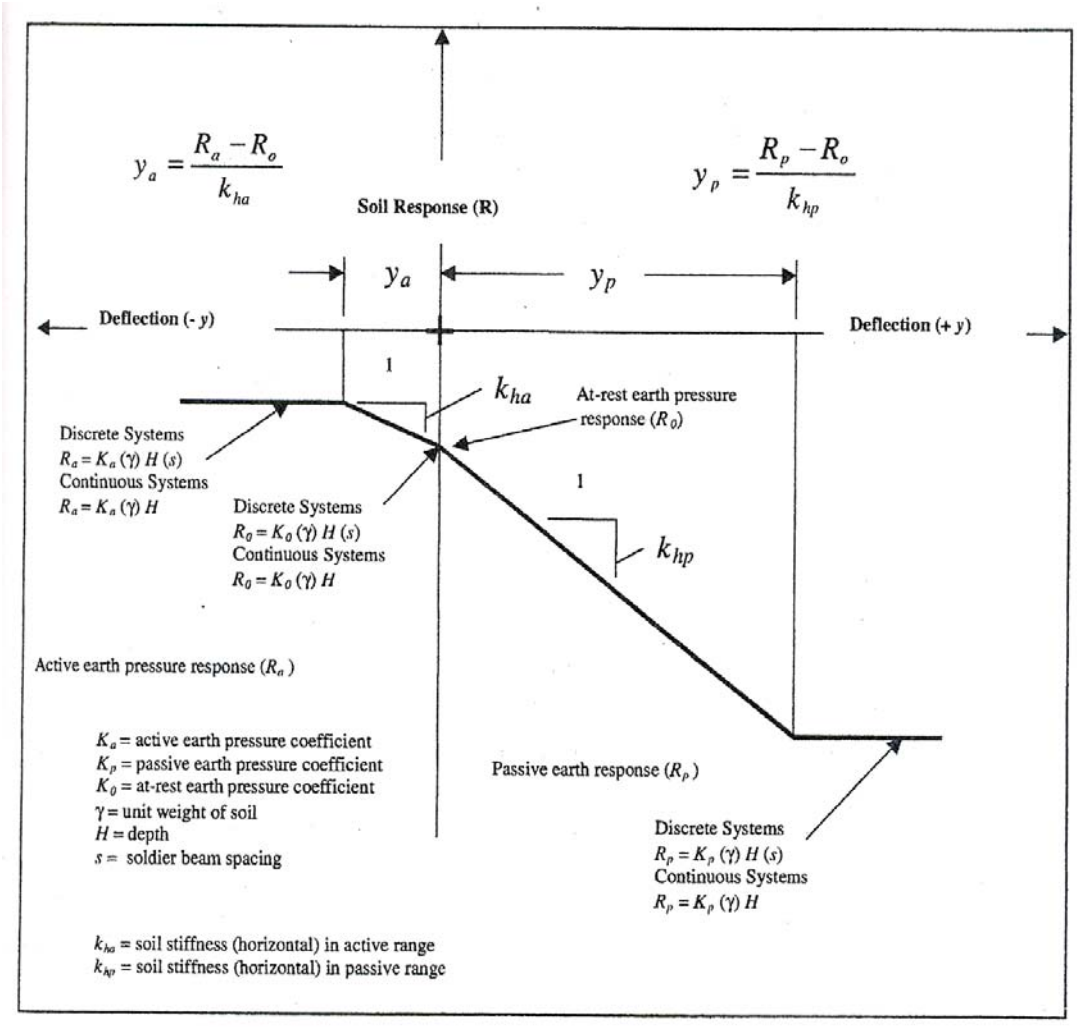

Figure 2.11 Idealized elastoplastic earth response deflection R-y curve (Dawkins 1994b)

2.3.2.1 Coefficient of Subgrade Reaction Method

In the coefficient of subgrade reaction method, the linear elastic portion of the R-y curve is developed using constants of subgrade reaction values or subgrade constants equal or similar to those described in Tables 2.1 and 2.2. A single constant of subgrade reaction or subgrade constant may be used to describe the linearelastic range between active and passive pressure, or different values may be used to define the region between at-rest and active and between at-rest and passive. Recall that at-rest pressure corresponds to zero deflection of the soil behind the retaining wall.
For the coefficient of subgrade reaction method, the elastic stiffness is determined directly for each point from the top of the wall to the toe. In practice, however, values are provided for discrete points usually representing a change in soil properties or change in effective stress. The computer program then, generates a series of infinitely closely spaced soil springs with a coefficient of subgrade reaction k_h varying linearly between the values described at the discrete points. In this way the coefficient of subgrade reaction can either vary linearly with depth (cohesionless soils, normally consolidated silts, and normally consolidated clays) or be constant with depth (cohesive soils). The deflections representing the change from linear elastic to active y_a and linear elastic to passive y_p are determined by the equations 2.12 and 2.13.

$$y_a = (R_0 - R_a) / k_{ha} \qquad (2.12)$$

$$y_p = (R_P - R_0) / k_{hp} \qquad (2.13)$$

where:

y_a : deflection representing the change from linear elastic to active

R_0 : at-rest stress state for soil spring (at zero deformation)

R_A : active stress state at- for soil spring

k_{ha} : horizontal coefficient of subgrade reaction – at rest to active (soil spring active state elastic stiffness)

y_p : deflection representing the change from linear elastic to passive

R_P : passive stress state at- for soil spring

k_{hp} : horizontal coefficient of subgrade reaction – at rest to passive (soil spring passive state elastic stiffness)

Often k_{ha} and k_{hp} are assumed to be equal (constant slope for linear elastic region). Active and passive stress states for the soil springs are usally based on conventional earth pressure theory (Rankine or Coulomb). However, passive soil failures related to the toe region of discrete soldier beam systems require the consideration of special failure mechanisms that can not be predicted by conventional earth pressure theory.

2.3.2.2 Reference Deflection Method

The reference deflection method differs from the coefficient of subgrade reaction method in that the deflections y_a and y_p are established values (dependent on soil type), rather than dependent on predetermined values of soil spring stiffness. In the reference deflection method, the soil spring stiffness is determined by the known limiting earth pressures and the known deflections of y_a and y_p as given in equations 2.14 and 2.15.

$$k_{ha} = (R_0 - R_a) / y_a \qquad (2.14)$$

$$k_{hp} = (R_P - R_0) / y_p \qquad (2.15)$$

With cohesionless soils, the limit state pressures (active and passive pressures) increase linearly with depth. Based on information presented above with respect to p-y curves, the displacements required to develop active or passive pressure will also increase linearly with depth. This suggests that the displacements required to generate active or passive conditions should be constant with depth, and gives rise to the reference deflection method for developing soil spring elastoplastic curves. The reference deflections are those necessary to mobilize active and passive soil resistance, and depend on soil type.

In Weatherby, Chung, Kim, and Briaud (1998), the reference deflections for sand were based on measurements obtained from the Texas A&M full-scale wall tests. The wall tested was 7.6 m high and consisted of soldier beams and wood lagging supported by one and two rows of pressure-injected ground anchors. The wall was constructed in a homogenous sand deposit. Earth pressures acting on the soldier beams were calculated by double differentiation of bending moments determined from strain gauge data. Earth pressures were plotted against measured lateral displacements. The deflection required to fully mobilize active earth pressure was found to be 0.13 cm. The deflection required to fully mobilize passive earth pressure was assumed to be 1.27 cm.

Reference deflections for day were assumed and verified by comparing the predicted behavior with case history results (Weatherby, Chung, Kim, and Briaud1998). An active reference deflection y_a of 0.13 cm and a passive reference deflection y_p of 1.27 cm have been used in the development of R-y curves for cohesionless soils.

The Weatherby, Chung, Kim, and Briaud (1998) also provides reference deflections for discrete and continuous wall systems constructed in clay. The R-y curve for cohesive soil has two different forms according to the critical depth where the active earth pressure is zero. Figure 2.12 and 2.13 shows the typical *R-y* curve construction using the reference deflection method for different portions of a continuous anchored wall supporting a cohesive soil. The Figures 2.12 and 2.13 are valid for both the drained and undrained conditions of the cohesive soil.

Parametric studies (Weatherby, Chung, Kim, and Briaud 1998) showed that the bending moments in flexible wall systems were not very sensitive to the slope of the R-y *c*urve (stiffness of the nonlinear spring).The parameters studies did show that the moments were sensitive to the values of the

maximum and minimum resistance used to define the plastic plateaus- of the elastoplastic curve. The studies indicated that the passive resistance had to be reduced by 50 percent to obtain results comparable to those of the test wall. Since the test wall was a discrete soldier beam system, the pressures acting on the back face will be considerably smaller than active Rankine or Coulomb earth pressures due to arching effects. The opposite is true for passive pressure resistance. The use of an active resistance pressure lower than Rankine/Coulomb, and a passive resistance pressure greater than Rankine/Coulomb, is therefore justified with respect to the Winkler spring analysis of discrete tieback wall systems. However, the actual relationship between arching effects and active pressure resistance is unknown.

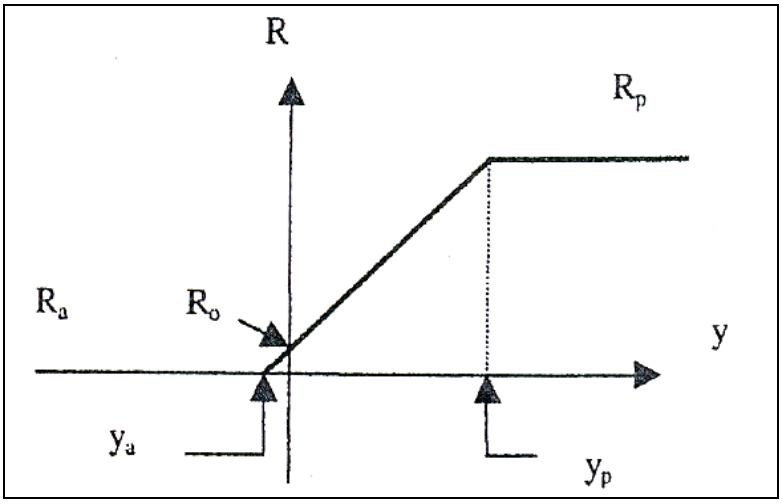

Figure 2.12 R-y curve for cohesive soils above the critical depth (Weatherby, Chung, Kim, and Briaud 1998)

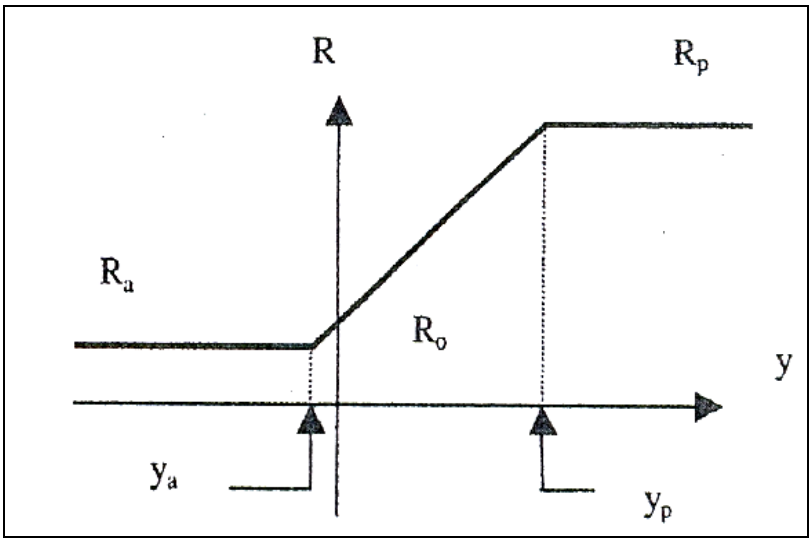

Figure 2.13 R-y curve for cohesive soils below the critical depth (Weatherby, Chung, Kim, and Briaud 1998)

Table 2.3 Reference deflections for R-y curves for clay according to S_u (Weatherby, Chung, Kim, and Briaud 1998)

	S_u < 190 kPa	190 kPa <S_u < 380 kPa	S_u > 380 kPa
y_a	-0.50 cm	-0.38 cm	-0.31 cm
y_p	2.54 cm	2.03 cm	1.02 cm

2.3.2.3 Pfister Method

Pfister developed relationships between soil strength and horizontal subgrade reaction for stiff continuous diaphragm walls (Pfister, Evers, Guillaud, and Davidson 1982). The Pfister relationships between soil strength and horizontal subgrade reaction are presented in Figure 2.14. They are generally used where no information other than the shear parameters of the loaded soils is available. The procedure used to develop elasto-plastic soil springs for a beam on elastic foundation analysis is illustrated in Pfister, Evers, Guillaud, and Davidson (1982).

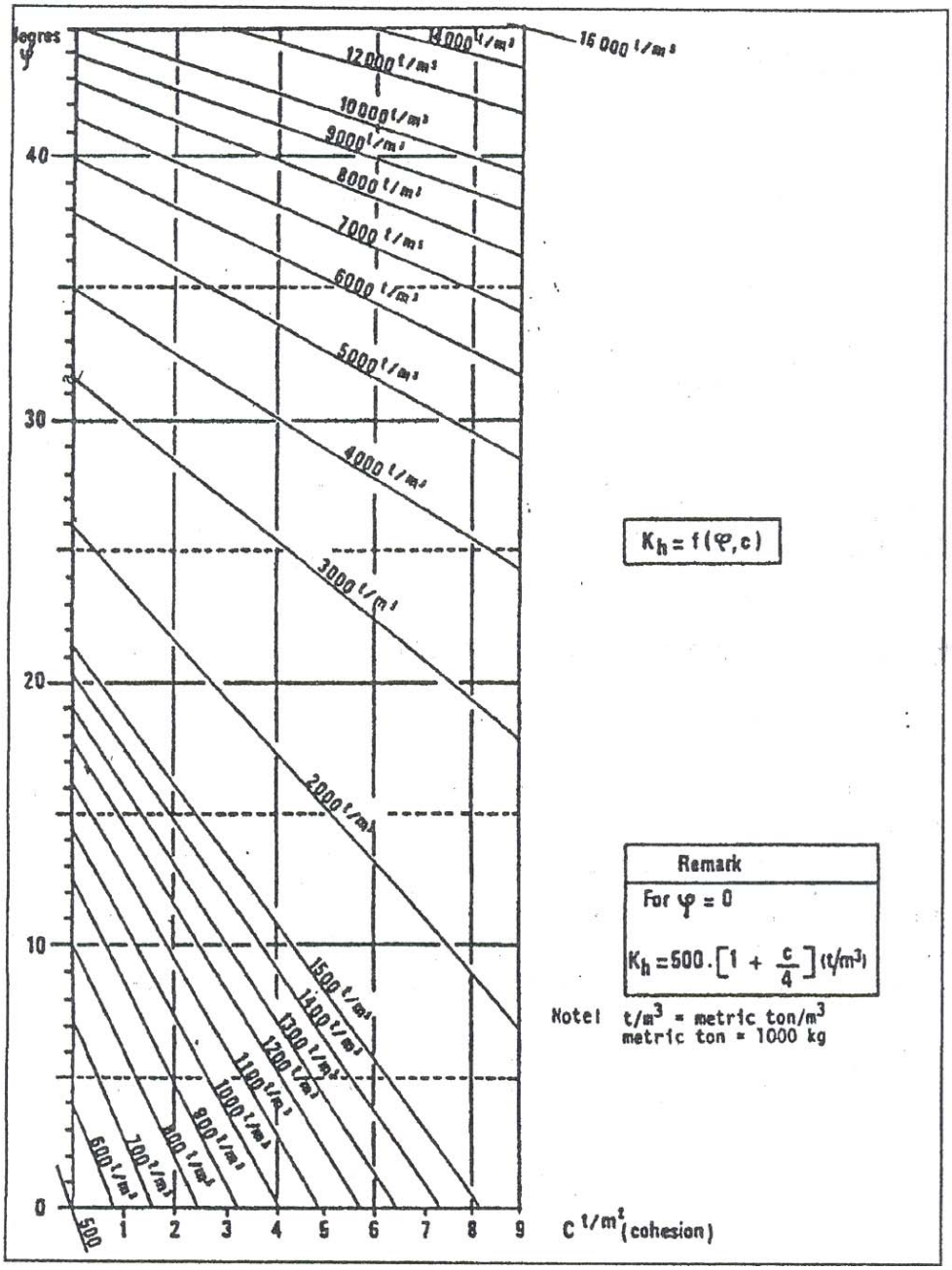

Figure 2.14 Horizontal subgrade moduli, k_h
(after Pfister,Evers, Guillaud, and Davidson 1982)

2.4 Pseudo Finite Element Method

The method is based on the finite element theory for the linear elastic two dimensional plane strain problems. In pseudo-finite element analysis, both the soil and the wall is discretised . The wall is actually modeled by as a

beam elements of zero thickness and the soil as an elastic continuum. The soil stiffness is characterized fairly crudely by means of stiffness of the elastic continuum. The pseudo-finite analysis takes full account of soil either side of and below the wall .The soil pressure between soil and wall is limited by pre-defined active and passive earth pressures (Rankine, Coulomb etc.). Props are generally modelled as springs or point loads and there may be some difficulty in representing real support conditions, especially where moment restraint is provided.

An elastic continuum analysis will calculate wall movements, bending moments and prop loads, but not ground movements around the wall.

Although actual construction sequences can be modeled, it should be stressed that these are approximate, not exact methods or solution. Its relevance to reality depends on the approximate selection of design input parameters. These should be calibrated against reliable field measurements of well monitored comparable excavations and wall systems. Even then, the inherent approximations and the relative simplicity of this method mean that the results obtained are only approximate.

2.5 Finite Element and Finite Difference Method

This category of analysis includes methods which attempt to satisfy all theoretical requirements, include realistic soil constitutive models and incorporate boundary conditions that realistically simulate field conditions. These methods involve full discretisation of both the soil and structural members. Because of the complexities involved and the nonlinearities in soil behaviour, all methods are numerical in nature. Approaches based on finite difference and finite element methods are those most widely used. These methods essentially involve a computer simulation of the history of the boundary value problem from green field conditions, through construction and in the long term.

Their ability to accurately reflect field conditions essentially depends on (i) the ability of the constitutive model to represent real soil behaviour and (ii) correctness of the boundary conditions imposed. The user has only to define the appropriate geometry, construction procedure, soil parameters and boundary conditions.

Structural members may be added and withdrawn during the numerical simulation to model field conditions. Retaining structures composed of several retaining walls, interconnected by structural components, can be considered and, because the soil mass is modelled in the analysis, the complex interaction between raking struts or ground anchors and the soil

can be accounted for. The effect of time on the development of pore water pressures can also be simulated by including coupled consolidation. No postulated failure mechanism or mode of behaviour of the problem is required, as these are predicted by the analysis. The analysis allows the complete history of the boundary value problem to be predicted and a single analysis can provide information on all design requirements.

Full numerical analysis can be used to predict the behaviour of complex field situations. It can also be used to investigate the fundamentals of soil/structure interaction and to calibrate some of the methods discussed above.

Ground movements as well as wall movements, bending moments and prop loads are calculated, but may be of limited value unless a well developed soil constitutive model has been used and the results calibrated against reliable measurements of well monitored comparable excavations and wall systems.

Finite element and finite difference methods are theoretically complete solutions yet are still relatively simple in their modeling of ground behavior. These methods require the user to have significant and specific experience of the particular software package being used and experience of modeling the ground conditions and construction sequence envisaged. It is unlikely that two users of the same software, modeling the same problem, will obtain identical results.

2.6 Requirements of a Complete Solution

To show the mathematical capabilities of the various method of analysis, the requirements of the complete theoretical solution for any mathematical problem is summarized in this section.

In general, an exact complete theoretical solution must satisfy equilibrium, compatibility, the material constitutive behaviour and boundary conditions (both force and displacement). Each of these conditions is defined separately below.

To quantify how forces are transmitted through a continuum engineers use the concept of stress (force/unit area). The magnitude and direction of a stress and the manner in which it varies spatially indicates how the forces are transferred. However, these stresses can not vary randomly but must obey certain rules (Potts and Zdravkovic, 1999). This condition is defined as equilibrium.

Compatible deformation involves no overlapping of material and no generation of holes. The physical meaning of compatibility can be explained by considering a plate composed of smaller plate elements, as shown in Figure 2.15a. After straining, the plate elements may be so distorted that they form the array shown in Figure 2.15b. This condition might represent failure by rupture. Alternatively, deformation might be such that the various

plate elements fit together (i.e. no holes created overlapping) as shown in Figure 2.15c. This condition represents a compatible deformation and satisfies the compatibility condition.

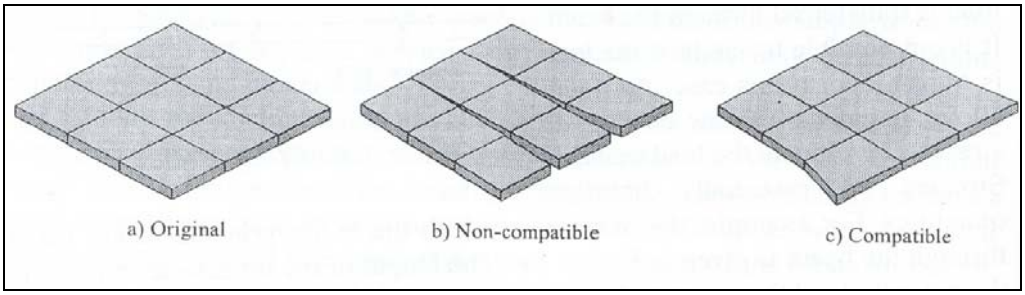

Figure 2.15 Modes of deformation (Potts and Zdravkovic, 1999)

The constitutive behaviour is a description of material behaviour. In simple terms it is the stress–strain behaviour of the soil. It usually takes the form of a relationship between the stresses and strains and therefore provides a link between equilibrium and compatibility.

The term boundary condition is used to cover all possible additional conditions that may be necessary to fully describe a particular problem. These are the load (point loads, line loads, surcharge pressures and body forces) and displacement (prescribed displacements,tied freedoms and springs) conditions which fully define the boundary value problem being analysed.

2.7 Comparison of Methods

As discussed in the previous sections, for a complete theoretical solution equilibrium, compatibility, material constitutive behaviour and boundary conditions shoul be satisfied. The ability of each analysis to satisfy the theoretical solution requirement are summarised in Table 2.4.

As design of the all geotechnical structures, design of embedded retaining walls should consider stability (local and overall), structural forces, deflections of the wall, movements of the adjacent ground, movements and structural forces induced in adjacent structures and/or services, too. The ability of each analysis method to consider these requirements are summarised in Table2.5.

Limit equilibrium method only give information on local stability and structural forces. Subgrade reaction method can provide information on local stability and on wall movements and structural forces. This method is therefore an improvement over the limit equilibrium method. However, they do not provide information on overall stability or on movements in the adjacent soil and the effects on adjacent structures or services. Altough the

same comments for the subgrade reaction method can be mentioned for pseudo finite element method, pseudo finite element method considers the full discretization of the wall and soil either side of and below the wall . Finite element and finite difference methods can provide information on all these requirements. A single analysis can be used to simulate the complete construction history of the retaining structure. In many respects they provide the ultimate method analysis, satisfying all the fundamental requirements. However, they require large amounts of computing resources and an experienced geotechnical designer.The advantages and limitation of each method is summarised in Tables 2.6 and 2.7.

The appropriate method of analysis to use in any given circumstances will depend on factors such as the complexity of the structure and the construction process, the information needed from the calculation, the input data available and the potential economic benefit from refining the analysis. For example, if the wall depth is governed by cut-off requirements or if a sheet pile wall section is governed by considerations of driveability, there may be little benefit in carrying out complex computations. Similarly, there is

little benefit to be obtained by using complex numerical analysis to reduce material costs of walls where there is little or no soil-structure interaction (e.g. cantilever walls).

Table 2.6 and 2.7 summarises the most widely used methods of analysis. Although some appear to give a large amount of design information, the reliability of this depends on the quality and suitability of the input data. Some of the more advanced numerical modelling techniques (finite element and finite difference) can be time consuming to set up and require considerable input data and appropriate operator knowledge and experience, and are unlikely to be cost-effective in the design of a straightforward retaining wall. It is sensible to carry out some simple calculations as a check on more advanced methods. For example, wherever possible, it is prudent to carry out simple limit equilibrium calculations with appropriate simplifying assumptions to obtain a conservative bound before

carrying out complex finite element or finite difference analyses. It is generally better to use a simple analysis with appropriate soil parameters than a complex analysis with inappropriate soil parameters.

Table 2.4 Basic solution requirements satisfied by the various methods of analysis (Potts and Zdravkovic, 1999)

Method of Analysis	Solution Requirement				
	Equilibrium	Compatibility	Constiutive Behaviour	Boundary Conditions	
				Force	Displacement
Limit Equilibrium	S	NS	Rigid with a failure criterion	S	NS
Subgrade Reaction (Winkler) Method	S	S	soil modelled by springs or elastic interaction factors	S	S
Pseudo Finite Element Method	S	S	linear elastic	S	S
Finite Element& Finite Difference Method	S	S	Any	S	S

S : Satisfied NS : Not satisfied

Table 2.5 Design requirements satisfied by the various methods of analysis (Potts and Zdravkovic, 1999)

Method of Analysis	Design Requirements						
	Stability			Wall & Support		Adjacent Structures	
	Wall & Support	Base heave	Overall	Structural force	Displacement	Structural force	Displacement
Limit Equilibrium	S	NS (seperate calculation required)	NS (seperate calculation required)	S	NS	NS	NS
Subgrade-Reaction (Winkler) Method	S	NS (seperate calculation required)	NS (seperate calculation required)	S	S	NS	NS
Pseudo Finite Element Method	S	NS (seperate calculation required)	NS (seperate calculation required)	S	S	NS	NS
Finite Element & Finite Difference Method	S	S	S	S	S	S	S

S : Satisfied NS : Not satisfied

Table2.6 Advantages and limitations of common methods of retaining wall analysis (Powrie, 2003)

Type of Analysis / Softwares	Advantages	Limitations
Limit Equilibrium e.g. Stawal Reward	- Needs only the soil strength - Simple and straightforward	- does not model soil-structure interaction - does not calculate deformations. Hand calculations of deformations possible by relating mobilised strength, soil shear strain and wall rotation (rarely done); or through empirical databases - statically indeterminate systems (e.g. multi-propped walls), non-uniform surcharges and berms require considerable idealisation - can model only drained (effective stress) or undrained (total stress) conditions - two dimensional only - results take no account of pre-excavation stress state
Subgrade Reaction e.g. Wallap	- full soil - structure interaction analysis is possible, modelling construction sequence, etc. - soil modelled as a bed of elastic springs - soil structure interaction taken into account - wall movements are calculated -relatively straightforward - results take account of pre excavation stress state	- idealisation of soil behaviour is likely to be crude - subgrade moduli can be difficult to assess - two dimensional only - berms and certain structural connections are difficult to model - global effects not modelled explicitly - ground movements around wall are not calculated

Table2.7 Advantages and limitations of common methods of retaining wall analysis (Powrie, 2003)

Type of Analysis / Softwares	Advantages	Limitations
Pseudo Finite Element Method e.g. Frew Wallap	- full soil structure interaction analysis is possible, modelling construction sequence, etc. - soil modelled as an elastic solid with soil stiffness matrices calculated using a finite element program - soil-structure interaction taken into account - wall movements are calculated -relatively straightforward - takes account of pre-excavation stress state	- two dimensional only - limited to linear elastic soil model, with active and passive limits - berms and certain structural connections are difficult to model - global effects not modelled explicitly - ground movements around wall are not calculated
Finite Element and Finite Difference method e.g. Safe Plaxis Crisp Flac Abaqous Dyna	- full soil-structure interaction analysis is possible, modelling construction sequence etc. - complex soil models can represent variation of stiffness with strain and anisotropy - takes account of pre-excavation stress state -can model complex wall and excavation geometry including structural and support details - wall and ground movements are computed -potentially good representation of pore water response - can model consolidation as soil moves from undrained to drained conditions - can carry out two-dimensional or three dimensional analyses	- can be time consuming to set up and difficult to model certain aspects, e.g. wall installation - quality of results dependent on availability of appropriate stress strain models for the ground - extensive high quality data (e.g. pre-excavation lateral stresses as well as soil stiffness and strength) needed to obtain most representative results - simple (linear elastic) soil model may give unrealistic ground movements - structural characterisation of many geotechnical finite element and finite difference packages may be crude - significant software – specific experience required by user - basic representation of pore water response

CHAPTER 3

ANALYSIS MADE BY DIFFERENT METHODS

3.1 Properties of the Wall Analysed

A single propped tangent pile embedded wall (Figure 3.1) in a deep normally consolidated cohesionless sand deposit is analysed with various soil parameters and wall types by limit equilibrium, subgrade reaction, pseudo-finite and finite element methods. The excavation width is 12 m and retained height h is 8 m. The wall is supported by a single strut at 2 m below the top (-2.00 level) with a center to center spacing of 5 m in horizontal direction.

The penetration depth of the wall d (the wall toe level) is determined by limit equilibrium method analysis. This wall depth is used in calculating structural forces by other methods, i.e. subgrade, pseudo finite and finite element method analysis.

The limiting earth pressures (active-passive) in limit equilibrium method are determined according to the Caquot&Kerisel (the wall/soil friction is taken as 0.67ϕ on the active side and 0.50ϕ on the passive side). The calculated limiting earth pressures for each soil type are given in Table 3.1. Depth of embedment values are calculated with a safety factor of 1.5 with respect to the gross pressures assuming free earth support condition.The calculated wall toe levels and strut forces and wall internal forces are listed in Table 3.2.

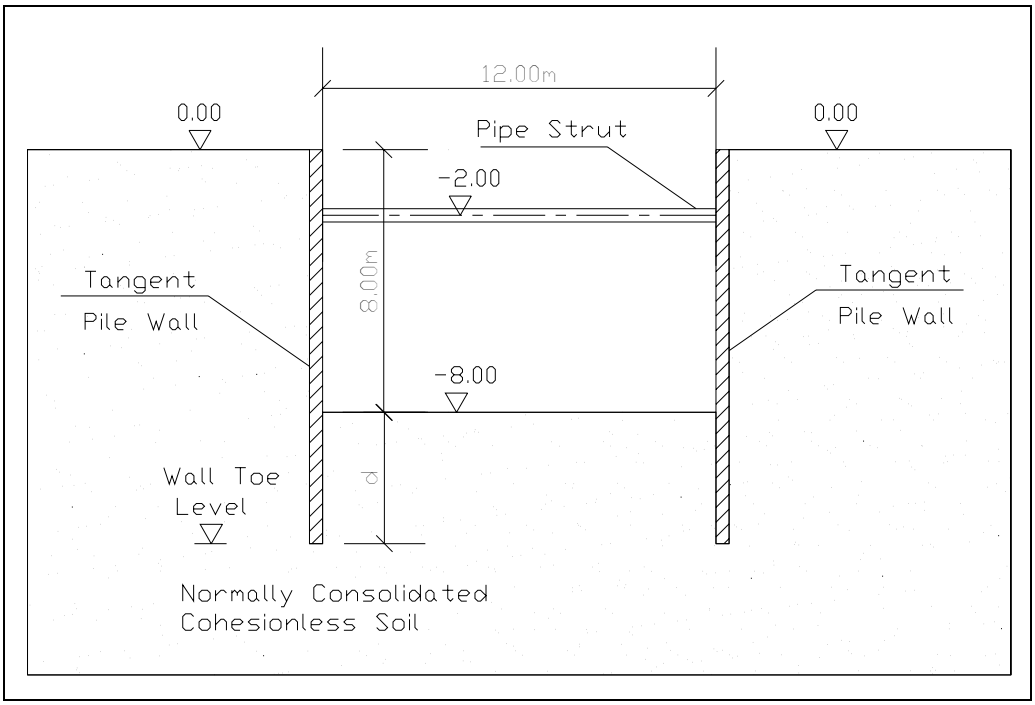

Figure 3.1 Analysed wall geometry

Table 3.1 Soil types limiting earth pressure coefficients

NAME	K_a	K_p
SOIL1A	0.285	4.288
SOIL1B		
SOIL1C		
SOIL2A	0.229	5.879
SOIL2B		
SOIL2C		
SOIL3A	0.182	8.378
SOIL3B		
SOIL3C		

Table 3.2 Summary of limit equilibrium analysis

NAME	Wall Toe Level	Strut Load (kN/m)	Wall Shear Force at strut level (kN / m)	Wall Stem Maximum Shear Force (kN / m)	Bending Moment at prop level (kNm/m)	Wall Stem Maximum Bending Moment (kNm/m)
SOIL1A	-11.00	92.31	83.78	81.77	6.84	191.48
SOIL1B						
SOIL1C						
SOIL2A	-10.00	68.51	62.36	66.36	5.50	134.24
SOIL2B						
SOIL2C						
SOIL3A	-9.50	52.67	46.73	53.84	4.37	95.93
SOIL3B						
SOIL3C						

3.1.1 Soil Parameters

The representative value of the bulk unit weight of the soil is considered as 18 kN/m^3. The coefficient of earth pressure at rest is determined according to the Jacky's formula (1 - sinϕ).

Analyses are carried out for three values of internal friction angle, i.e. $\phi=30^0$, 35^0, and 40^0 . In order to estimate elastic moduli corresponding these friction angles, it is assumed that average SPT blow counts are $N_{60}=10$, $N_{60}=24$ and $N_{60}=46$ for $\phi=30^0$, 35^0, and 40^0 respectively (Peck,1974, modified by Carter&Bertley 1991.). The range of elastic moduli of the backfill, E_{soil}, are assessed from the following relationships.

E_{soil} = 500 x (N_{60}+15) (Tan et al 1991)

E_{soil} = (15000 to 22000) ln (N_{60}) (Bowles, 1988)

Angle of dilation is estimated from:

$\psi=\phi$-30

As suggested by PLAXIS computer program manual

The minimum and maximum deformation moduli for each N_{60} SPT blow count value are taken into account and three different (minimum, maximum and intermediate) deformation moduli are assigned for each value of ϕ. Poissons ratio is taken as 0.25 for all soil types.

A list of the soil types considered in the analyses together with relevant soil parameters are as given in Table 3.3.

Table 3.3 Soil types and parameters

NAME	N_{60}	ϕ	ψ	K_0	ν	E_{soil} (kPa)
SOIL1A	10	30	0	0.500	0.25	12500
SOIL1B	10	30	0	0.500	0.25	23500
SOIL1C	10	30	0	0.500	0.25	34500
SOIL2A	24	35	5	0.426	0.25	19500
SOIL2B	24	35	5	0.426	0.25	33585
SOIL2C	24	35	5	0.426	0.25	47670
SOIL3A	46	40	10	0.357	0.25	30500
SOIL3B	46	40	10	0.357	0.25	57365
SOIL3C	46	40	10	0.357	0.25	84230

3.1.2 Wall Properties

The wall is assumed to consist of tangent piles. Three different pile diameters are taken into account for each soil and wall type.
The concrete class is taken as C20. The material properties for C20 concrete class are as follows:

E_{conc} = 28000 MPa

γ_{conc} = 25 kN / m^3 (for PLAXIS analysis)

ν = 0.10 (for PLAXIS analysis)

Soil/wall friction angle, δ, is taken as δ=0.67ϕ.

The list of the wall types considered in the analysis are as given in Table 3.4.

Table 3.4 Wall types and properties

NAME	Diameter	δ
WALL1	650 mm	0.67ϕ
WALL2	800 mm	0.67ϕ
WALL3	1000 mm	0.67ϕ

3.1.3 Strut Properties

The ST37 class steel pipe struts are included in the analysis. The Young's modulus of steel is taken as $2.1x10^8$ kPa . The pipe strut having a outer diameter of 323.9 mm and thickness of 16 mm are adopted in the subgrade reaction, pseudo finite and finite element analysis. The dimension of the pipe strut is determined considering the maximum strut load obtained from the limit equilibrium analysis considering the lateral buckling and capacity ratio of the steel elements.

3.2 Analysis Cases

A summary of the cases studied are presented in Table 3.5.

3.3 Stages of Analysis

For all the cases investigated, construction stages are considered. The following steps are included in the analysis:

1^{st} step : excavate to -2.00 level (strut level)
2^{nd} step : install strut
3^{rd} step : excavate to -8.00 level (final excavation level)

Table 3.5 A summary of the cases studied

NAME	SOIL TYPE	WALL TYPE	WALL TOE LEVEL
CASE1	SOIL1A	WALL1	-11.00
CASE2	SOIL1B	WALL1	-11.00
CASE3	SOIL1C	WALL1	-11.00
CASE4	SOIL2A	WALL1	-10.00
CASE5	SOIL2B	WALL1	-10.00
CASE6	SOIL2C	WALL1	-10.00
CASE7	SOIL3A	WALL1	-9.50
CASE8	SOIL3B	WALL1	-9.50
CASE9	SOIL3C	WALL1	-9.50
CASE10	SOIL1A	WALL2	-11.00
CASE11	SOIL1B	WALL2	-11.00
CASE12	SOIL1C	WALL2	-11.00
CASE13	SOIL2A	WALL2	-10.00
CASE14	SOIL2B	WALL2	-10.00
CASE15	SOIL2C	WALL2	-10.00
CASE16	SOIL3A	WALL2	-9.50
CASE17	SOIL3B	WALL2	-9.50
CASE18	SOIL3C	WALL2	-9.50
CASE19	SOIL1A	WALL3	-11.00
CASE20	SOIL1B	WALL3	-11.00
CASE21	SOIL1C	WALL3	-11.00
CASE22	SOIL2A	WALL3	-10.00
CASE23	SOIL2B	WALL3	-10.00
CASE24	SOIL2C	WALL3	-10.00
CASE25	SOIL3A	WALL3	-9.50
CASE26	SOIL3B	WALL3	-9.50
CASE27	SOIL3C	WALL3	-9.50

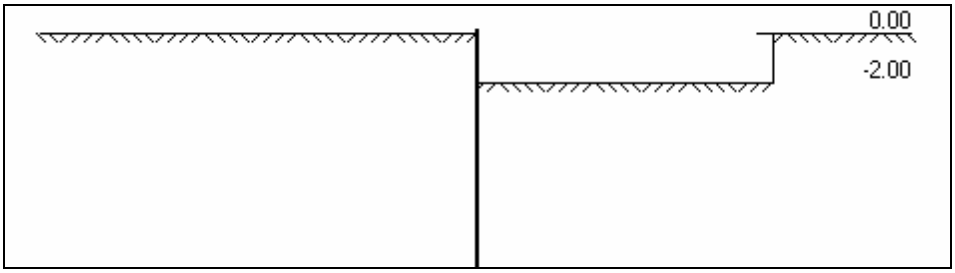

Figure 3.2 Stage1

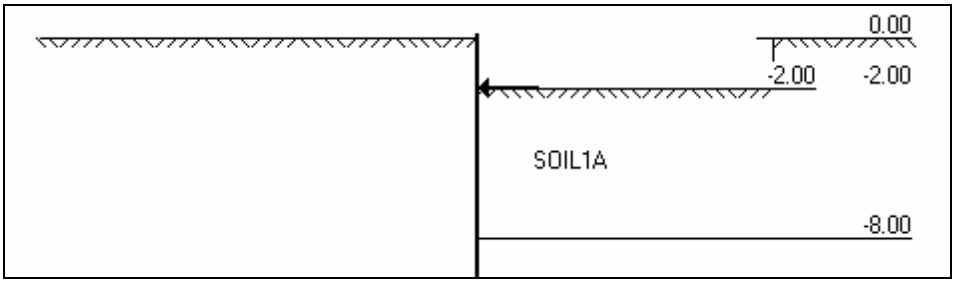

Figure 3.3 Stage 2

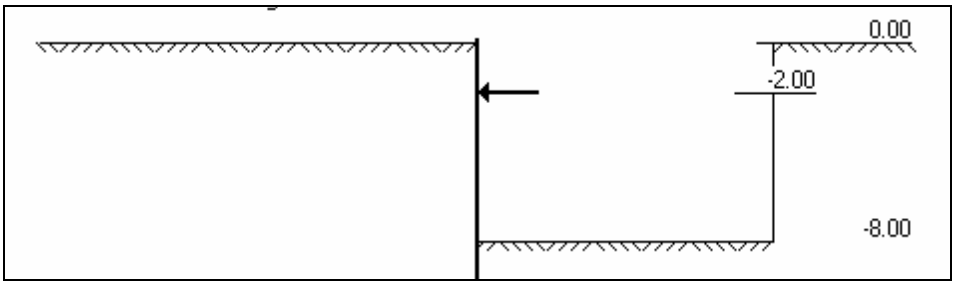

Figure 3.4 Stage 3

CHAPTER 4

RESULTS OF ANALYSIS

4.1 General Considerations

The 27 cases defined in the section 3.2 are analysed by soil structure interaction methods (subgrade reaction method, pseudo finite element method and finite element method) using WALLAP and PLAXIS softwares. Total 81 numbers of analysis are performed.

The structural forces obtained from the analysis are examined by Young's modulus of soil, wall flexural rigidity and method of analysis.

The strut loads and maximum wall internal forces at prop level and wall stem (Figure 4.1 and Figure 4.2) obtained from these analyses are normalised with respect to the limit equilibrium analyses results as defined in equations 4.1, 4.2 and 4.3 below. The calculated and normalised quantities of the structural forces are represented both tabularly and graphically in the sections 4.2, 4.3 and 4.4.

$$N.S.L. = P_{SSI} / P_{LEQ} \qquad (4.1)$$

N.S.L. : normalised strut load

P_{SSI} : strut load obtained from the subgrade reaction, pseudo finite and finite element methods

P_{LEQ} : strut load obtained from the limit equilibrium analysis

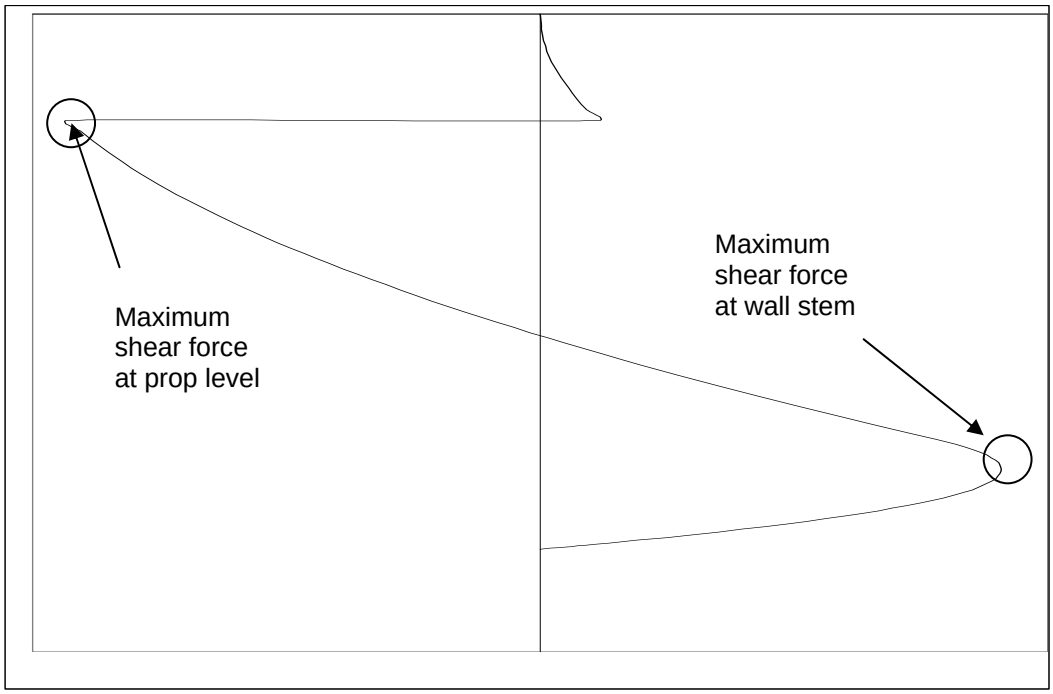

Figure 4.1 Peak shear forces considered in the analysis

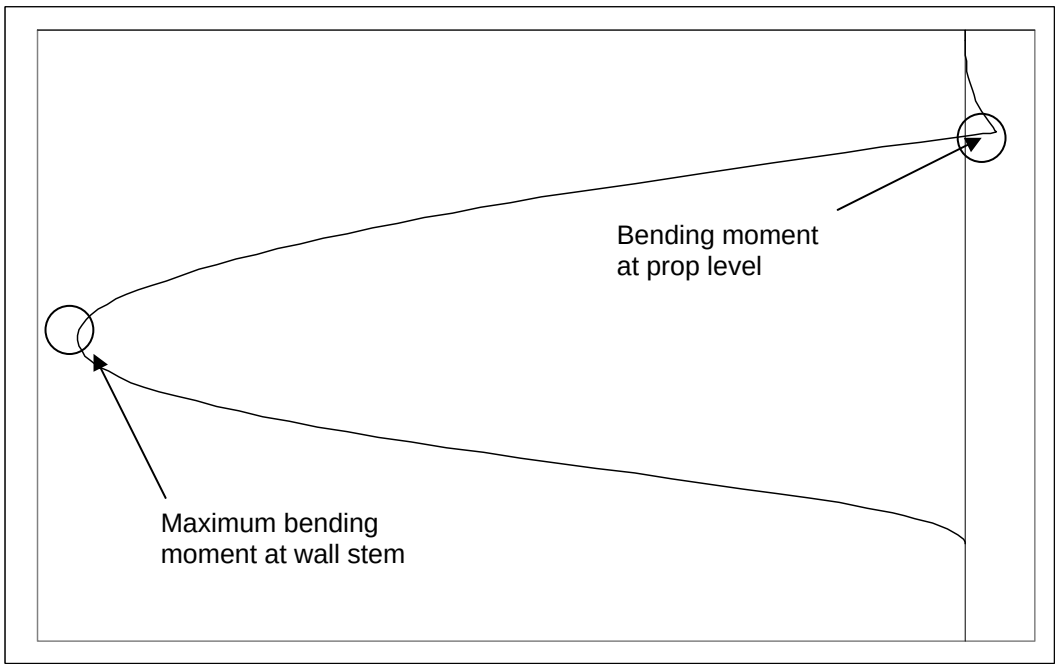

Figure 4.2 Peak bending moments considered in the analysis

$N.B.M. = M_{SSI} / M_{LEQ}$ (4.2)

N.B.M. : normalised bending moment

M_{SSI} : bending moment obtained from the subgrade reaction, pseudo finite and finite element methods

M_{LEQ} : bending moment obtained from the limit equilibrium analysis

$N.S.F. = V_{SSI} / V_{LEQ}$ (4.3)

N.S.F. : normalised shear force

V_{SSI} : shear force obtained from the subgrade reaction, pseudo finite and finite element methods

V_{LEQ} : shear force obtained from the limit equilibrium analysis

4.2 Strut Loads

The strut loads obtained from the analysis and normalised strut loads are represented in Table 4.1 and Table 4.2. The variation of normalised strut loads are plotted for varying soil Young's modulus (at a constant wall flexural rigidity) and for varying wall flexural rigidity (at a constant soil Young's modulus).

Effect of E_{soil} on strut loads (Figures 4.3 – 4.11):

For all of the analysis cases and internal friction angle values of 30^o, 35^o, and 40^o normalized strut loads decrease as Young's modulus increases.

Effect of EI_{wall} on strut loads (Figures 4.12–4.20):

It is observed that for all of the wall configurations and soil friction angle values, normalised strut loads increase as the wall flexural rigidity, EI_{wall}, increases. This is due to the fact that stiffer wall does not deflect much as compared to less stiff system, which results in higher strut loads.

Effect of method of analysis on strut loads (Figures 4.21– 4.23):

As seen from figures through Figure 4.21– 4.23, maximum strut load in each case is obtained in finite element method while the minimum prop load is obtained in subgrade reaction.

In $\phi=30^0$ group analysis cases (CASE1-2-3-10-11-12-19-20-21), the maximum normalised strut loads of 1.13, 1.207 and 1.325 are obtained in subgrade reaction method, pseudo finite element method and finite element method respectively.

In $\phi=35^0$ group analysis cases (CASE4-5-6-13-14-15-22-23-24), the maximum normalised strut loads of 1.08, 1.13 and 1.30 are obtained in subgrade reaction method, pseudo finite element method and finite element method respectively.

In $\phi=40^0$ group analysis cases (CASE7-8-9-16-17-18-25-26-27), the maximum normalised strut loads of 1.07, 1.14 and 1.24 are obtained in subgrade reaction method, pseudo finite element method and finite element method respectively.

Table 4.1 Summary of strut loads obtained from the analysis (kN/m)

CASE NAME	Subgrade Reaction	Pseudo Finite	Finite Element
CASE1	101.32	111.89	114.41
CASE2	98.87	104	110.67
CASE3	97.42	100.49	106.44
CASE4	74.18	80.06	85.65
CASE5	73.07	75.54	81.89
CASE6	73.73	73.36	78.97
CASE7	55.74	60.54	61.31
CASE8	55.05	55.63	59.51
CASE9	54.8	55.06	57.65
CASE10	103.32	111.18	120.05
CASE11	100.39	101.33	114.15
CASE12	98.52	99.37	111.12
CASE13	75.2	77.12	88.54
CASE14	73.63	74.34	84.61
CASE15	72.9	73.87	80.53
CASE16	56.1	57.52	64.38
CASE17	55.33	56.09	60.22
CASE18	54.95	55.39	57.80
CASE19	106.42	113.5	124.62
CASE20	103	104.04	119.82
CASE21	100.95	101.29	114.21
CASE22	76.5	77.28	92.01
CASE23	74.77	75.01	89.25
CASE24	73.73	74.34	84.28
CASE25	56.75	57.02	66.26
CASE26	55.67	56.36	62.68
CASE27	55.06	55.74	59.51

Table 4.2 Summary of normalised strut loads

CASE NAME	Subgrade Reaction	Pseudo Finite	Finite Element
CASE1	1.077	1.190	1.217
CASE2	1.051	1.106	1.177
CASE3	1.036	1.069	1.132
CASE4	1.051	1.134	1.213
CASE5	1.035	1.070	1.160
CASE6	1.044	1.039	1.119
CASE7	1.046	1.136	1.151
CASE8	1.033	1.044	1.117
CASE9	1.029	1.033	1.082
CASE10	1.099	1.182	1.277
CASE11	1.068	1.078	1.214
CASE12	1.048	1.057	1.182
CASE13	1.065	1.092	1.254
CASE14	1.043	1.053	1.199
CASE15	1.033	1.046	1.141
CASE16	1.053	1.080	1.208
CASE17	1.038	1.053	1.130
CASE18	1.031	1.040	1.085
CASE19	1.132	1.207	1.325
CASE20	1.095	1.106	1.274
CASE21	1.073	1.077	1.215
CASE22	1.084	1.095	1.303
CASE23	1.059	1.062	1.264
CASE24	1.044	1.053	1.194
CASE25	1.065	1.070	1.244
CASE26	1.045	1.058	1.176
CASE27	1.033	1.046	1.117

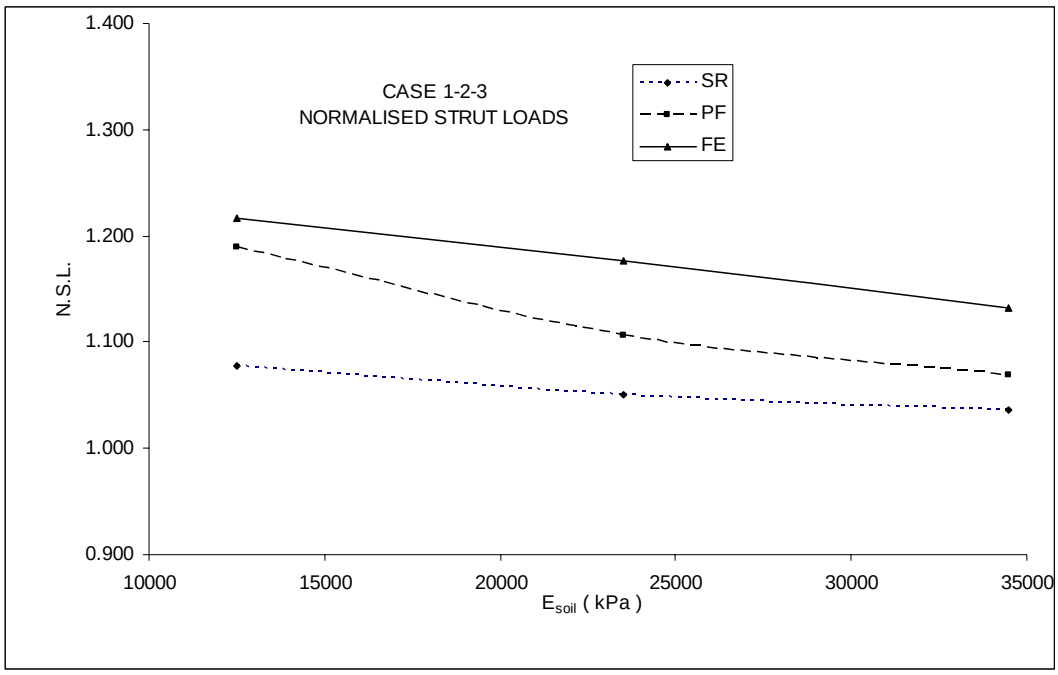

Figure 4.3 Normalised strut loads vs E_{soil}

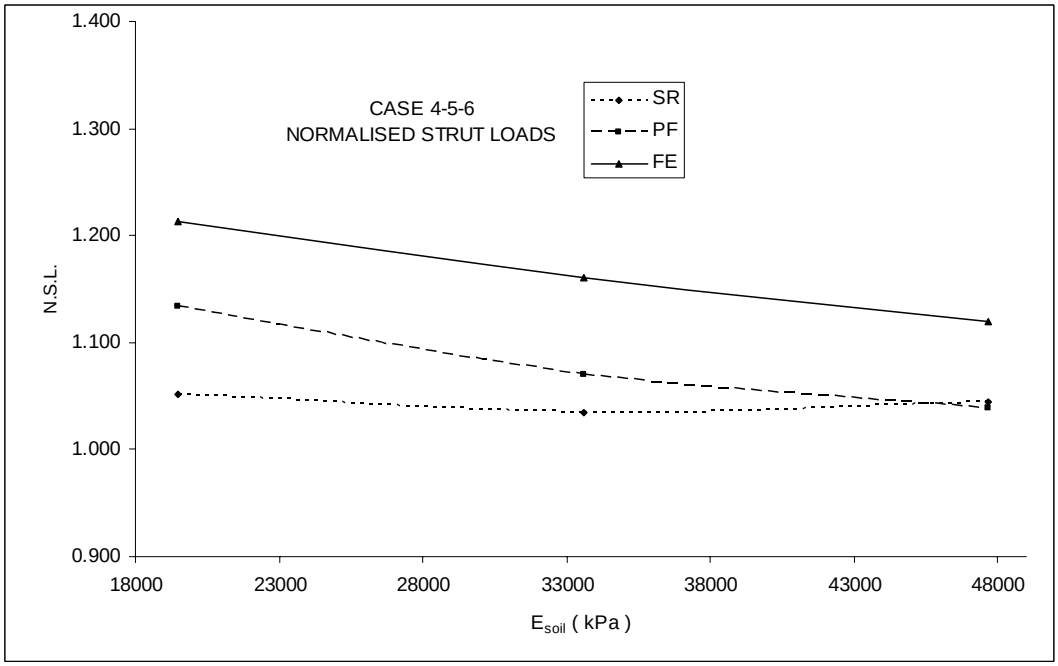

Figure 4.4 Normalised strut loads vs E_{soil}

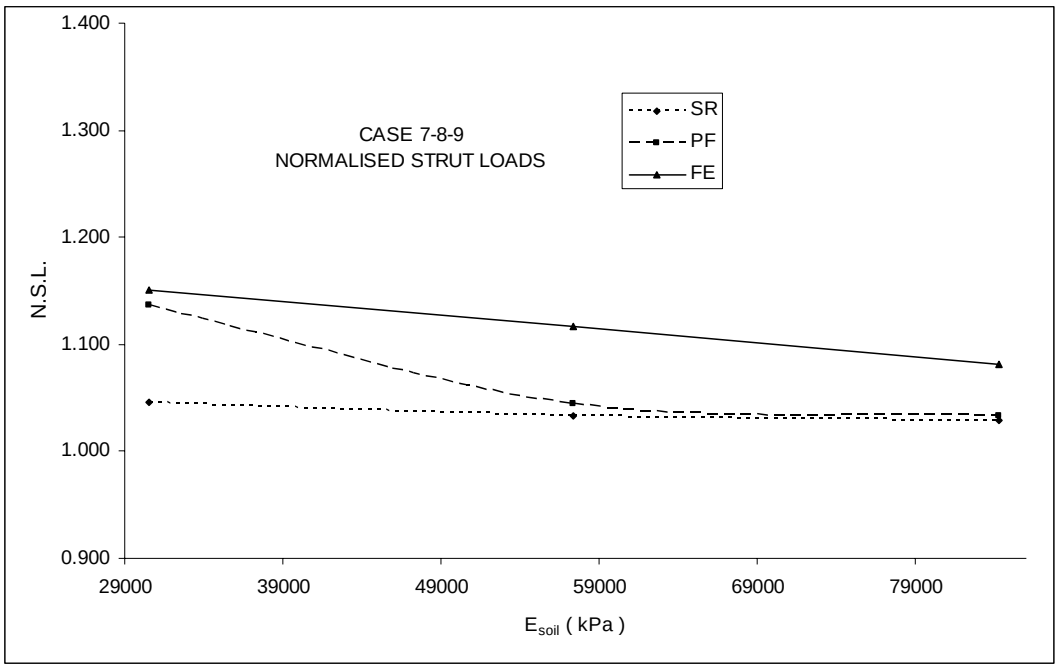

Figure 4.5 Normalised strut loads vs E_{soil}

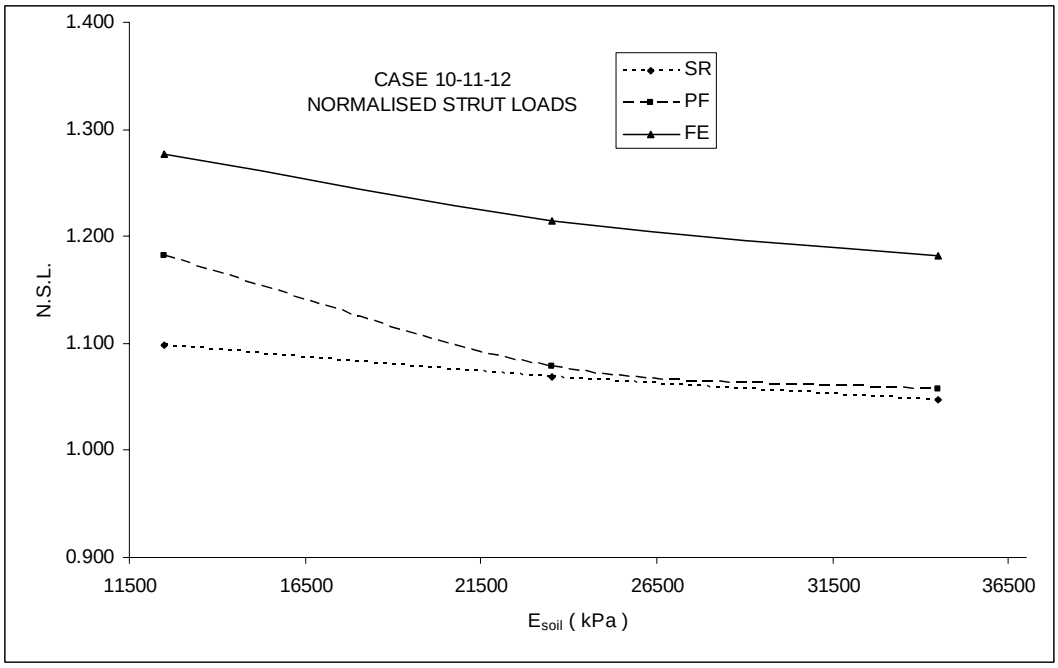

Figure 4.6 Normalised strut loads vs E_{soil}

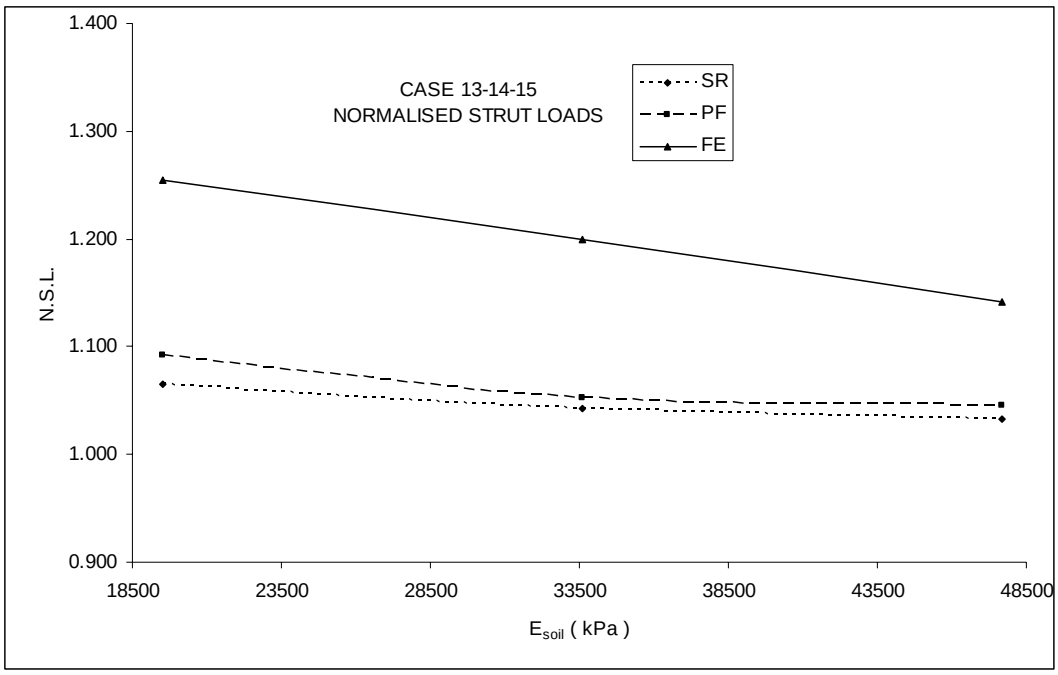

Figure 4.7 Normalised strut loads vs E_{soil}

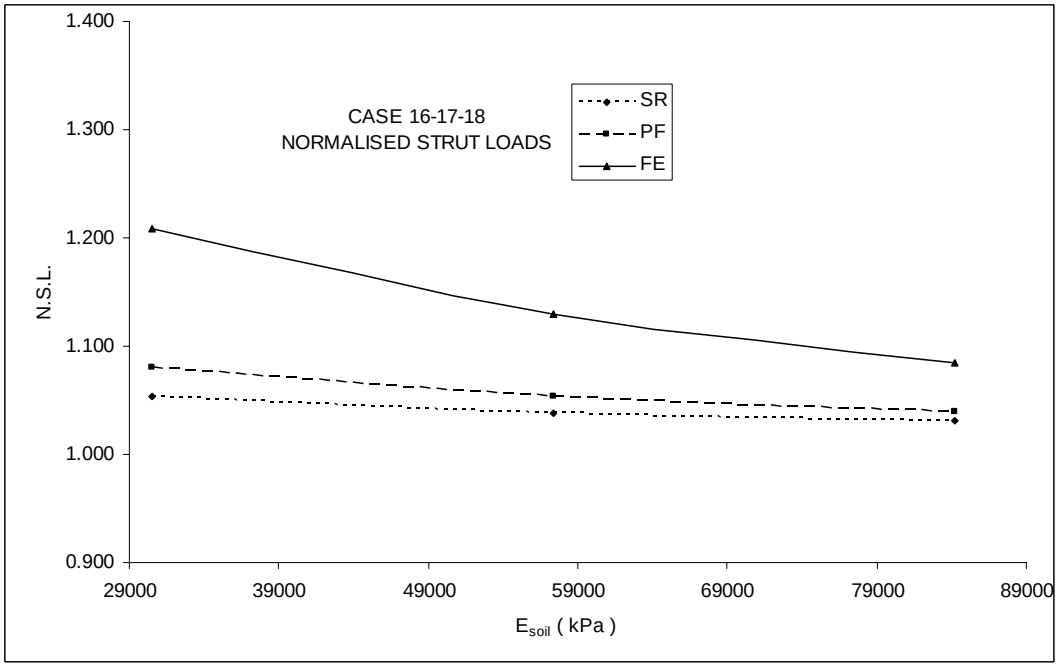

Figure 4.8 Normalised strut loads vs E_{soil}

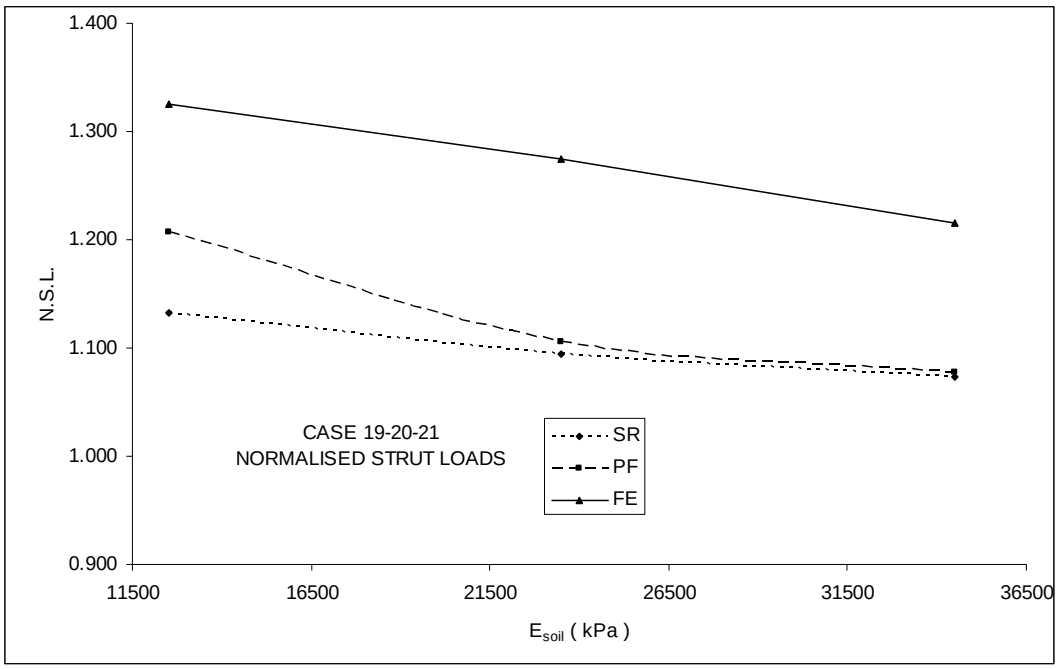

Figure 4.9 Normalised strut loads vs E_{soil}

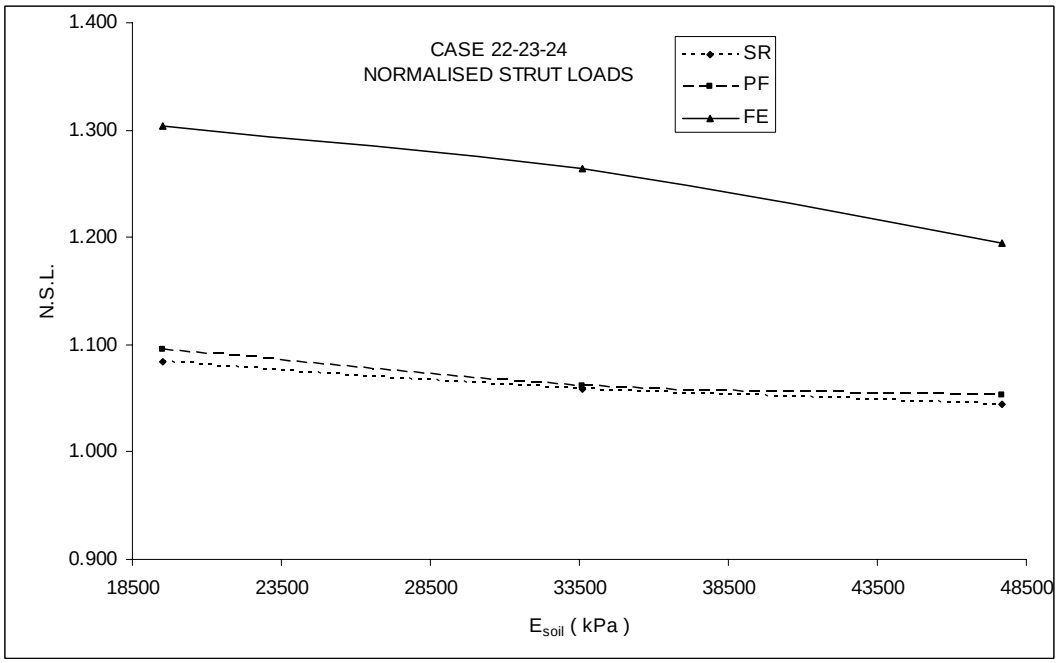

Figure 4.10 Normalised strut loads vs E_{soil}

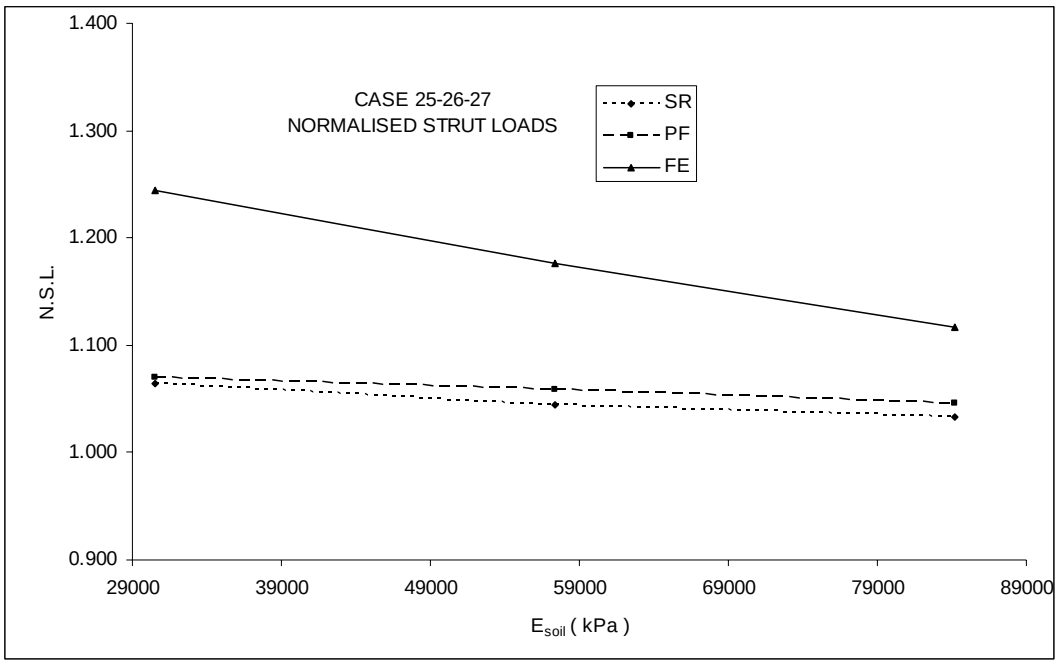

Figure 4.11 Normalised strut loads vs E_{soil}

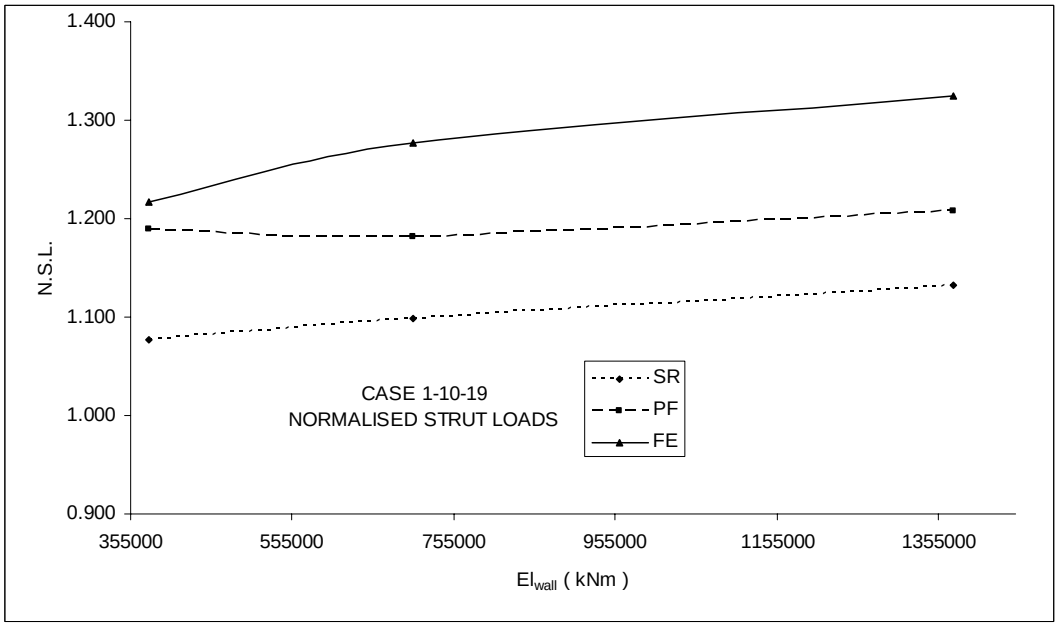

Figure 4.12 Normalised strut loads vs EI_{wall}

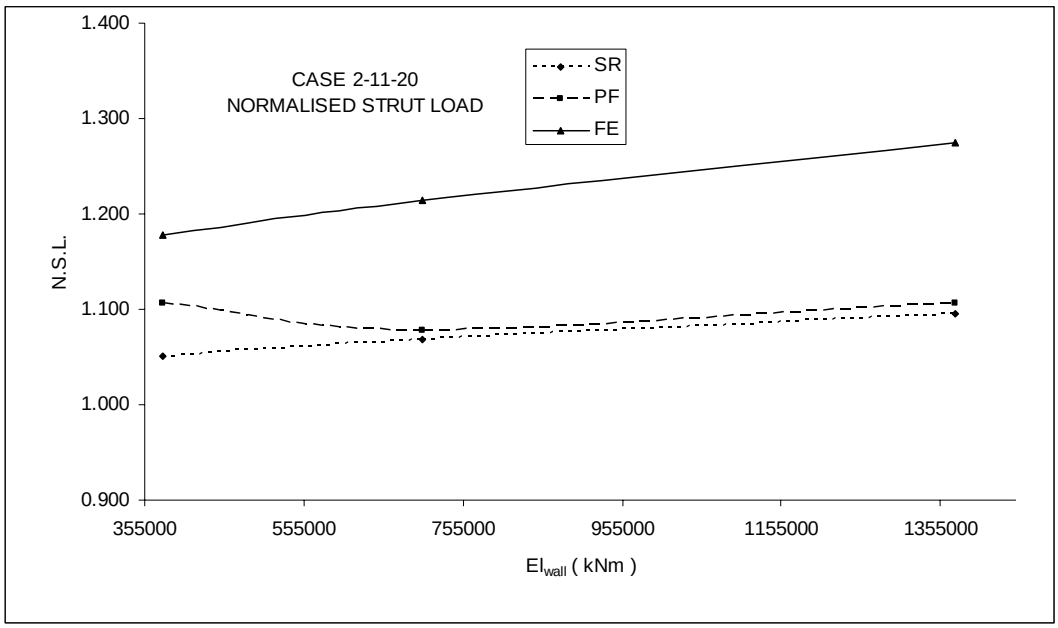

Figure 4.13 - Normalised strut loads vs EI_{wall}

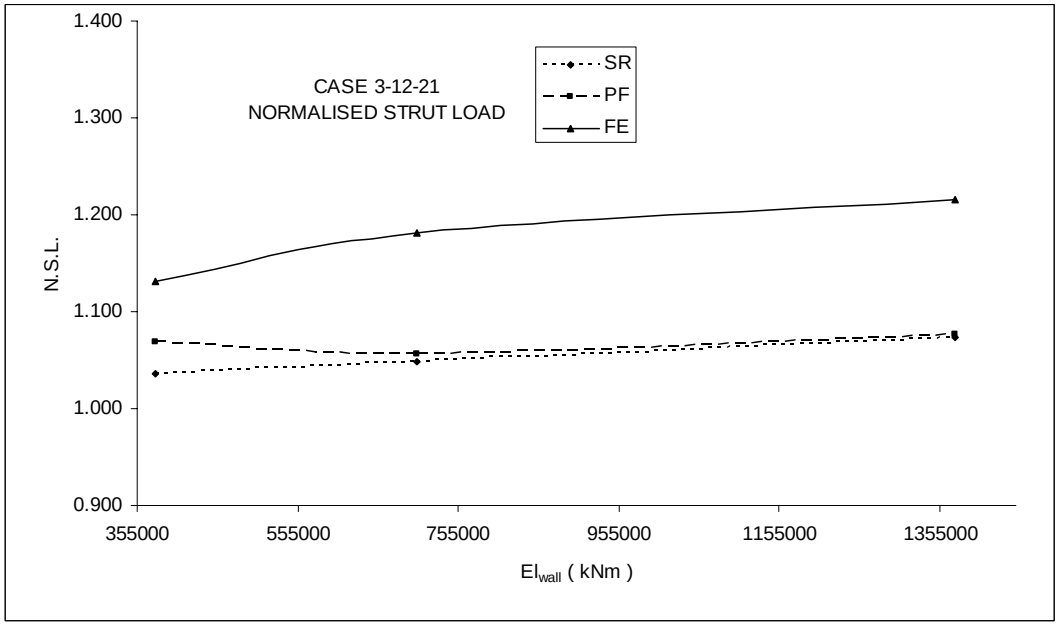

Figure 4.14 - Normalised strut loads vs EI_{wall}

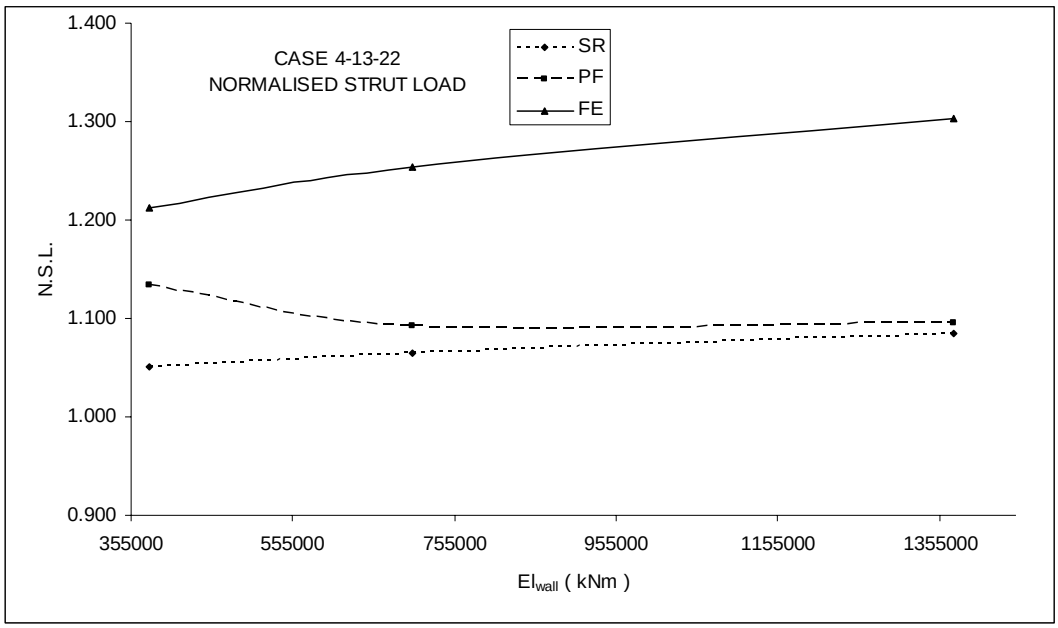

Figure 4.15 - Normalised strut loads vs EI_{wall}

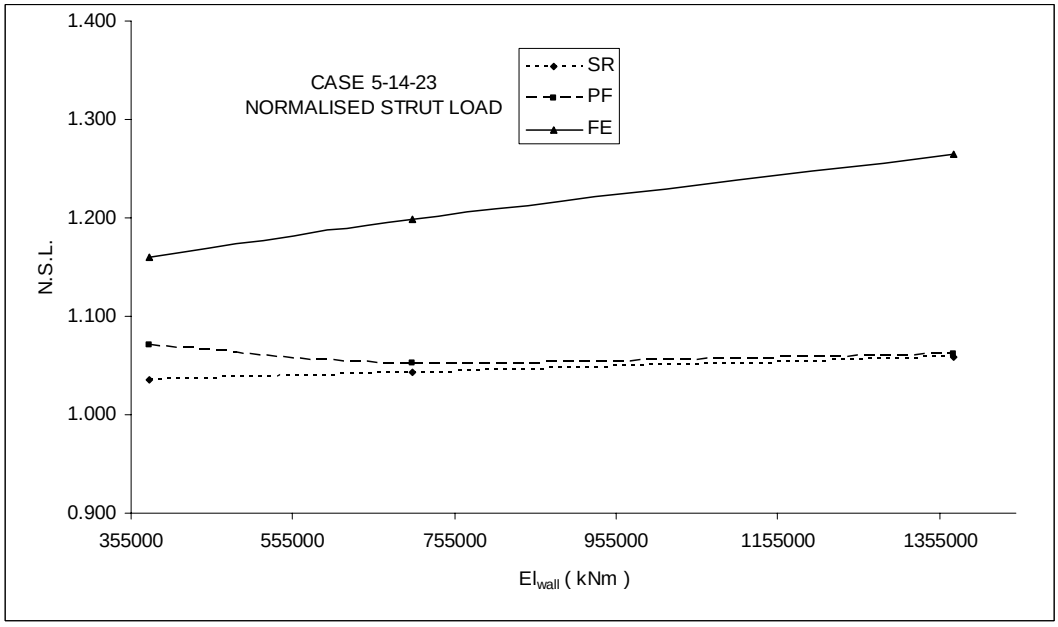

Figure 4.16 Normalised strut loads vs EI_{wall}

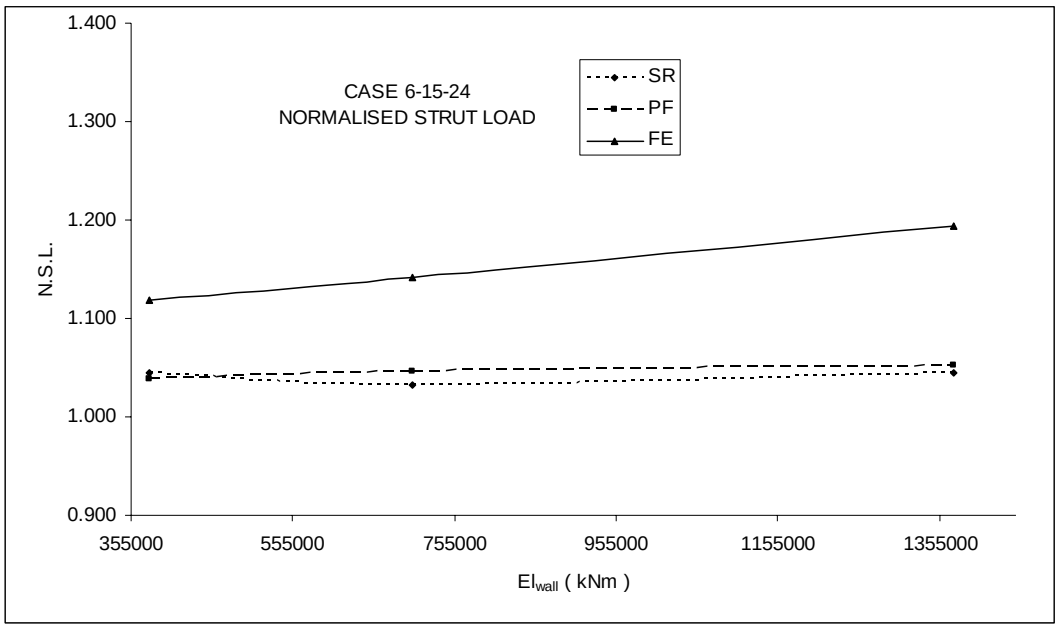

Figure 4.17 Normalised strut loads vs EI_{wall}

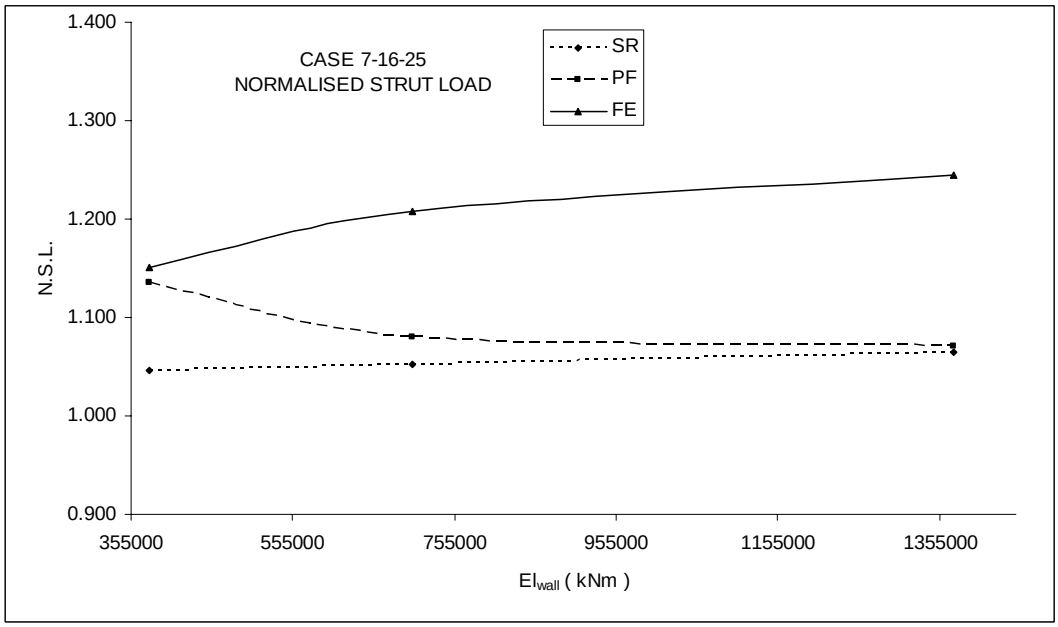

Figure 4.18 Normalised strut loads vs EI_{wall}

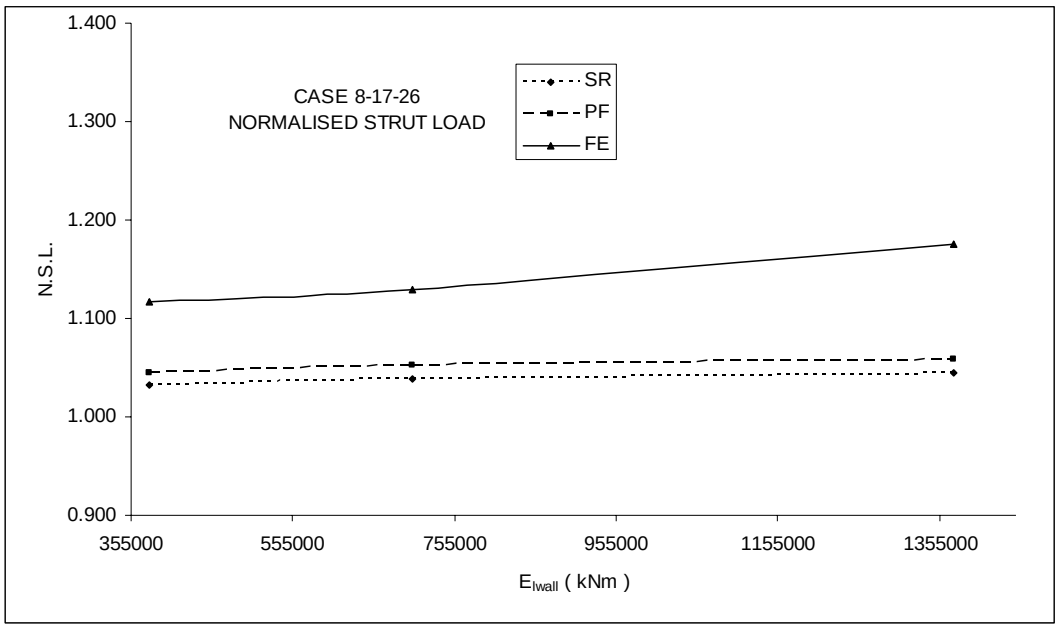

Figure 4.19 Normalised strut loads vs EI_{wall}

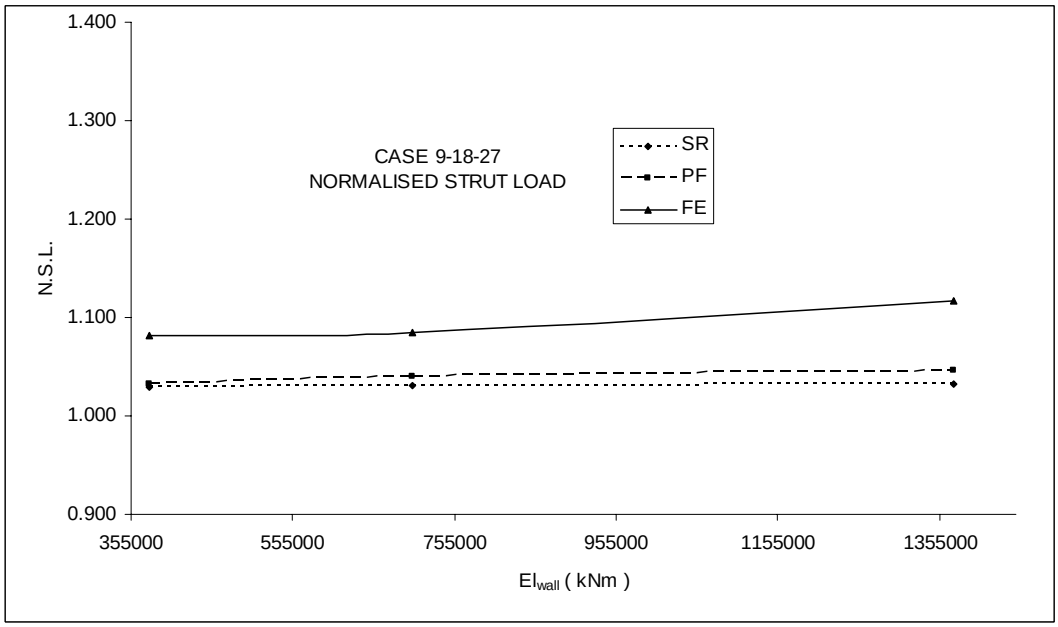

Figure 4.20 Normalised strut loads vs EI_{wall}

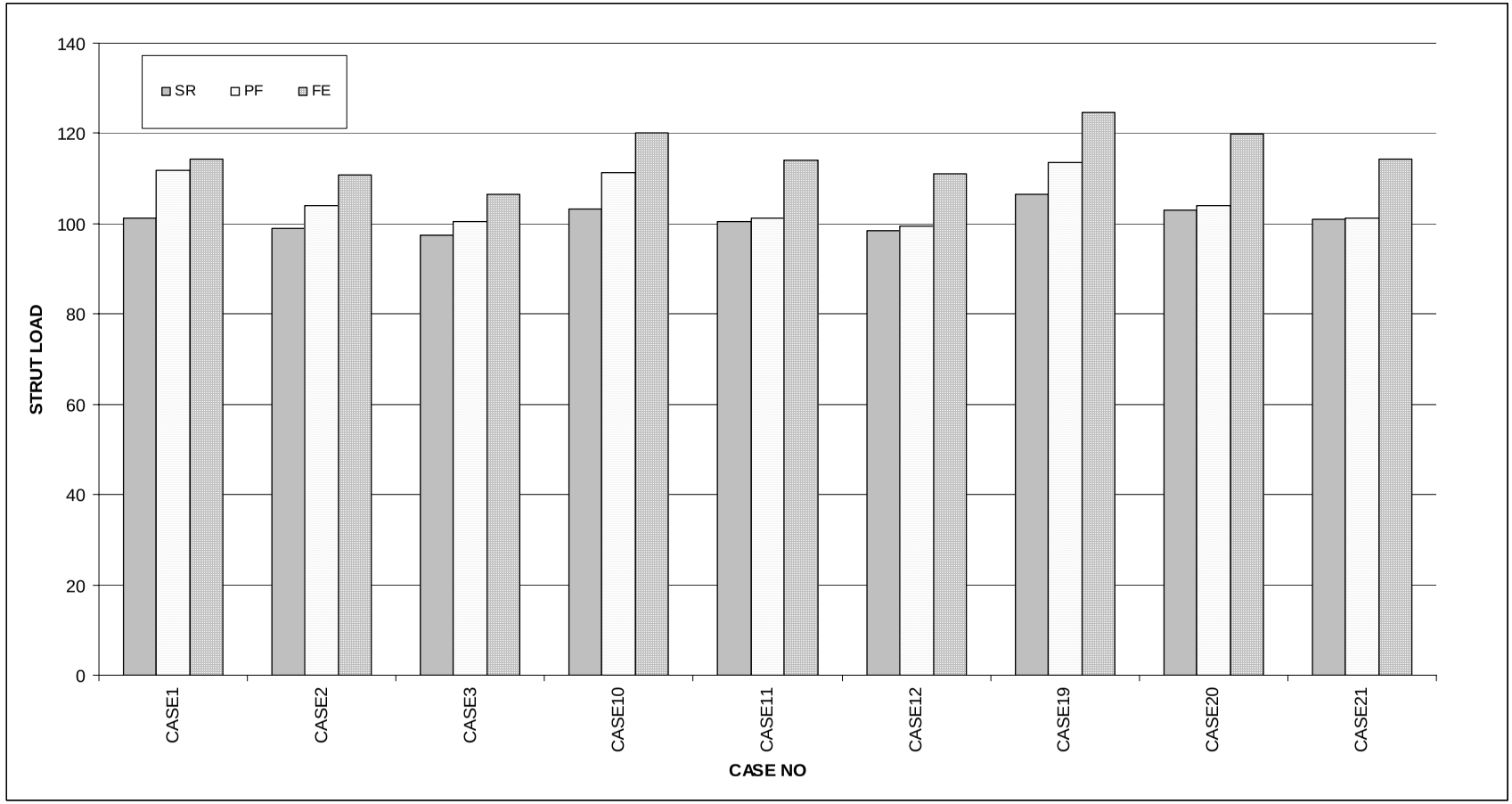

Figure 4.21 CASE 1-2-3-10-11-12-19-20-21 strut loads (kN)

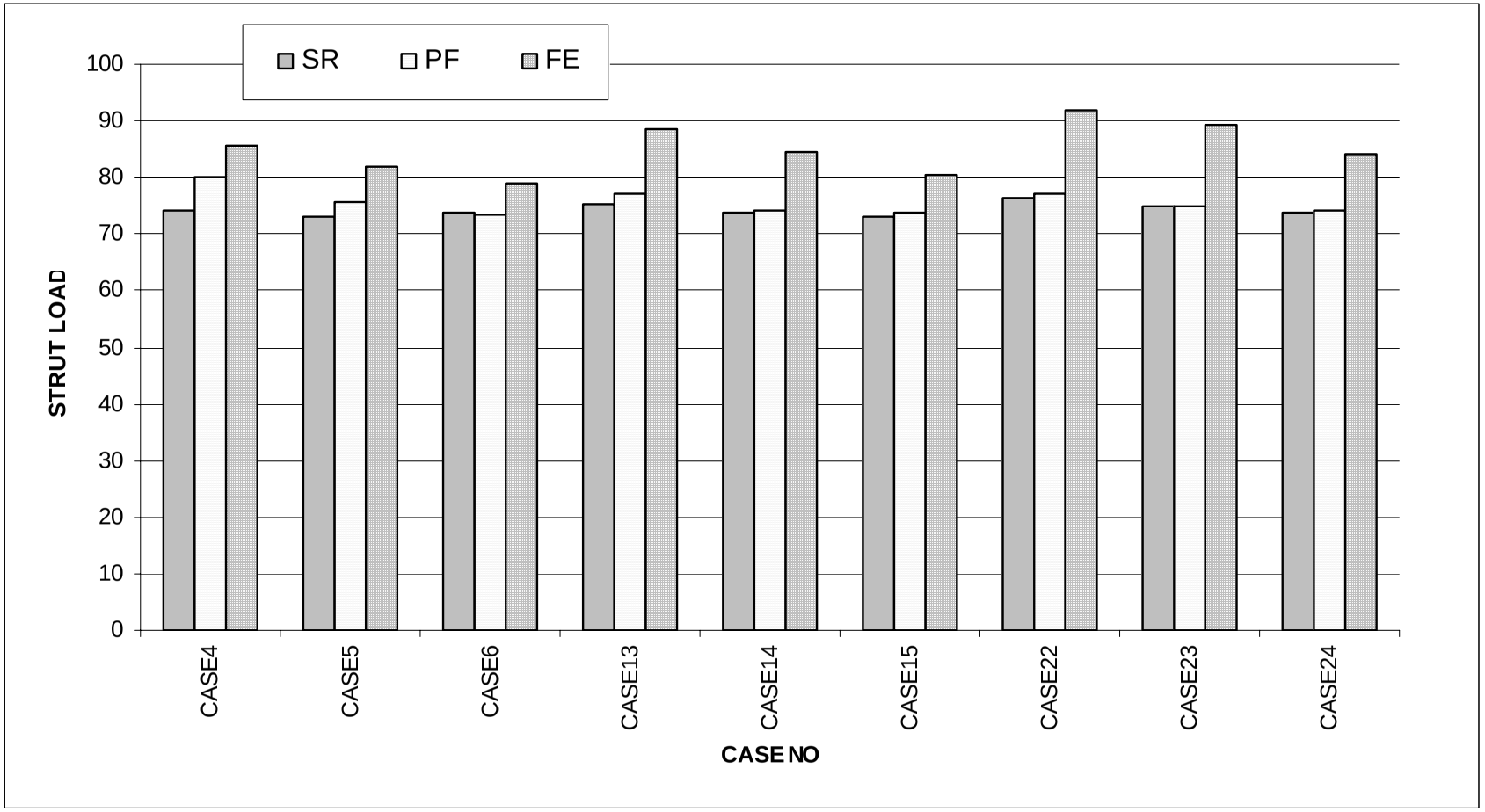

Figure 4.22 CASE 4-5-6-13-14-15-22-23-24 strut loads (kN)

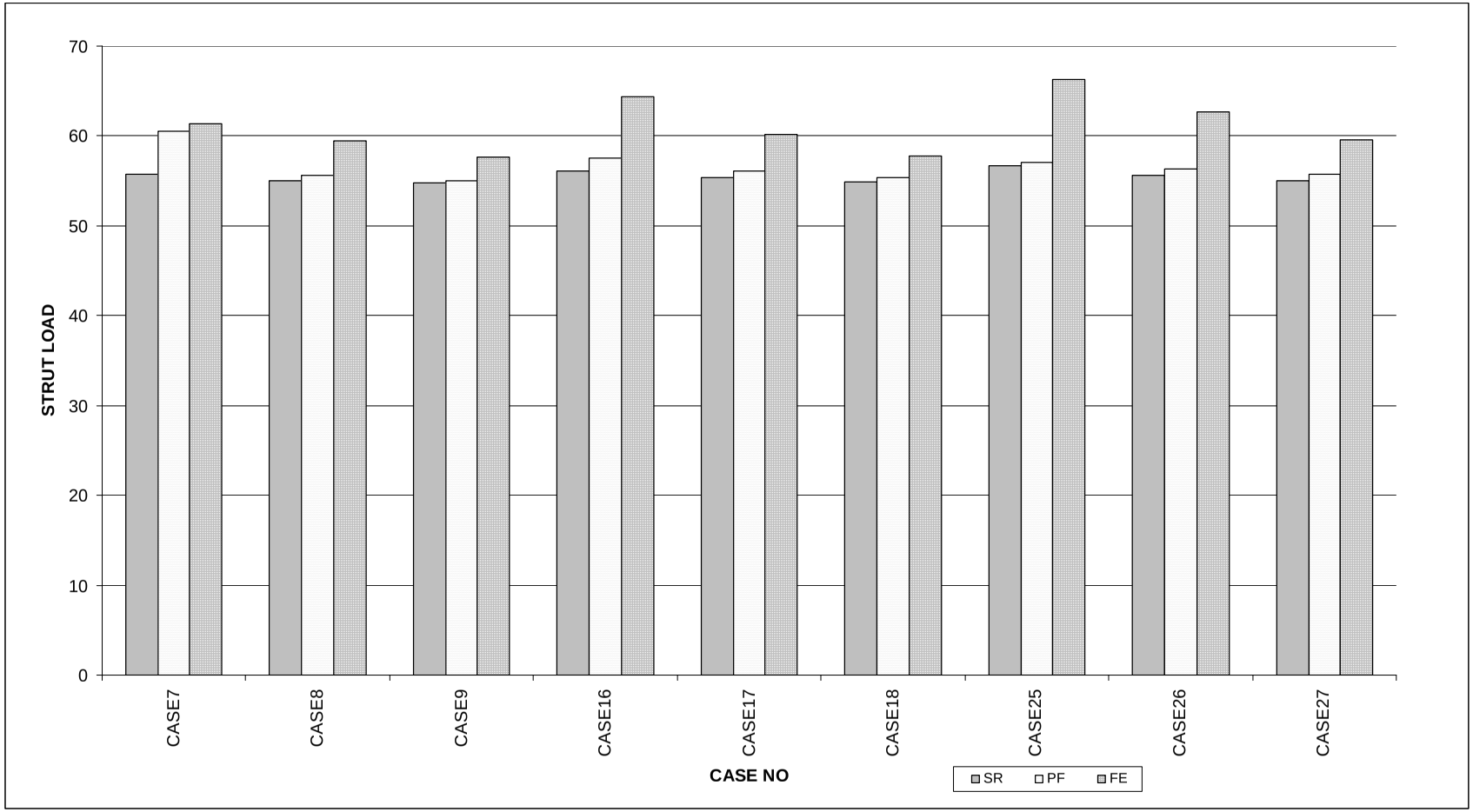

Figure 4.23 CASE 7-8-9-16-17-18-25-26-27 strut loads (kN)

4.3 Bending Moments

The wall bending moment at prop level and the maximum bending moment in the wall stem are examined by normalising with respect to bending moment as found by limit equilibrium method . The list of bending moments obtained in the analysis and normalised bending moments are represented in Tables 4.3-4.4-4.5-4.6.

Effect of E_{soil} on bending moments (Figures 4.24 4.32&Figures 4.42-4.50):

Results of the analyses indicate that normalised maximum wall stem bending moment decreases by increasing soil stiffness in pseudo-finite element approach, whereas it increases in finite element method, for all the selected wall configurations and backfill friction angle values of 30^0, 35^0, and 40^0.

Effect of EI_{wall} on bending moments (Figures 4.33–4.41&4.51-4.59):

Normalised wall bending moment at strut level decreases with increasing wall rigidity in finite element and pseudo-finite element methods, for all the wall configurations studied and backfill internal friction angles of 30^0, 35^0, and 40^0. However, in subgrade reaction method normalized bending moment at strut level is not affected by change in wall rigidity.

Effect of method of analysis (Figures 4.60–4.62):

The subgrade reaction method yields almost the same wall bending moment at prop level with the limit equilibrium method. The finite element method yields greater bending moments as compared to the results obtained by limit equilibrium method. The pseudo finite element method

yields values of bending moments at prop level between those of obtained by subgrade reaction and finite element methods.

In $\phi=30^0$ group analysis cases, normalised maximum wall stem bending moments are obtained in the range of 1.07-1.25, 1.06–1.36 and 0.91–1.40 in subgrade reaction method, pseudo finite element method and finite element method respectively. In $\phi=30^0$ group analysis cases, normalised wall bending moments are obtained at the prop level in the range of 1.00-1.03, 1.05–2.48 and 2.36–3.85 by subgrade reaction method, pseudo finite element method and finite element method respectively.

In $\phi=35^0$ group analysis cases, normalised maximum wall stem bending moments are obtained in the range of 1.06-1.16, 1.07–1.18 and 0.91–1.34 by subgrade reaction method, pseudo finite element method and finite element method respectively. In $\phi=35^0$ group analysis cases, normalised wall bending moment at the prop level are obtained in the range of 1.00-1.03, 1.06–2.16 and 2.36–3.61 by subgrade reaction method, pseudo finite element method and finite element method respectively.

In $\phi=40^0$ group analysis cases, normalised maximum wall stem bending moments are obtained in the range of 1.05-1.13, 1.05–1.13 and 0.85–1.30 by subgrade reaction, pseudo finite element and finite element methods respectively. In $\phi=40^0$ group analysis cases, normalised wall bending moment at the prop level are obtained in the range of 1.00-1.05, 1.05–2.14 and 1.89–3.55 by subgrade reaction, pseudo finite element and finite element methods respectively.

Table 4.3 Summary of maximum wall stem bending moments obtained from the analysis (kNm / m)

CASE NAME	Subgrade Reaction	Pseudo Finite	Finite Element
CASE1	220.25	219.8	219.84
CASE2	210.48	207.81	194.54
CASE3	204.62	202.28	173.66
CASE4	147.99	145.45	150.22
CASE5	143.49	144.74	134.02
CASE6	146.14	143.62	122.22
CASE7	104.53	105.09	102.66
CASE8	101.77	103.44	91.36
CASE9	100.8	101.16	81.14
CASE10	227.7	241.12	250.57
CASE11	216.51	219.06	222.60
CASE12	209.08	211.23	204.96
CASE13	152.04	151.17	165.36
CASE14	145.78	147.53	151.60
CASE15	142.9	145.67	140.16
CASE16	105.95	107.97	115.97
CASE17	102.86	105.25	102.84
CASE18	101.35	102.46	95.57
CASE19	240.3	259.74	267.23
CASE20	226.9	231.06	252.51
CASE21	218.72	218.88	232.46
CASE22	156.19	159.06	179.64
CASE23	150.29	150.19	168.94
CASE24	146.14	147.52	158.43
CASE25	108.53	108.97	124.55
CASE26	104.2	106.32	114.64
CASE27	101.77	103.87	105.71

Table 4.4 Summary of normalised maximum wall stem bending moments

CASE NAME	Subgrade Reaction	Pseudo Finite	Finite Element
CASE1	1.150	1.148	1.148
CASE2	1.099	1.085	1.016
CASE3	1.069	1.056	0.907
CASE4	1.102	1.084	1.119
CASE5	1.069	1.078	0.998
CASE6	1.089	1.070	0.910
CASE7	1.090	1.095	1.070
CASE8	1.061	1.078	0.952
CASE9	1.051	1.055	0.846
CASE10	1.189	1.259	1.309
CASE11	1.131	1.144	1.163
CASE12	1.092	1.103	1.070
CASE13	1.133	1.126	1.232
CASE14	1.086	1.099	1.129
CASE15	1.065	1.085	1.044
CASE16	1.104	1.126	1.209
CASE17	1.072	1.097	1.072
CASE18	1.056	1.068	0.996
CASE19	1.255	1.356	1.396
CASE20	1.185	1.207	1.319
CASE21	1.142	1.143	1.214
CASE22	1.164	1.185	1.338
CASE23	1.120	1.119	1.258
CASE24	1.089	1.099	1.180
CASE25	1.131	1.136	1.298
CASE26	1.086	1.108	1.195
CASE27	1.061	1.083	1.102

Table 4.5 Summary of wall bending moments at prop level obtained from the analysis (kNm / m)

CASE NAME	Subgrade Reaction	Pseudo Finite	Finite Element
CASE1	7.02	16.98	20.65
CASE2	7.05	12.82	24.59
CASE3	6.84	10.69	26.35
CASE4	5.68	11.89	17.18
CASE5	5.5	7.8	18.96
CASE6	5.65	5.83	19.85
CASE7	4.37	9.33	11.58
CASE8	4.37	4.63	14.27
CASE9	4.37	4.63	15.50
CASE10	7.01	11.71	17.50
CASE11	7.02	7.2	20.15
CASE12	7.04	7.2	22.05
CASE13	5.66	7.77	14.79
CASE14	5.67	5.83	15.82
CASE15	5.68	5.83	15.78
CASE16	4.62	5.45	10.24
CASE17	4.37	4.63	10.84
CASE18	4.37	4.63	11.32
CASE19	7	8.35	16.13
CASE20	7	7.2	16.94
CASE21	7	7.2	17.33
CASE22	5.65	5.83	13.12
CASE23	5.65	5.83	14.14
CASE24	5.65	5.83	12.99
CASE25	4.6	4.63	8.25
CASE26	4.6	4.63	8.94
CASE27	4.6	4.63	8.35

Table 4.6 Summary of normalised wall bending moments at prop level

CASE NAME	Subgrade Reaction	Pseudo Finite	Finite Element
CASE1	1.026	2.482	3.019
CASE2	1.031	1.874	3.596
CASE3	1.000	1.563	3.852
CASE4	1.033	2.162	3.123
CASE5	1.000	1.418	3.447
CASE6	1.027	1.060	3.609
CASE7	1.000	2.135	2.651
CASE8	1.000	1.059	3.266
CASE9	1.000	1.059	3.546
CASE10	1.025	1.712	2.559
CASE11	1.026	1.053	2.946
CASE12	1.029	1.053	3.223
CASE13	1.029	1.413	2.689
CASE14	1.031	1.060	2.877
CASE15	1.033	1.060	2.869
CASE16	1.057	1.247	2.342
CASE17	1.000	1.059	2.481
CASE18	1.000	1.059	2.591
CASE19	1.023	1.221	2.358
CASE20	1.023	1.053	2.477
CASE21	1.023	1.053	2.533
CASE22	1.027	1.060	2.386
CASE23	1.027	1.060	2.570
CASE24	1.027	1.060	2.361
CASE25	1.053	1.059	1.888
CASE26	1.053	1.059	2.045
CASE27	1.053	1.059	1.912

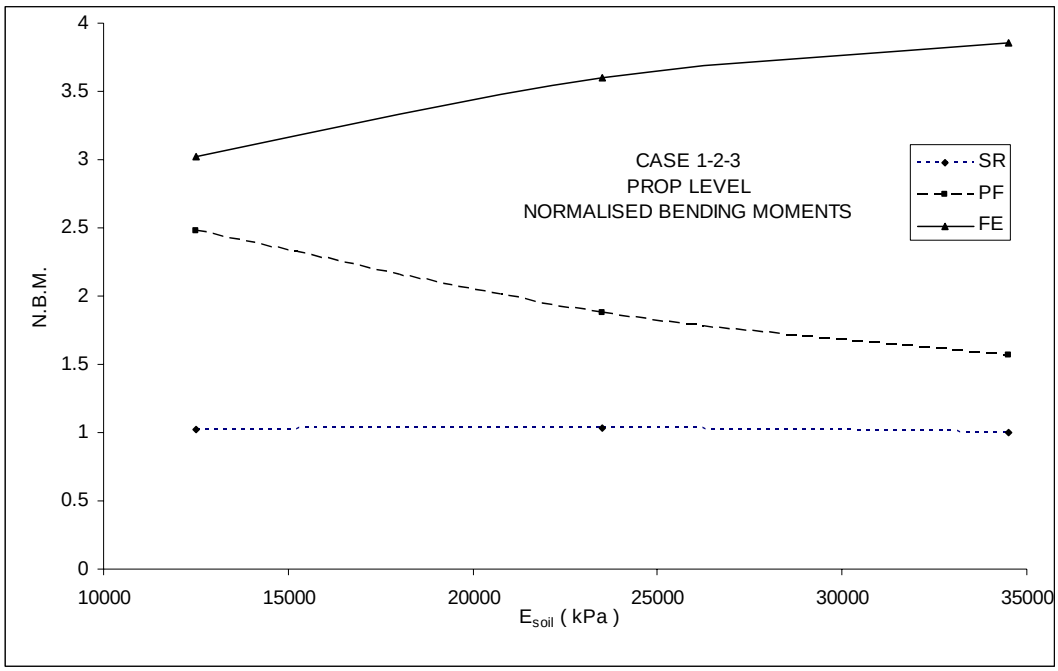

Figure 4.24 Prop level normalised bending moment vs E_{soil}

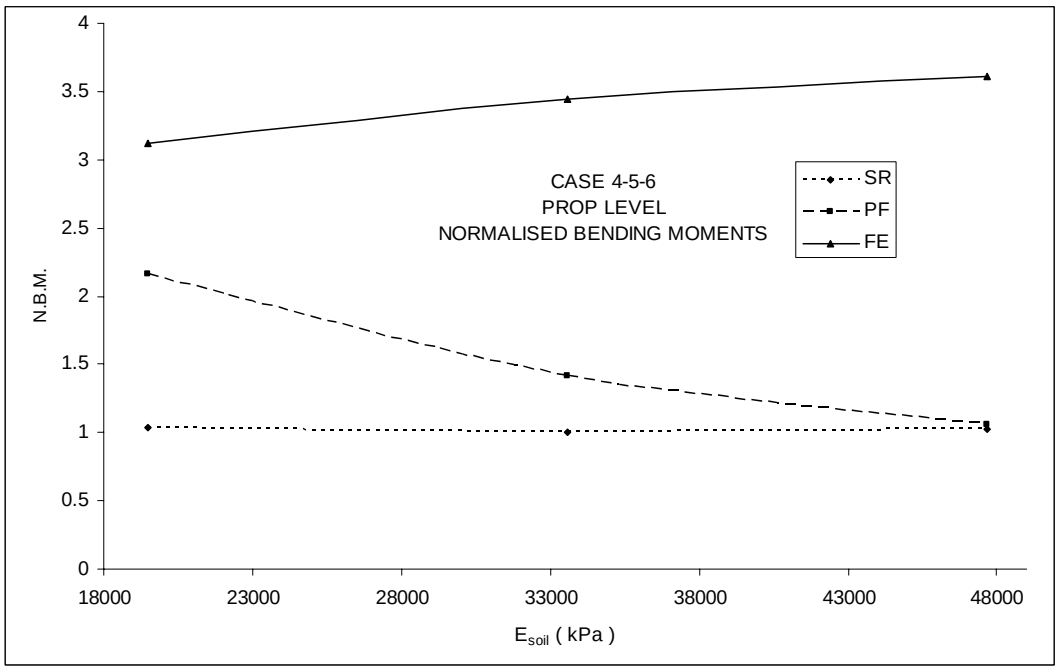

Figure 4.25 Prop level normalised bending moment vs E_{soil}

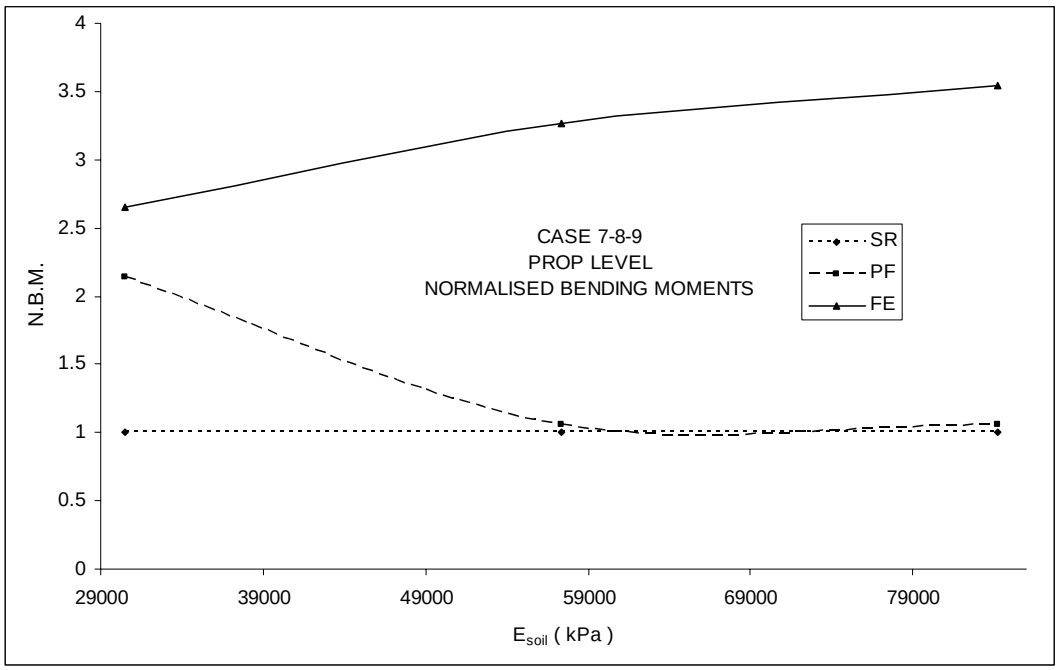

Figure 4.26 Prop level normalised bending moment vs E_{soil}

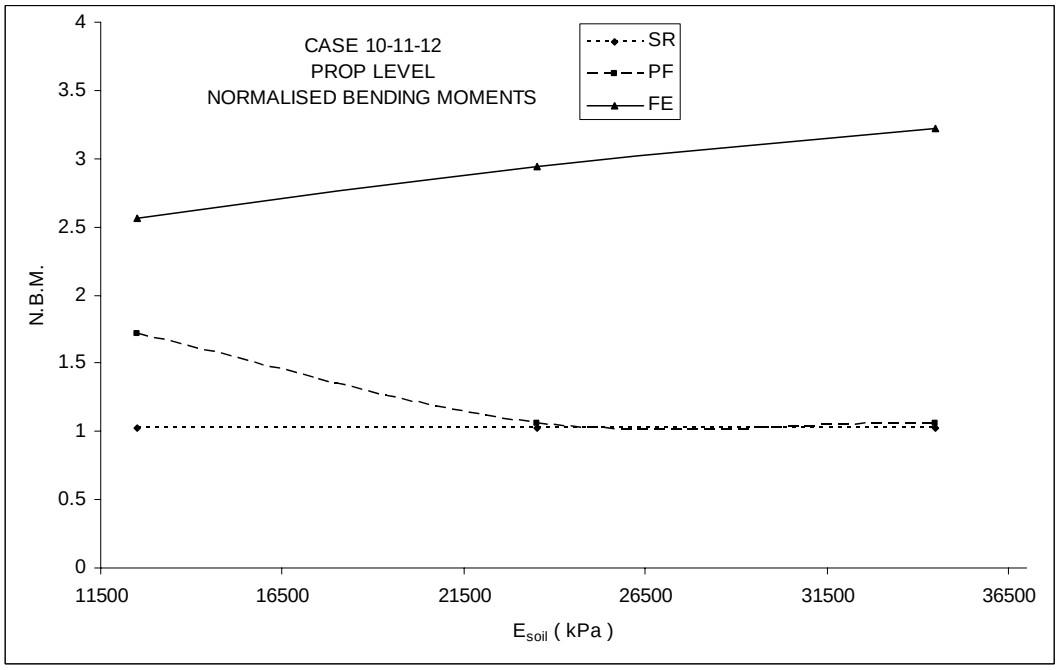

Figure 4.27 Prop level normalised bending moment vs E_{soil}

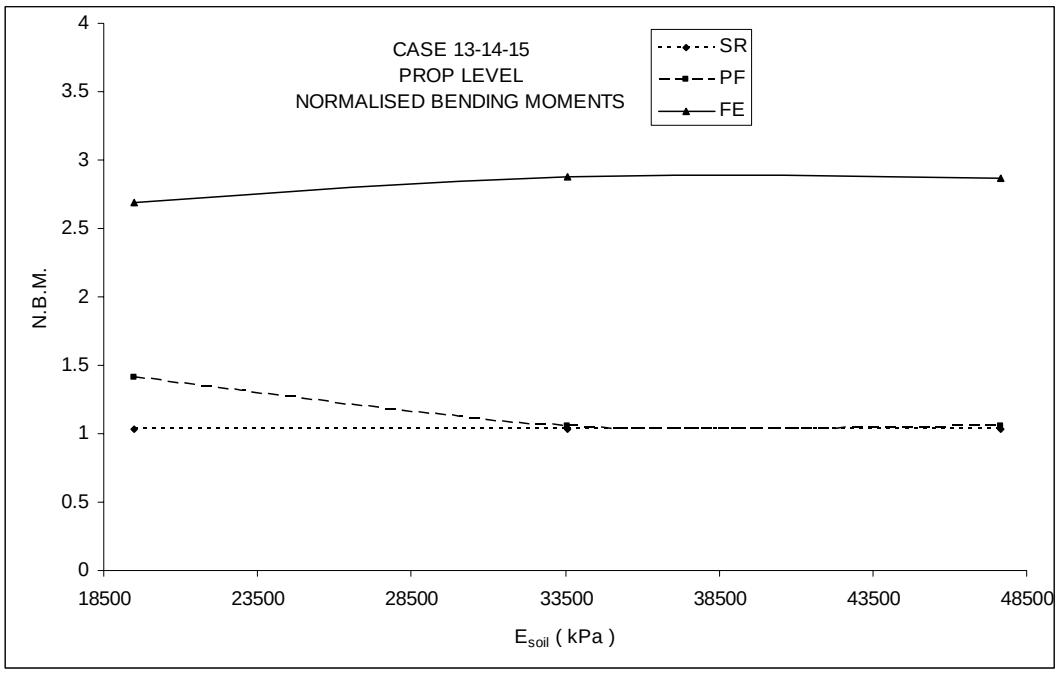

Figure 4.28 Prop level normalised bending moment vs E_{soil}

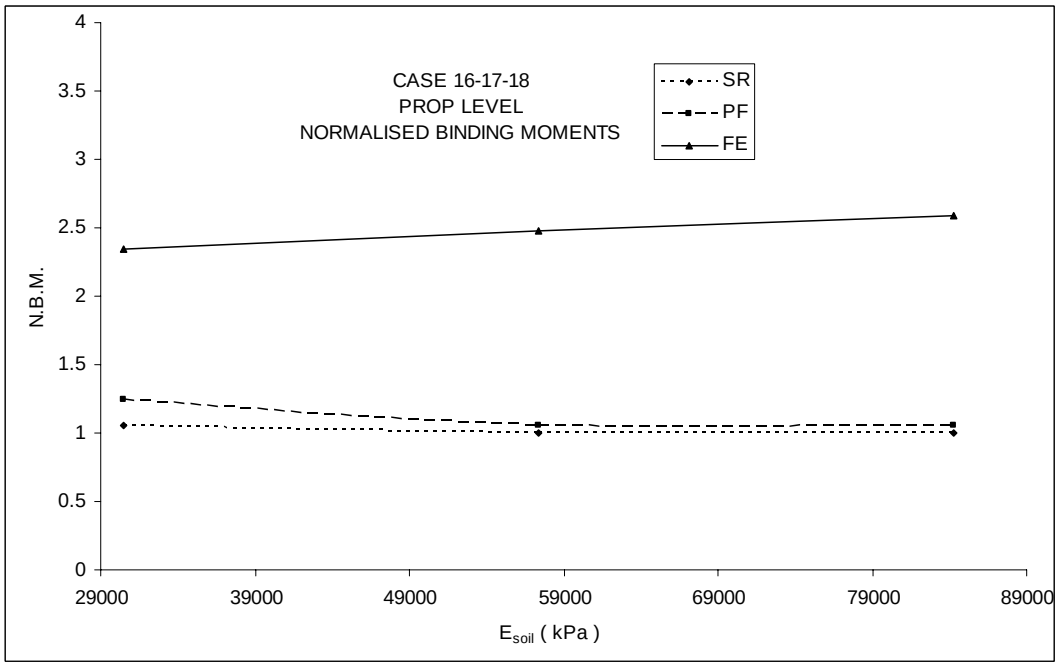

Figure 4.29 Prop level normalised bending moment vs E_{soil}

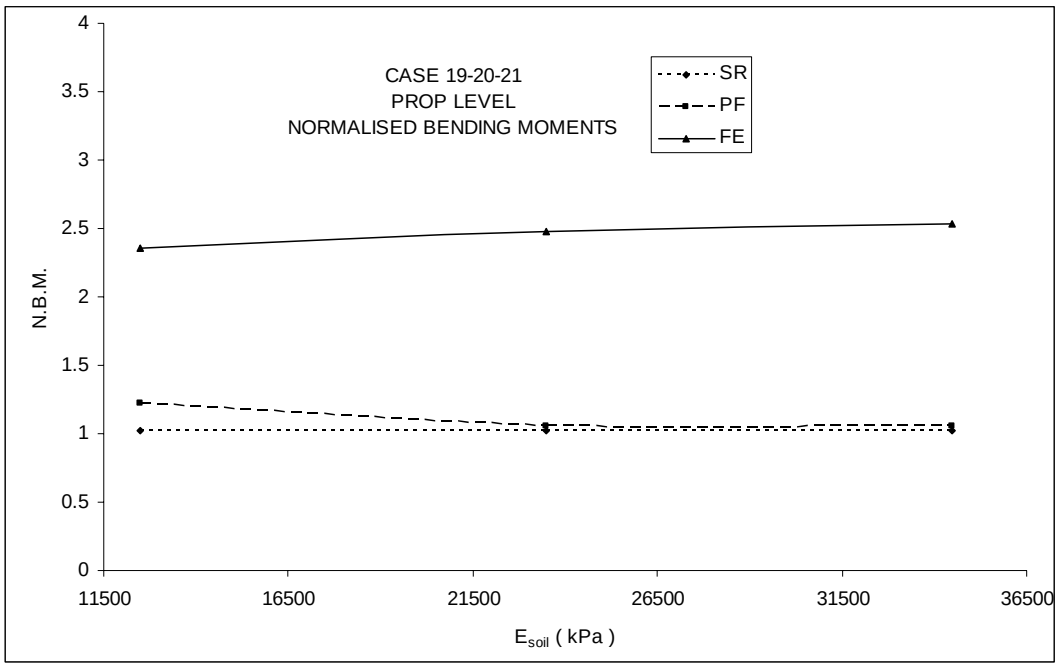

Figure 4.30 Prop level normalised bending moment vs E_{soil}

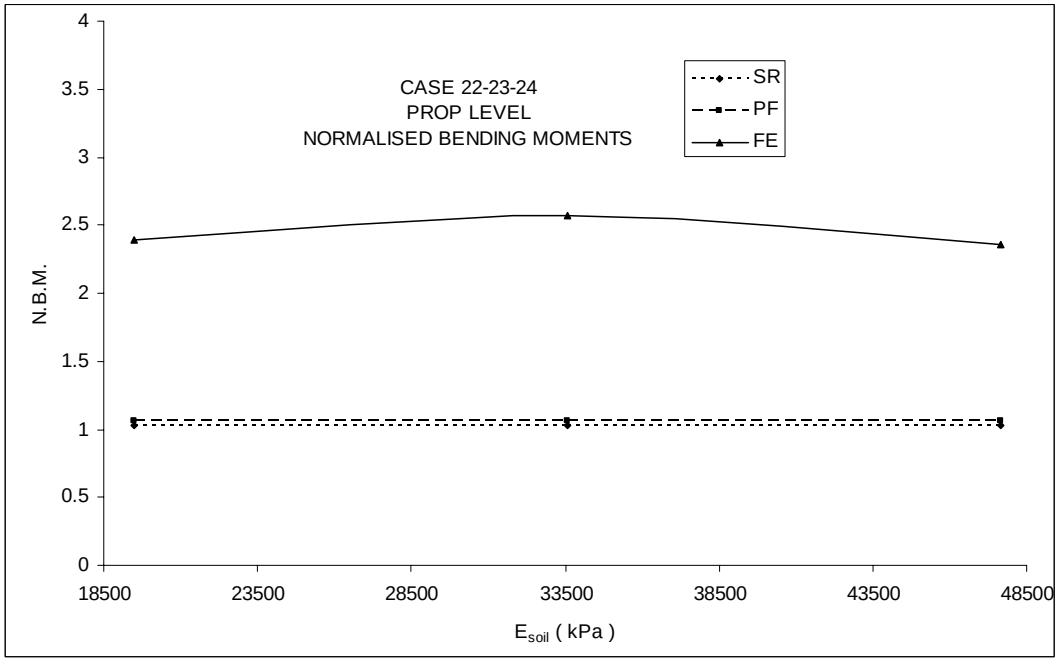

Figure 4.31 Prop level normalised bending moment vs E_{soil}

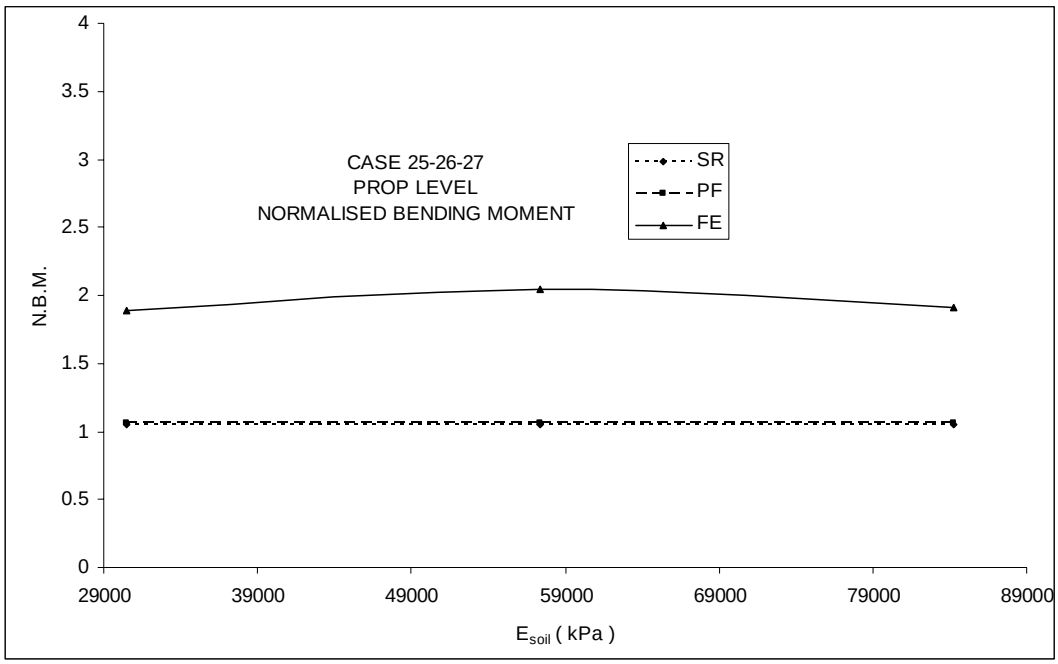

Figure 4.32 Prop level normalised bending moment vs E_{soil}

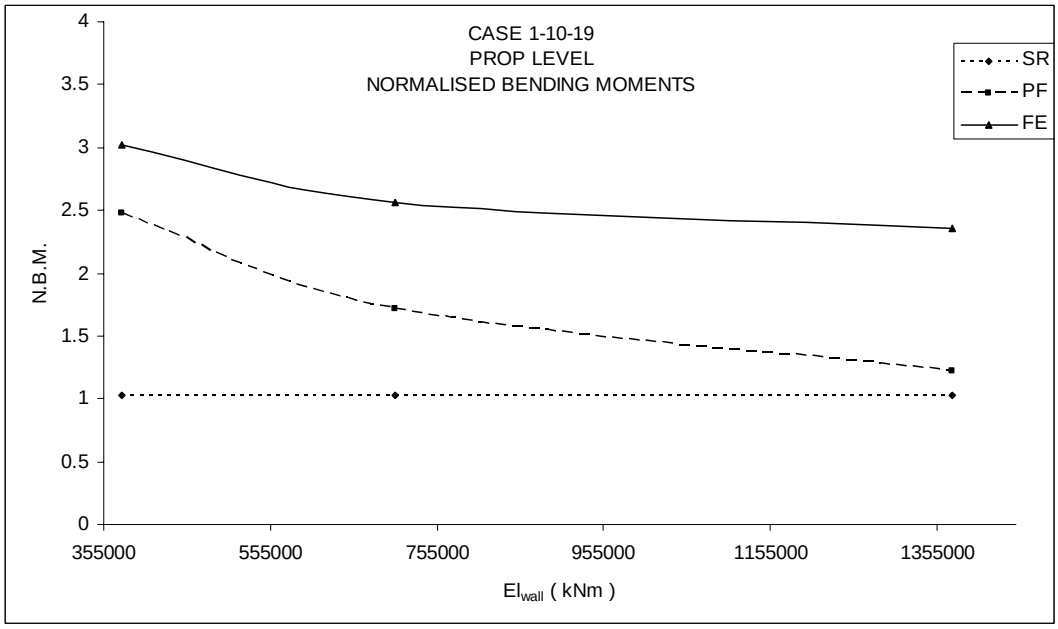

Figure 4.33 Prop level normalised bending moment vs EI_{wall}

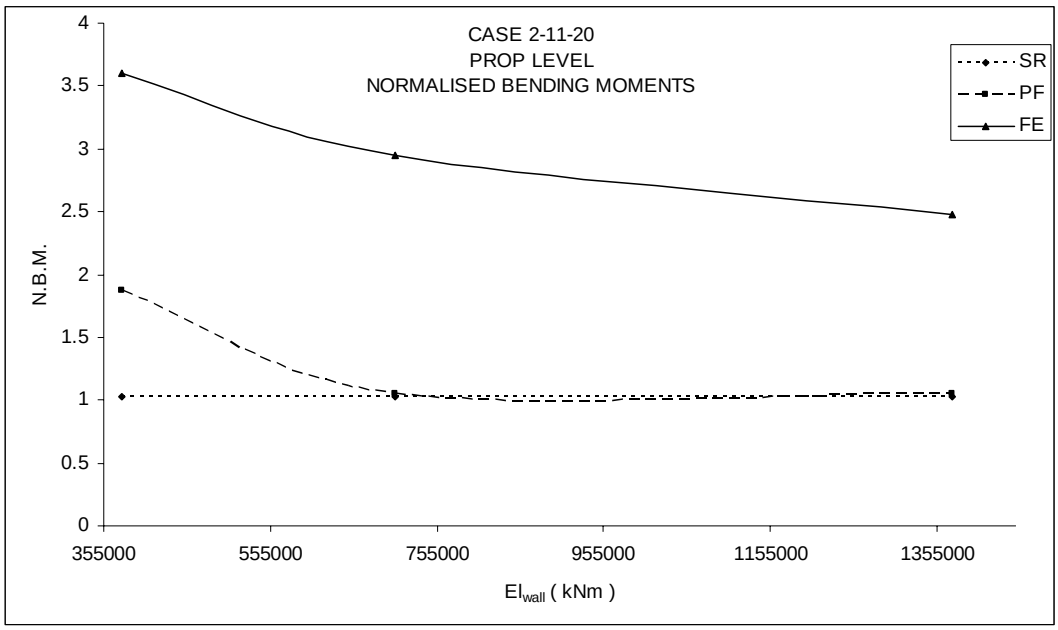

Figure 4.34 Prop level normalised bending moment vs EI_{wall}

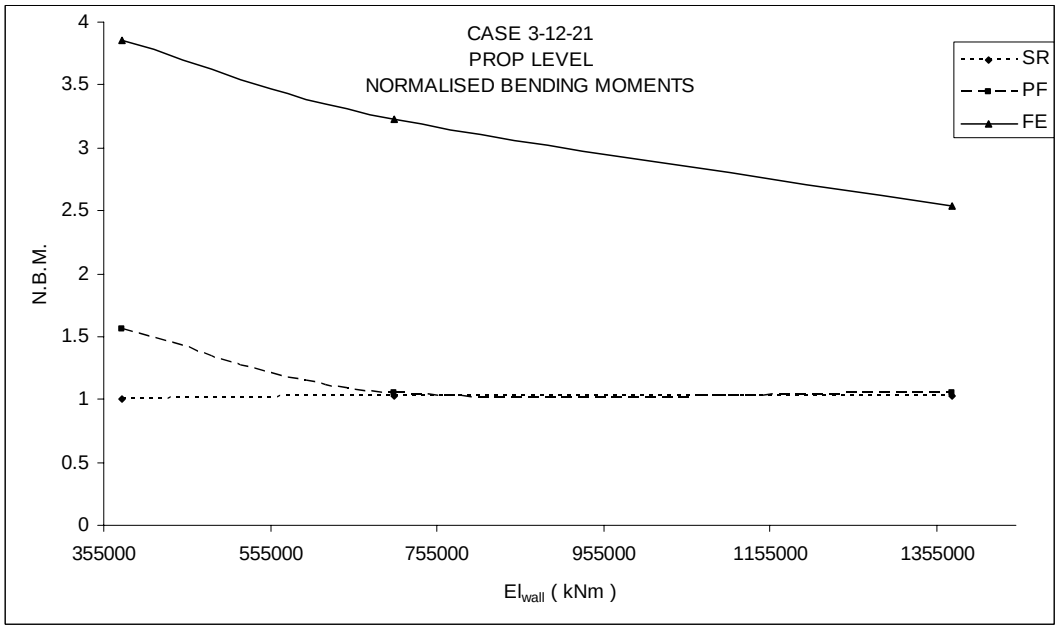

Figure 4.35 Prop level normalised bending moment vs EI_{wall}

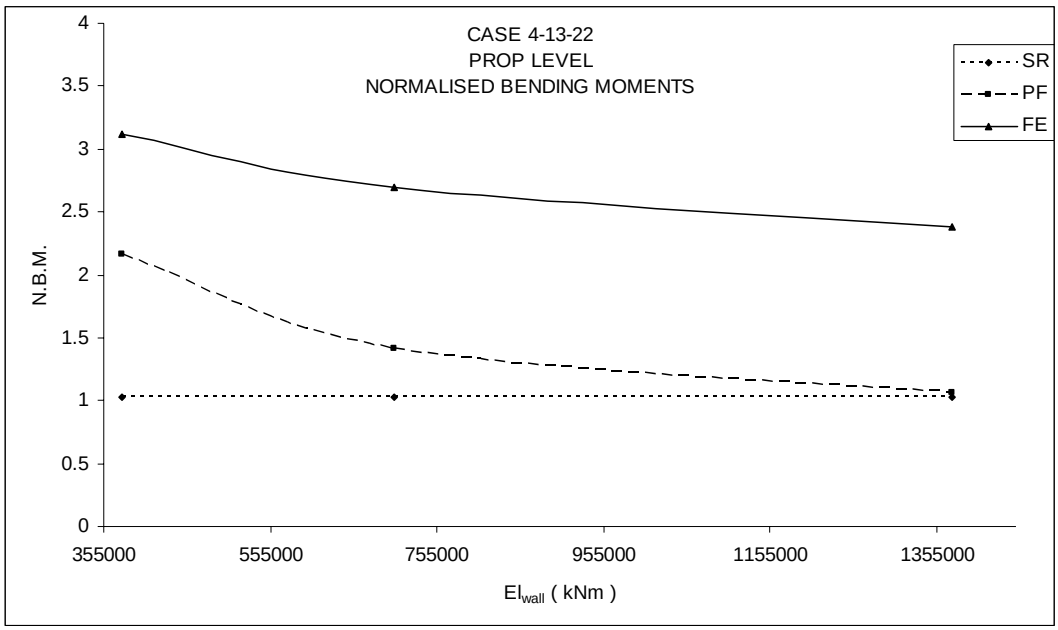

Figure 4.36 Prop level normalised bending moment vs EI_{wall}

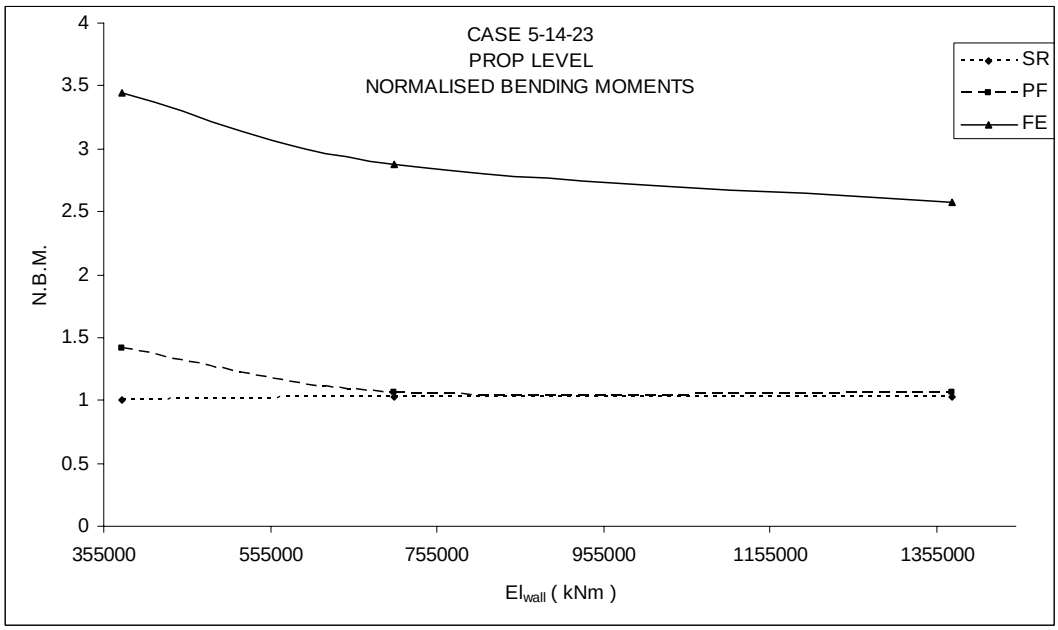

Figure 4.37 Prop level normalised bending moment vs EI_{wall}

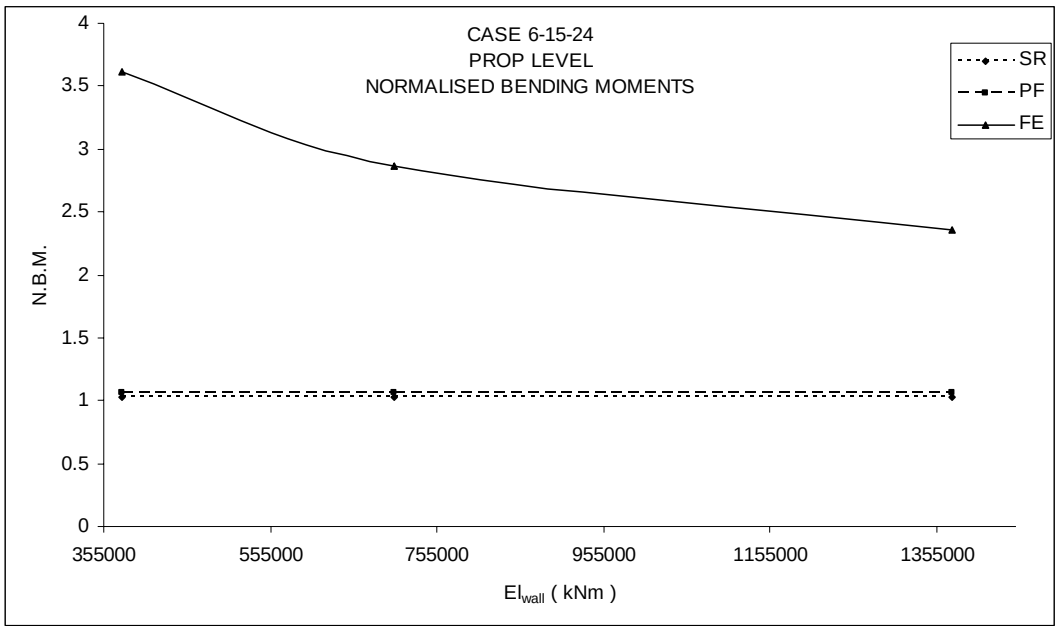

Figure 4.38 Prop level normalised bending moment vs EI_{wall}

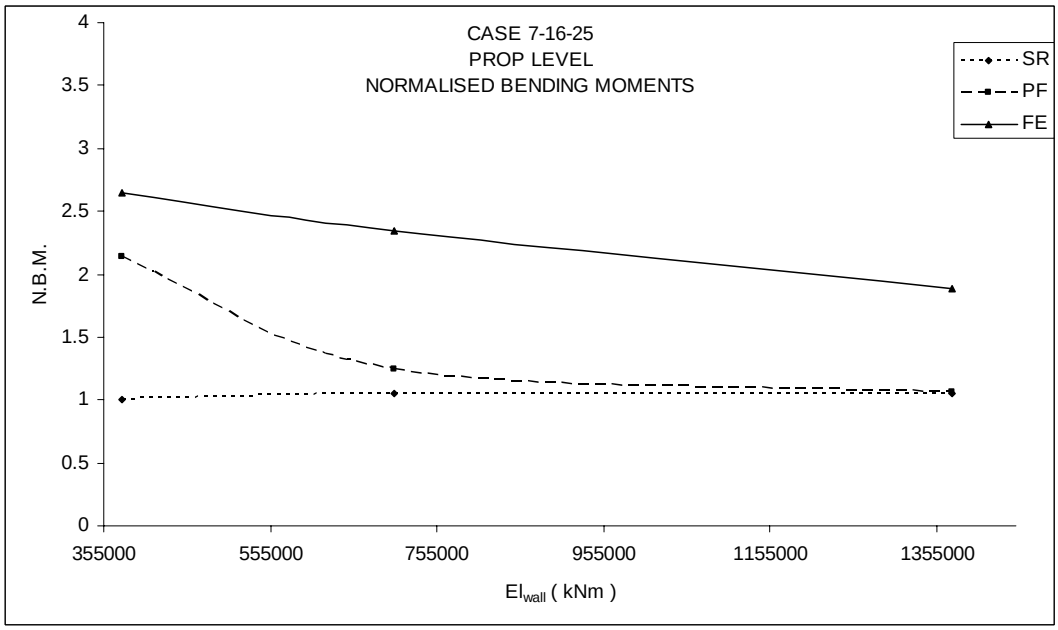

Figure 4.39 Prop level normalised bending moment vs EI_{wall}

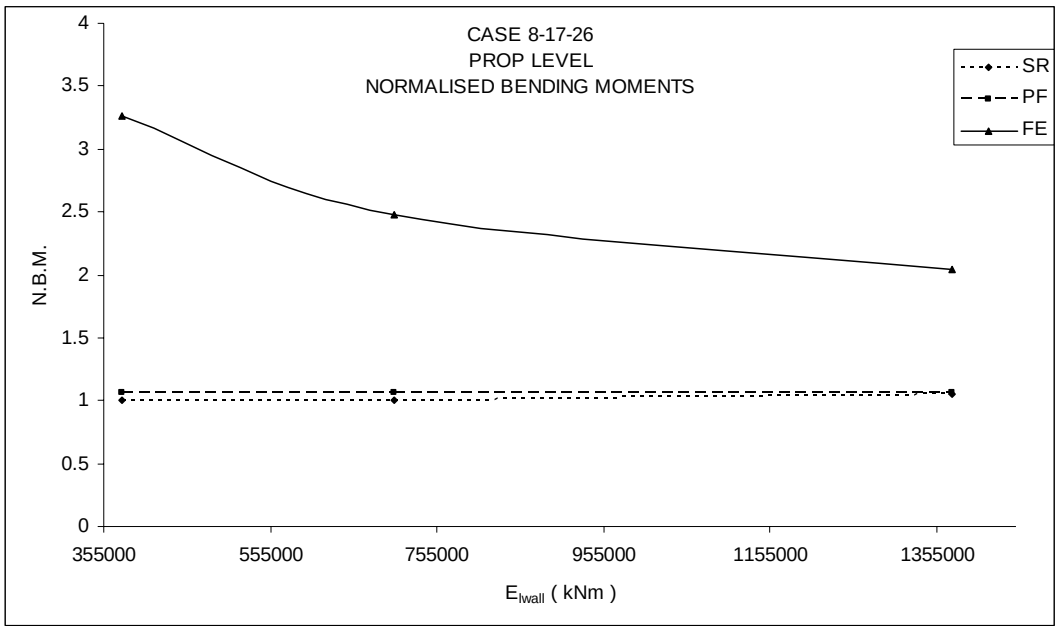

Figure 4.40 Prop level normalised bending moment vs EI_{wall}

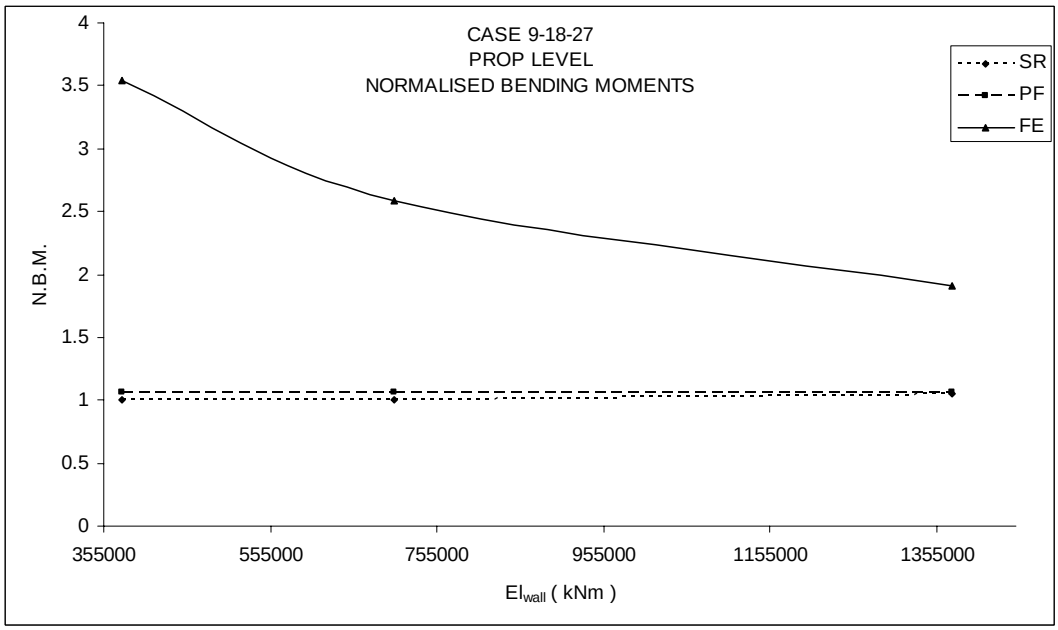

Figure 4.41 Prop level normalised bending moment vs EI_{wall}

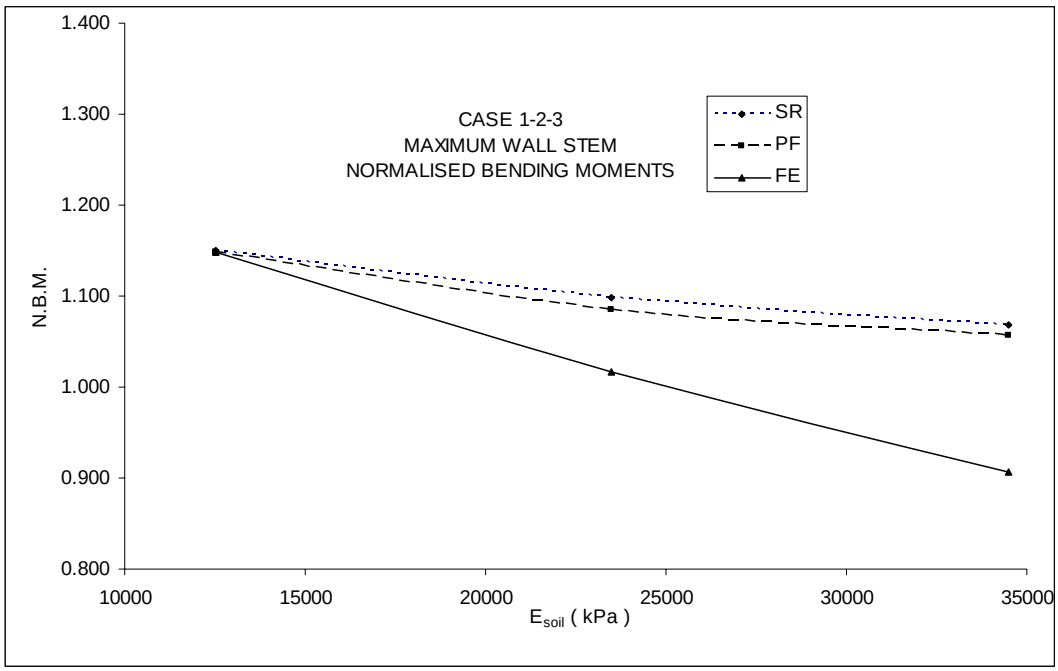

Figure 4.42 Wall stem normalised maximum bending moment vs E_{soil}

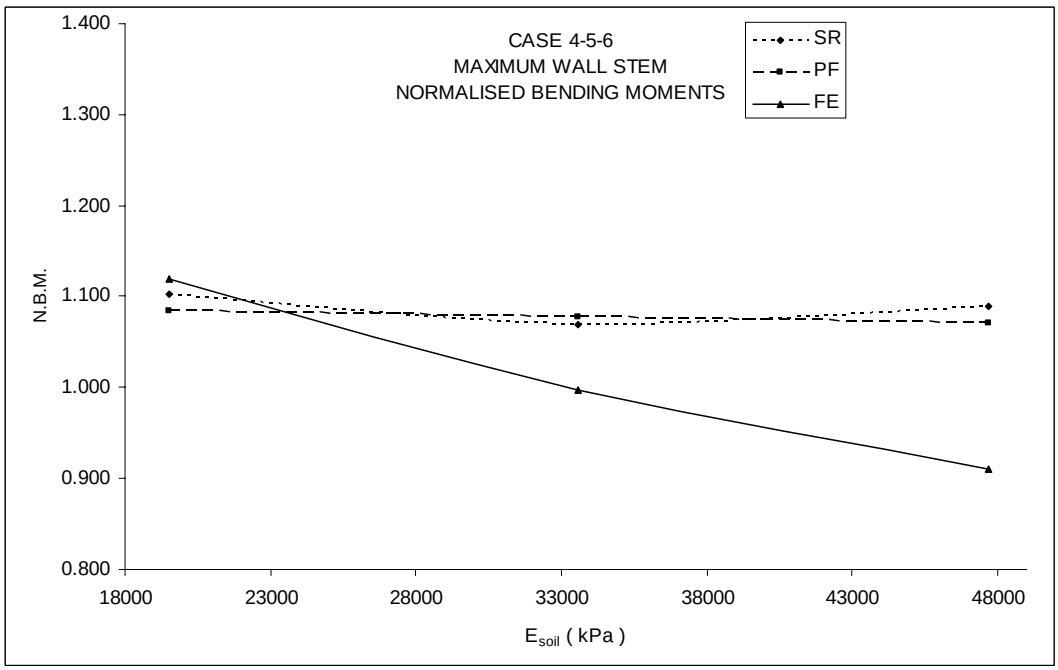

Figure 4.43 Wall stem normalised maximum bending moment vs E_{soil}

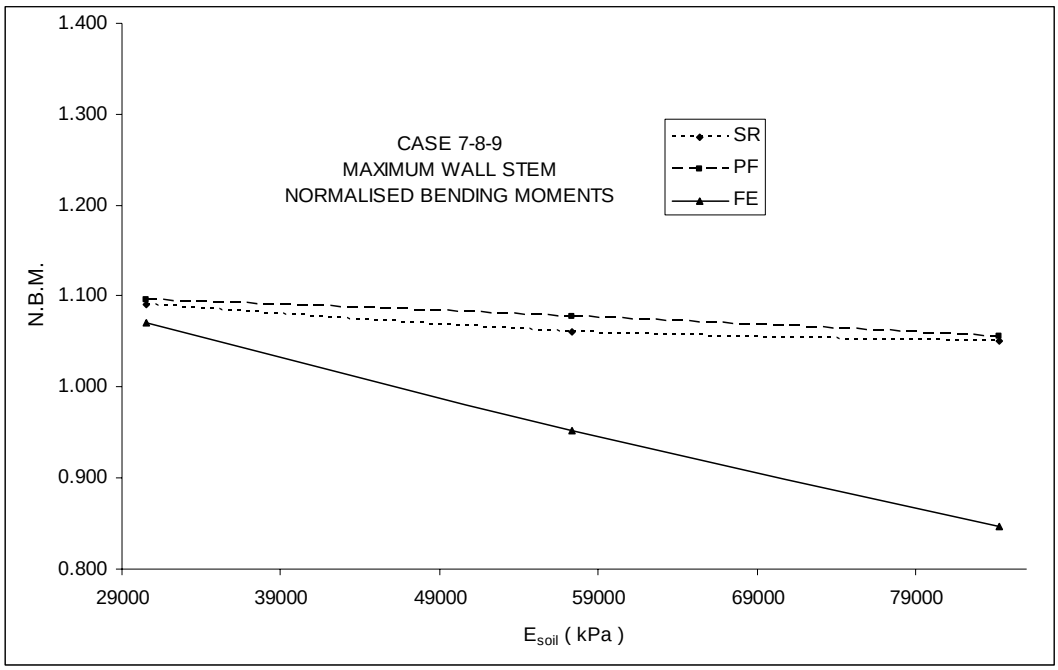

Figure 4.44 Wall stem normalised maximum bending moment vs E_{soil}

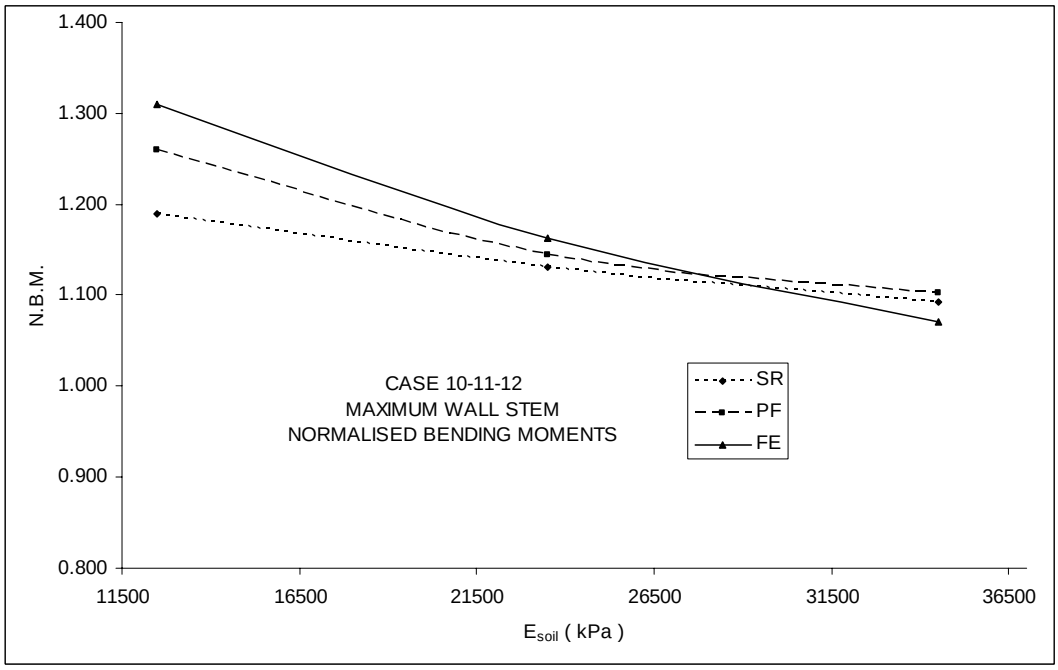

Figure 4.45 Wall stem normalised maximum bending moment vs E_{soil}

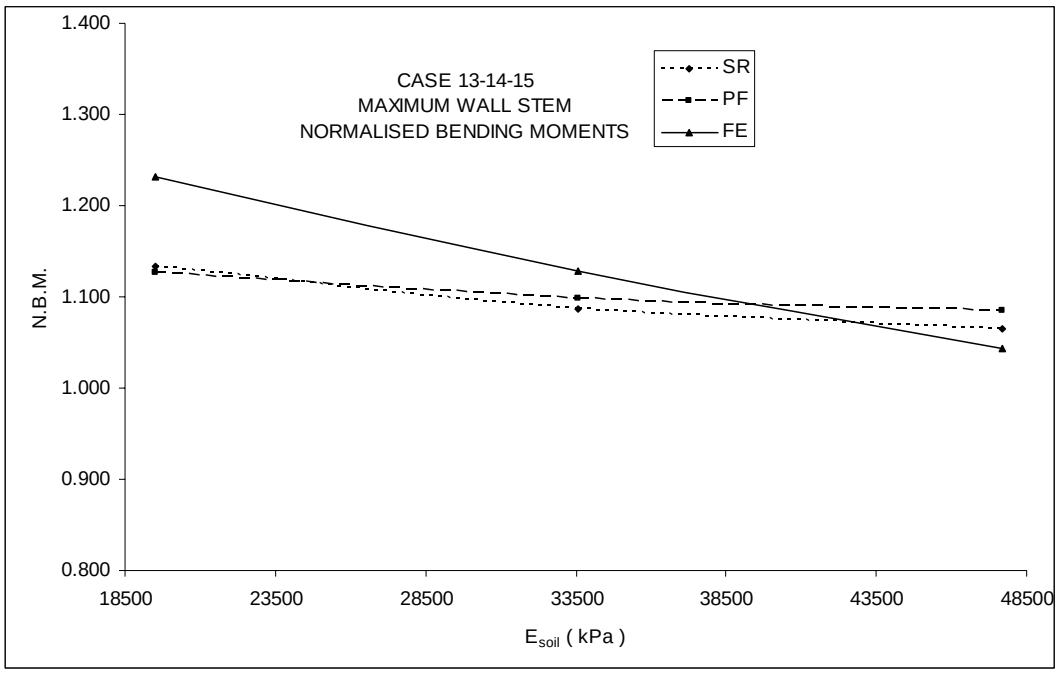

Figure 4.46 Wall stem normalised maximum bending moment vs E_{soil}

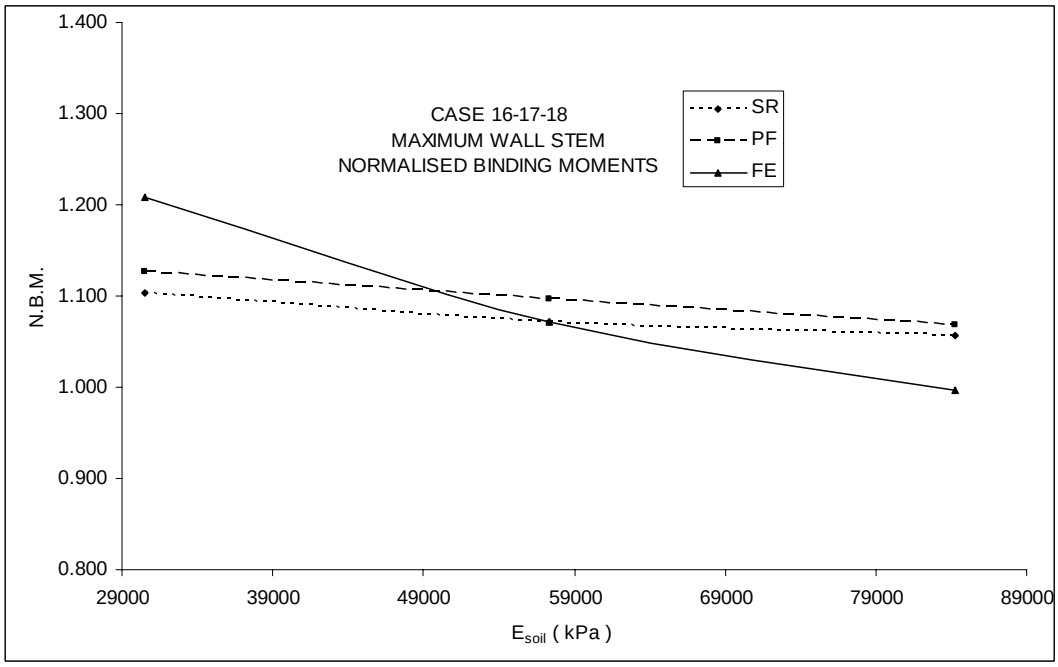

Figure 4.47 Wall stem normalised maximum bending moment vs E_{soil}

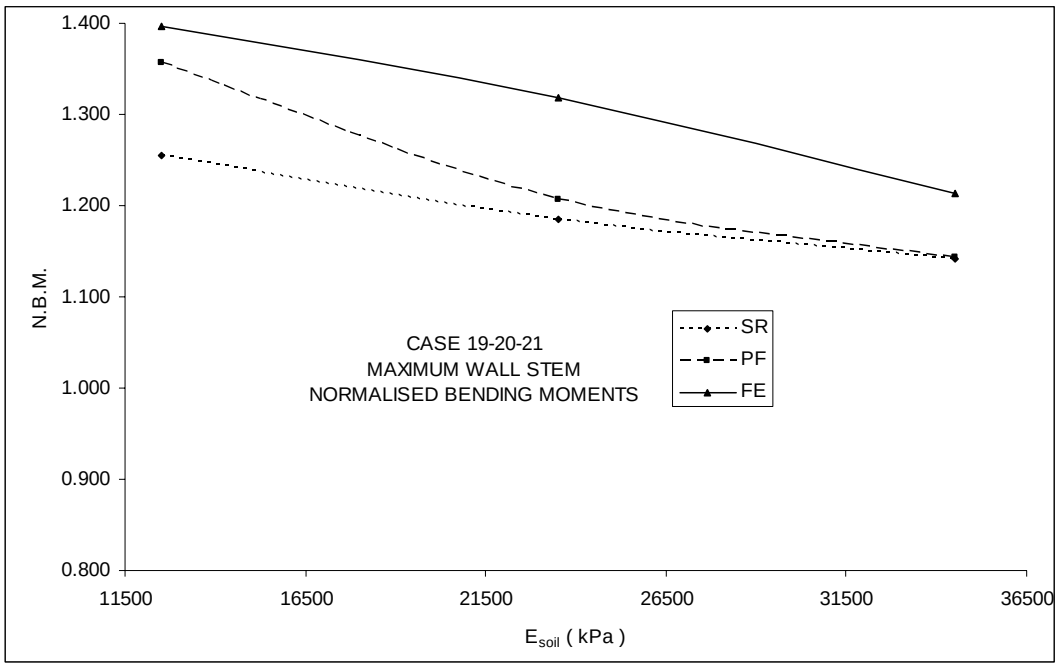

Figure 4.48 Wall stem normalised maximum bending moment vs E_{soil}

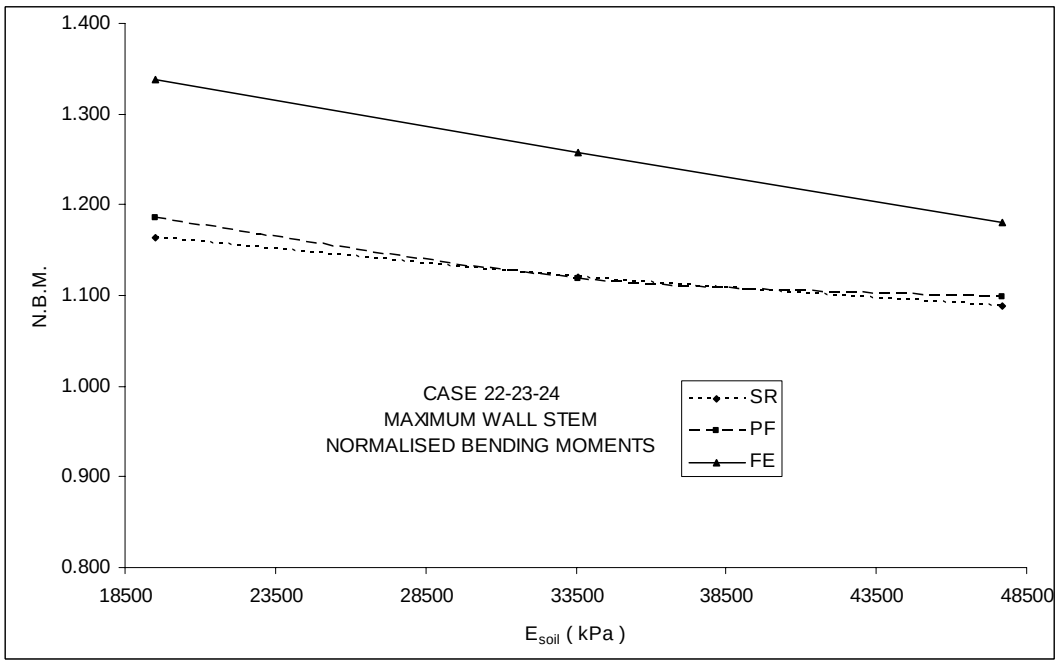

Figure 4.49 Wall stem normalised maximum bending moment vs E_{soil}

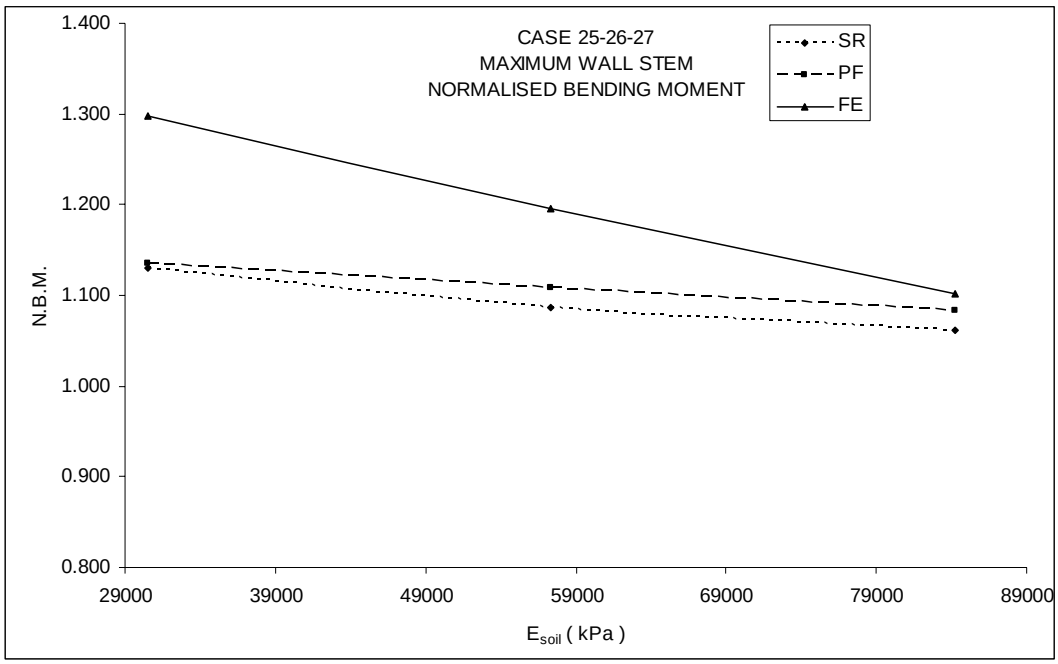

Figure 4.50 Wall stem normalised maximum bending moment vs E_{soil}

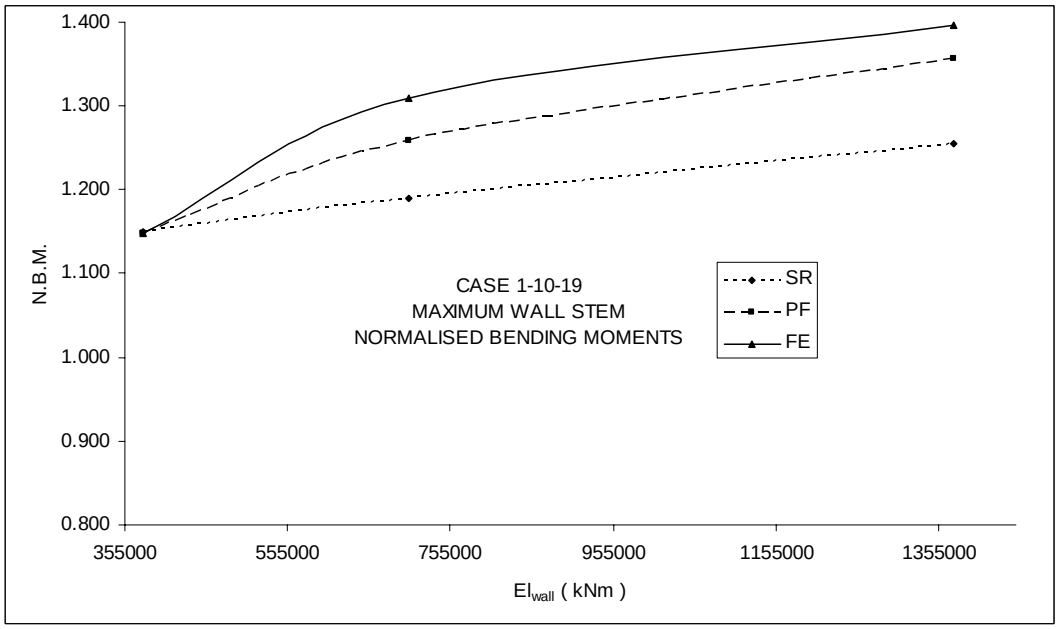

Figure 4.51 Wall stem normalised maximum bending moment vs EI_{wall}

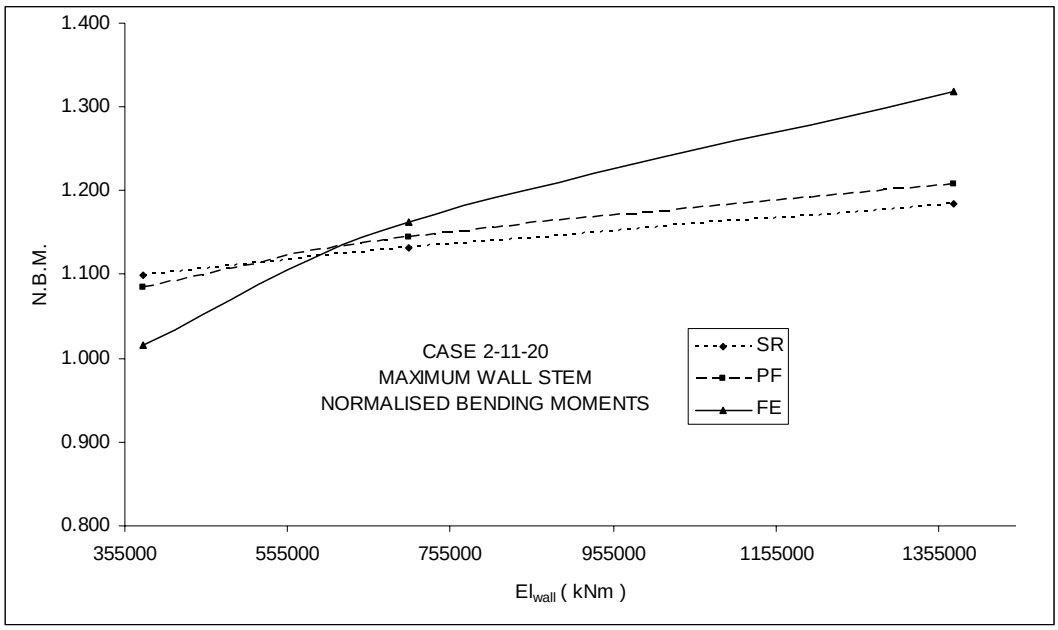

Figure 4.52 Wall stem normalised maximum bending moment vs EI_{wall}

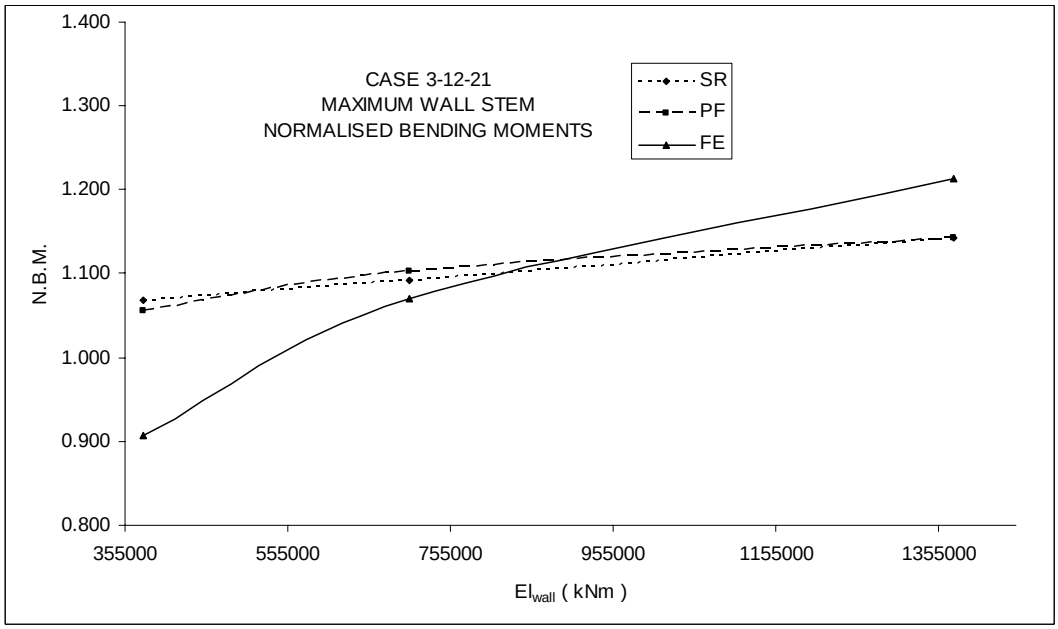

Figure 4.53 Wall stem normalised maximum bending moment vs EI_{wall}

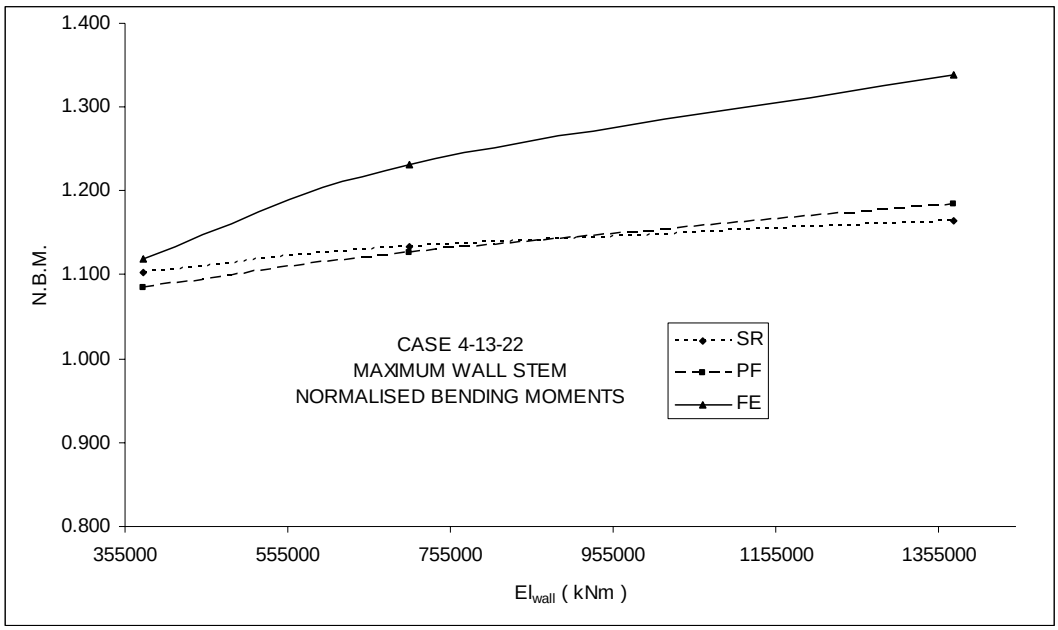

Figure 4.54 Wall stem normalised maximum bending moment vs EI_{wall}

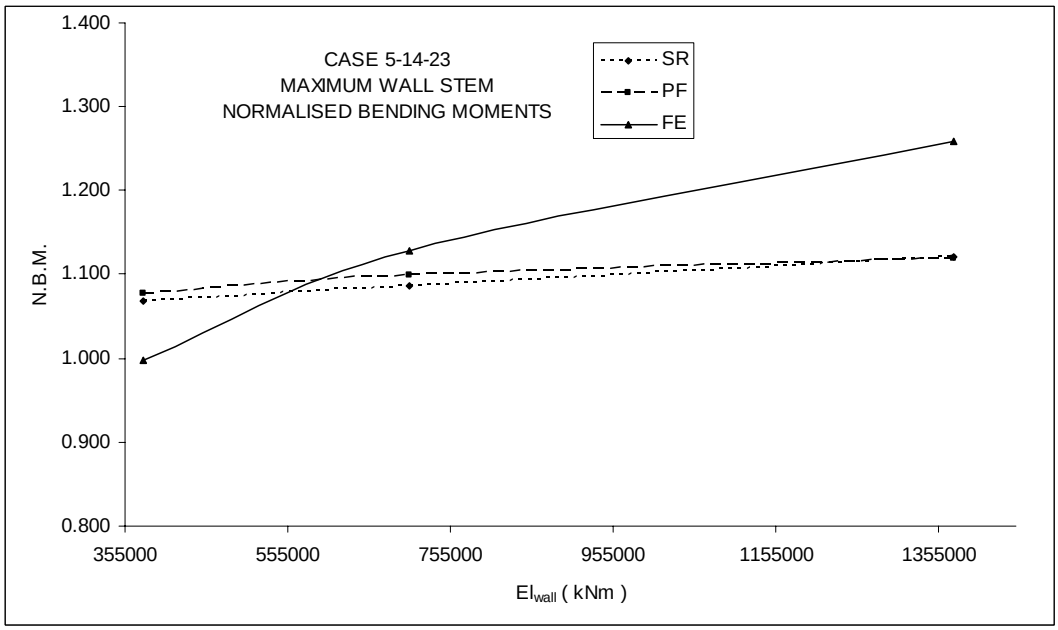

Figure 4.55 Wall stem normalised maximum bending moment vs EI_{wall}

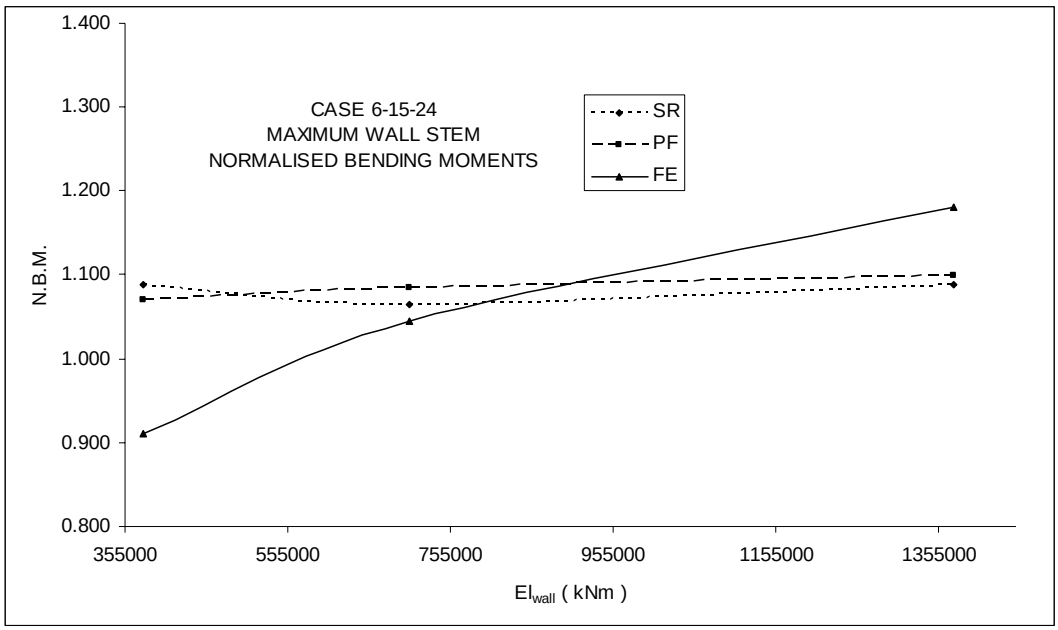

Figure 4.56 Wall stem normalised maximum bending moment vs EI_{wall}

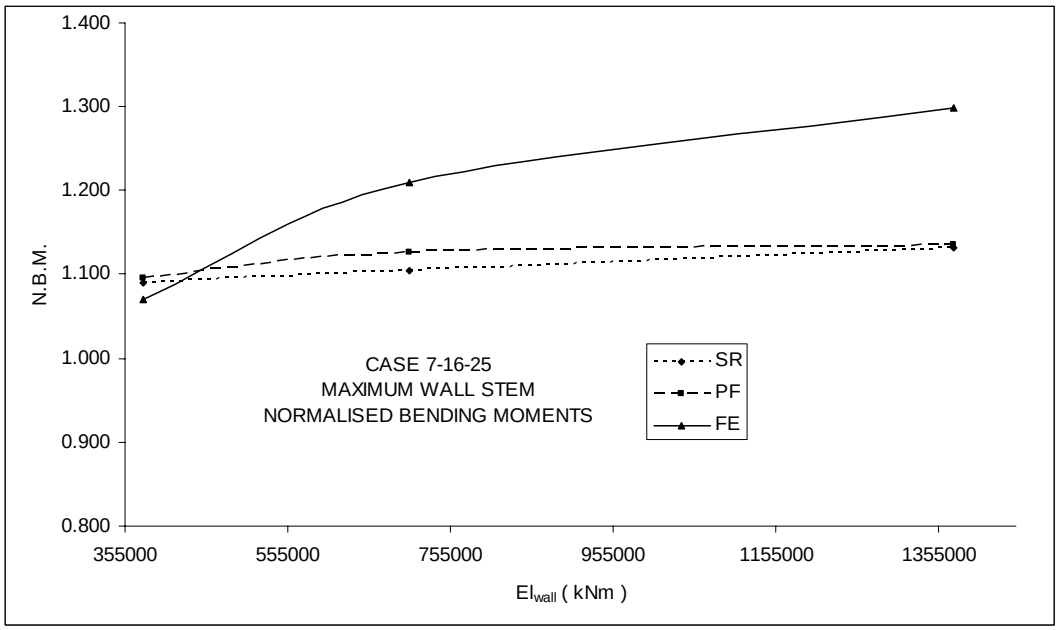

Figure 4.57 Wall stem normalised maximum bending moment vs EI_{wall}

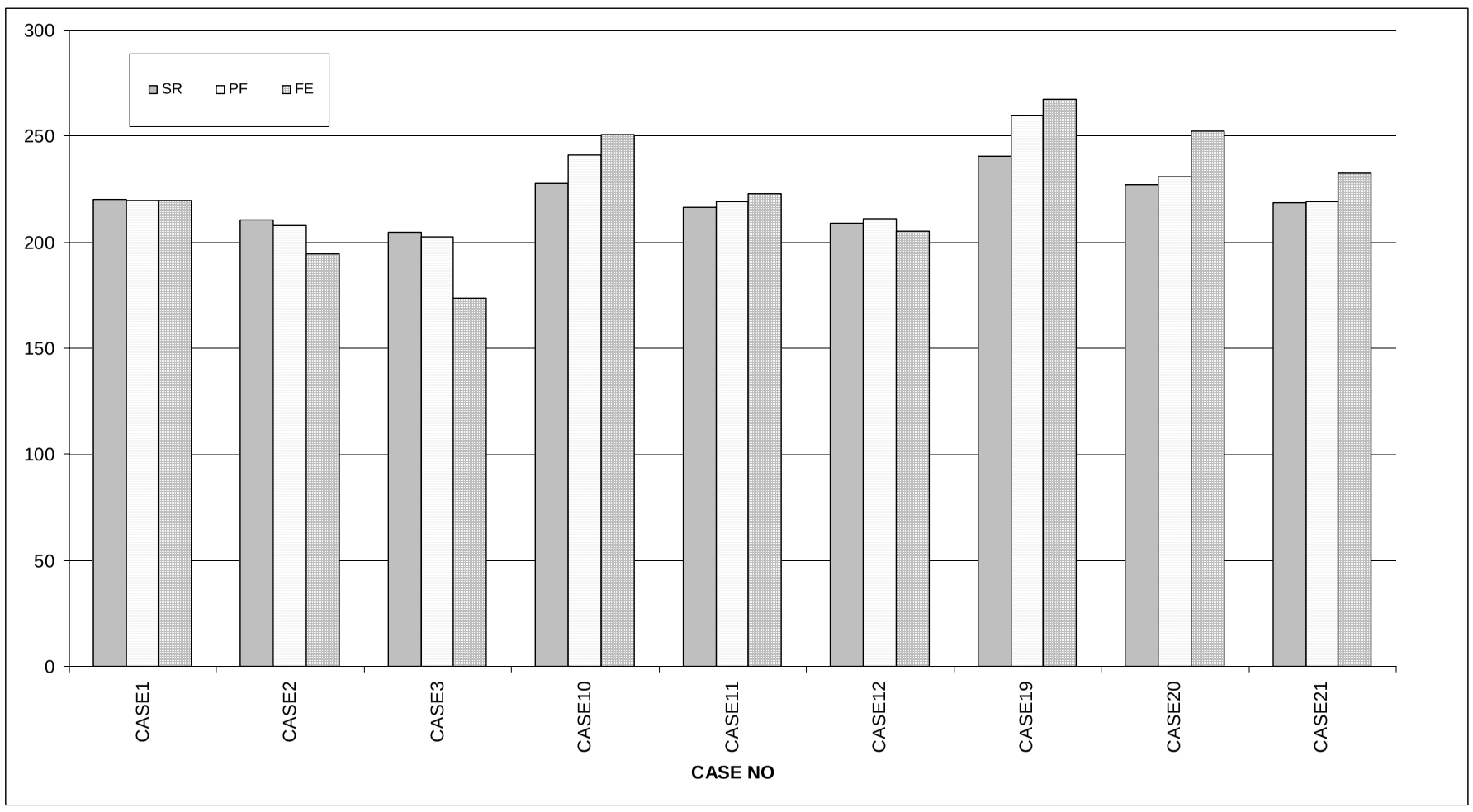

Figure 4.58 CASE 1-2-3-10-11-12-19-20-21 wall stem maximum bending moments (kNm / m)

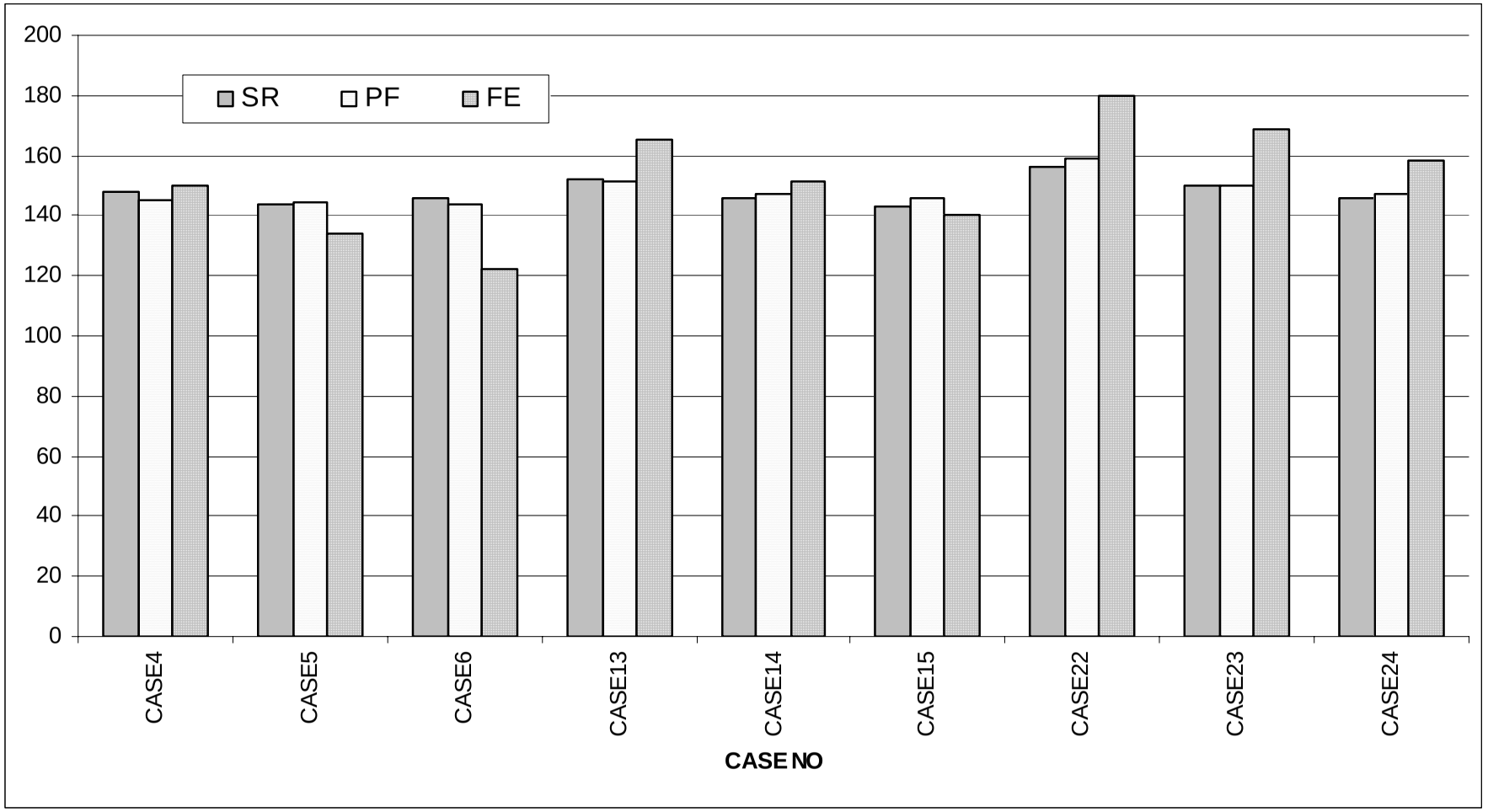

Figure 4.59 CASE 4-5-6-13-14-15-22-23-24 wall stem maximum bending moments (kNm / m)

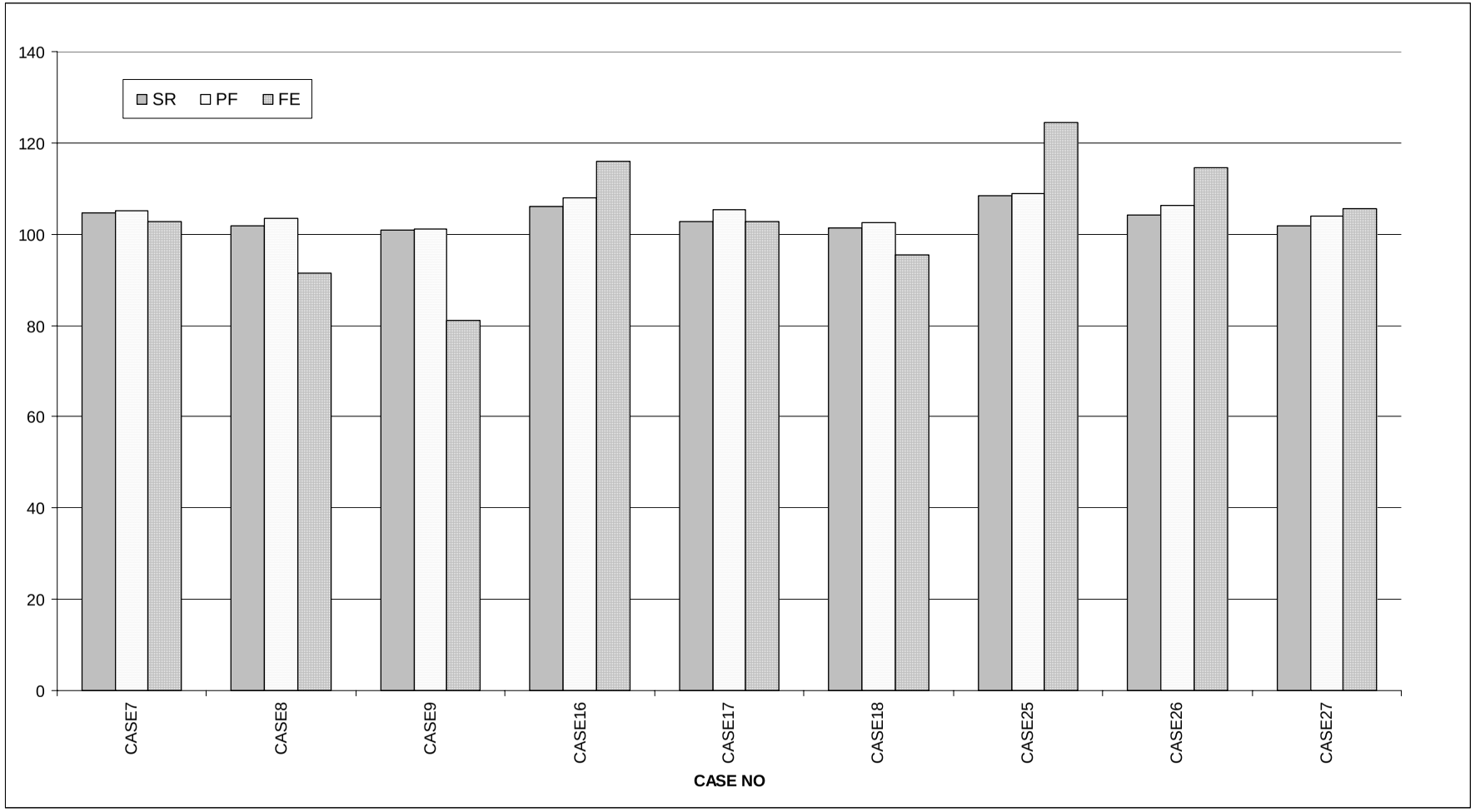

Figure 4.60 CASE 7-8-9-16-17-18-25-26-27 wall stem maximum bending moments (kNm / m)

4.4 Shear Forces

The wall shear forces at prop level and the maximum shear force at wall stem are examined by normalising with respect to shear forces as found by limit equilibrium method. The list of shear forces obtained in the analysis and normalised shear forces are represented in Tables 4.7-4.8-4.9-4.10.

Effect of E_{soil} on shear forces (Figures 4.61–4.69 & Figures 4.79 – 4.87) :

For all of the analysis cases and internal friction angle values of 30^0, 35^0, and 40^0, the normalised shear force at prop level decreases by increasing soil stiffness. It is also observed that for all of the wall-soil configurations, normalised maximum shear force at wall stem increases by increasing soil stiffness in finite element analyses.

Effect of EI_{wall} on shear forces (Figures 4.70–4.78 & 4.88&4.96):

For all of the analysis cases and internal friction angle values of 30^0, 35^0, and 40^0, the normalised shear force at prop level increases by increasing wall stiffness. It is also observed that for all of the wall-soil configurations, normalised maximum shear force at wall stem increases by increasing wall stiffness in finite element analyses.

Effect of method of analysis:

In $\phi=30^0$ group analysis cases (CASE1-2-3-10-11-12-19-20-21), normalised wall shear force at prop level is found to vary in the range of 1.04-1.14, 1.05–1.22 and 0.97–1.28 for subgrade reaction method, pseudo finite element method and finite element method respectively. In $\phi=30^0$ group analysis cases (CASE1-2-3-10-11-12-19-20-21), maximum normalised wall stem shear force is obtained to be in the range of 0.96-1.08, 0.93–1.08 and 0.94–1.17 by subgrade reaction method, pseudo finite element method and finite element method respectively.

In $\phi=35^0$ group analysis cases (CASE4-5-6-13-14-15-22-23-24), normalised wall shear force at prop level is found to be in the range of 1.04-1.09, 1.04–1.11 and 0.98–1.26 by subgrade reaction method, pseudo finite element method and finite element method respectively. In $\phi=35^0$ group analysis cases (CASE4-5-6-13-14-15-22-23-24) , maximum normalised wall stem shear force varies in the range of 0.98-1.08, 0.92–1.00 and 1.04–1.33 are obtained in subgrade reaction method, pseudo finite element method and finite element method respectively.

In $\phi=40^0$ group analysis cases (CASE7-8-9-16-17-18-25-26-27), normalised wall shear force at prop level is found to be in the range of 1.03-1.07, 1.04–1.08 and 0.93–1.23 by subgrade reaction method, pseudo finite element method and finite element method respectively. In $\phi=35^0$ group analysis cases (CASE4-5-6-13-14-15-22-23-24) , maximum normalised wall stem shear force varies in the range of 0.92-0.98, 0.88–0.92 and 0.95–1.27 as obtained by subgrade reaction method, pseudo finite element method and finite element method respectively.

Table 4.7 Summary of wall shear forces at prop level obtained from the analysis (kN / m)

CASE NAME	Subgrade Reaction	Pseudo Finite	Finite Element
CASE1	91.06	93.45	94.16
CASE2	88.61	89.66	87.14
CASE3	87.16	87.74	81.08
CASE4	67.1	67.1	69.91
CASE5	64.83	65.89	64.93
CASE6	65.48	65.12	61.10
CASE7	49.19	50.67	50.79
CASE8	48.5	49.08	46.88
CASE9	48.25	48.51	43.66
CASE10	93.06	97.39	101.93
CASE11	91.07	91.07	94.39
CASE12	88.26	89.11	89.57
CASE13	66.95	67.5	74.05
CASE14	65.38	66.1	69.92
CASE15	64.66	65.63	66.14
CASE16	49.55	50.42	54.64
CASE17	48.78	49.54	50.28
CASE18	48.39	48.84	47.58
CASE19	96.16	102.42	107.25
CASE20	92.74	93.78	102.18
CASE21	90.69	91.03	96.47
CASE22	68.26	69.04	78.51
CASE23	66.52	66.77	74.98
CASE24	65.48	66.1	71.25
CASE25	50.2	50.47	57.44
CASE26	49.11	49.81	53.68
CASE27	48.51	49.19	50.59

Table 4.8 Summary of normalised wall shear forces at prop level

CASE NAME	Subgrade Reaction	Pseudo Finite	Finite Element
CASE1	1.087	1.115	1.124
CASE2	1.058	1.070	1.040
CASE3	1.040	1.047	0.968
CASE4	1.076	1.076	1.121
CASE5	1.040	1.057	1.041
CASE6	1.050	1.044	0.980
CASE7	1.053	1.084	1.087
CASE8	1.038	1.050	1.003
CASE9	1.033	1.038	0.934
CASE10	1.111	1.162	1.217
CASE11	1.087	1.087	1.127
CASE12	1.053	1.064	1.069
CASE13	1.074	1.082	1.187
CASE14	1.048	1.060	1.121
CASE15	1.037	1.052	1.061
CASE16	1.060	1.079	1.169
CASE17	1.044	1.060	1.076
CASE18	1.036	1.045	1.018
CASE19	1.148	1.222	1.280
CASE20	1.107	1.119	1.220
CASE21	1.082	1.087	1.151
CASE22	1.095	1.107	1.259
CASE23	1.067	1.071	1.202
CASE24	1.050	1.060	1.143
CASE25	1.074	1.080	1.229
CASE26	1.051	1.066	1.149
CASE27	1.038	1.053	1.083

Table 4.9 Summary of maximum shear forces at wall stem obtained from the analysis (kN / m)

CASE NAME	Subgrade Reaction	Pseudo Finite	Finite Element
CASE1	82.07	77.62	84.24
CASE2	79.3	76.02	82.89
CASE3	78.78	77.67	76.51
CASE4	67.15	61.01	77.13
CASE5	65.13	61.54	69.48
CASE6	66.58	62.31	68.96
CASE7	50.69	47.61	58.10
CASE8	49.78	49.2	53.51
CASE9	50.03	49.77	51.25
CASE10	84.72	83.39	94.17
CASE11	80.91	77.57	87.89
CASE12	78.97	76.83	81.17
CASE13	69.49	63.43	83.25
CASE14	66.41	61.83	78.54
CASE15	64.83	61.89	73.91
CASE16	51.47	48.39	62.03
CASE17	49.98	48.74	57.30
CASE18	49.89	49.44	55.01
CASE19	88.31	88.38	95.97
CASE20	84.35	80.98	94.62
CASE21	81.56	77.86	89.70
CASE22	71.85	66.46	88.55
CASE23	68.67	63.16	83.79
CASE24	66.58	62.23	82.46
CASE25	52.86	48.89	68.15
CASE26	50.48	48.47	62.67
CASE27	49.77	49.09	59.71

Table 4.10 Summary of normalised maximum wall shear forces at wall stem

CASE NAME	Subgrade Reaction	Pseudo Finite	Finite Element
CASE1	1.004	0.949	1.030
CASE2	0.970	0.930	1.014
CASE3	0.963	0.950	0.936
CASE4	1.012	0.919	1.162
CASE5	0.981	0.927	1.047
CASE6	1.003	0.939	1.039
CASE7	0.941	0.884	1.079
CASE8	0.925	0.914	0.994
CASE9	0.929	0.924	0.952
CASE10	1.036	1.020	1.152
CASE11	0.989	0.949	1.075
CASE12	0.966	0.940	0.993
CASE13	1.047	0.956	1.255
CASE14	1.001	0.932	1.184
CASE15	0.977	0.933	1.114
CASE16	0.956	0.899	1.152
CASE17	0.928	0.905	1.064
CASE18	0.927	0.918	1.022
CASE19	1.080	1.081	1.174
CASE20	1.032	0.990	1.157
CASE21	0.997	0.952	1.097
CASE22	1.083	1.002	1.334
CASE23	1.035	0.952	1.263
CASE24	1.003	0.938	1.243
CASE25	0.982	0.908	1.266
CASE26	0.938	0.900	1.164
CASE27	0.924	0.912	1.109

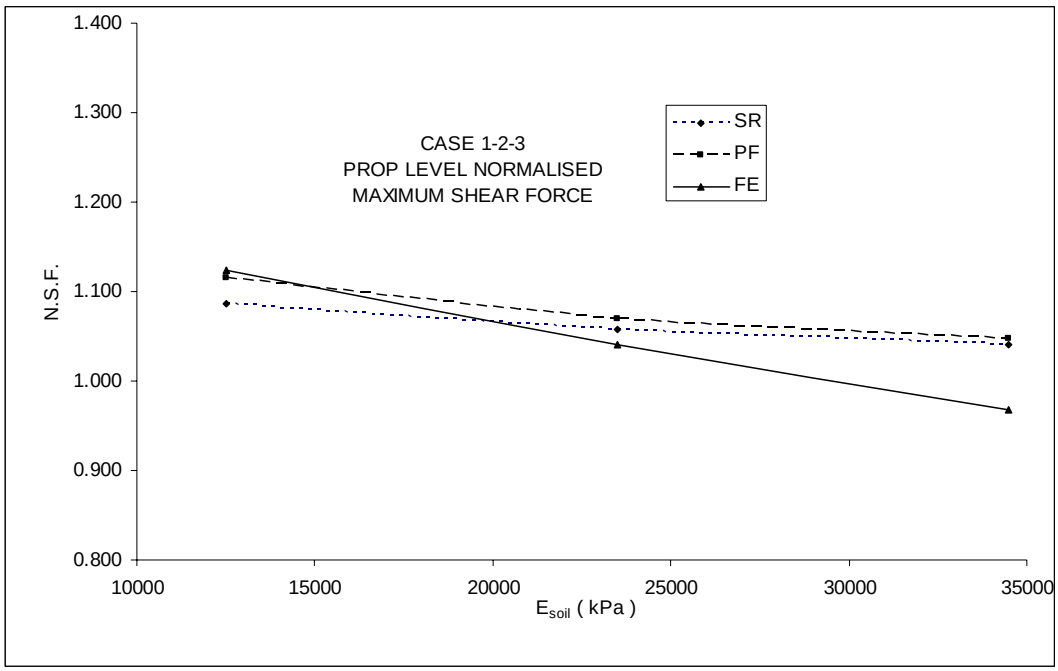

Figure 4.61 Prop level normalised maximum shear force vs E_{soil}

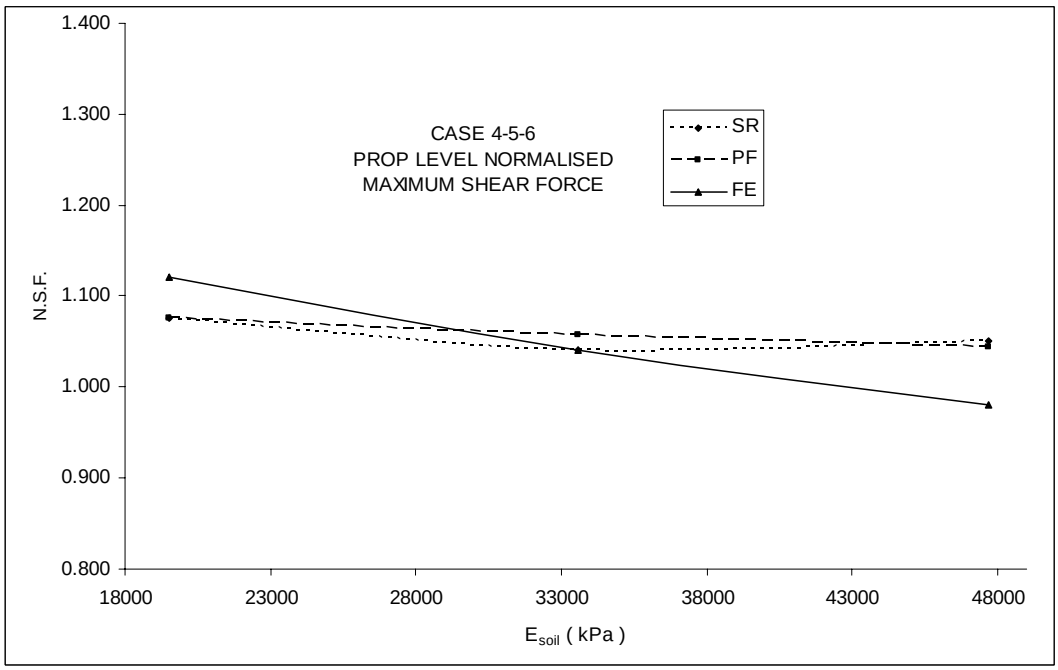

Figure 4.62 Prop level normalised maximum shear force vs E_{soil}

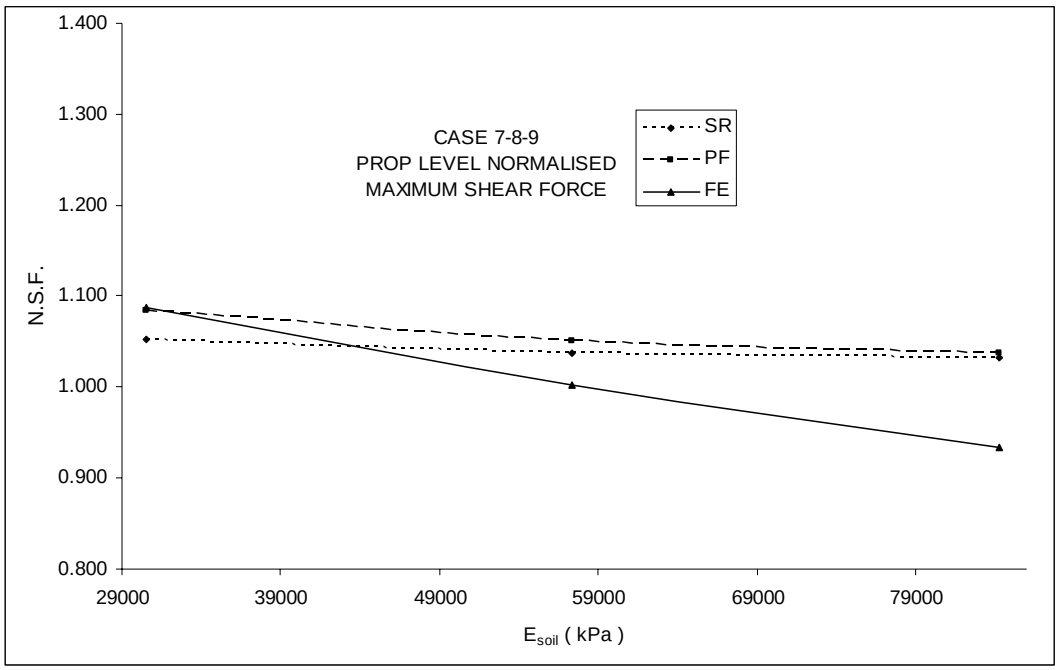

Figure 4.63 Prop level normalised maximum shear force vs E_{soil}

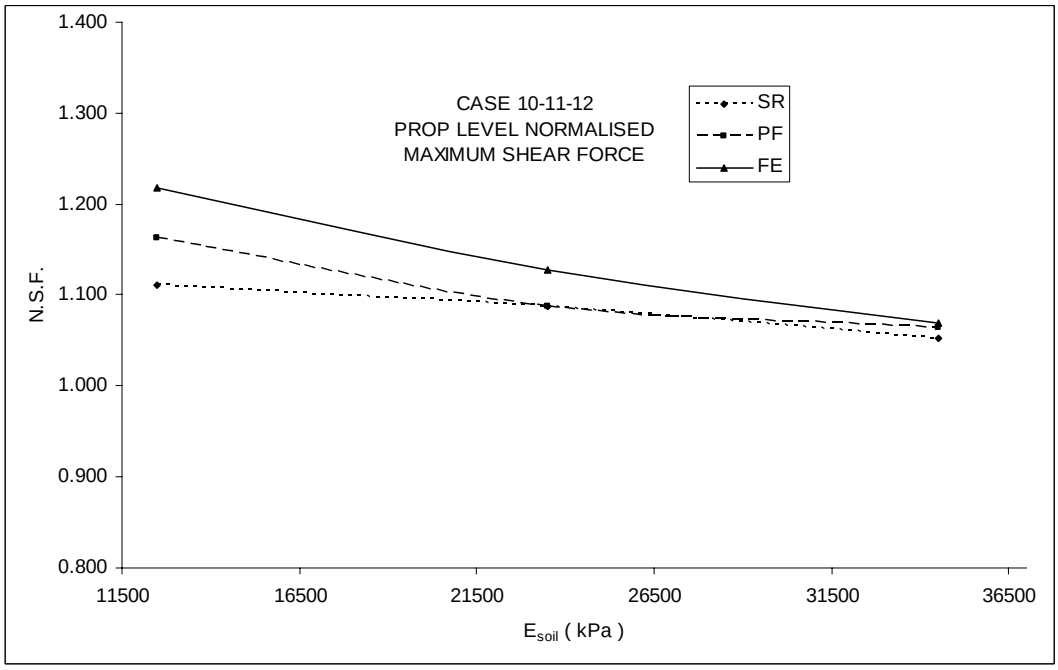

Figure 4.64 Prop level normalised maximum shear force vs E_{soil}

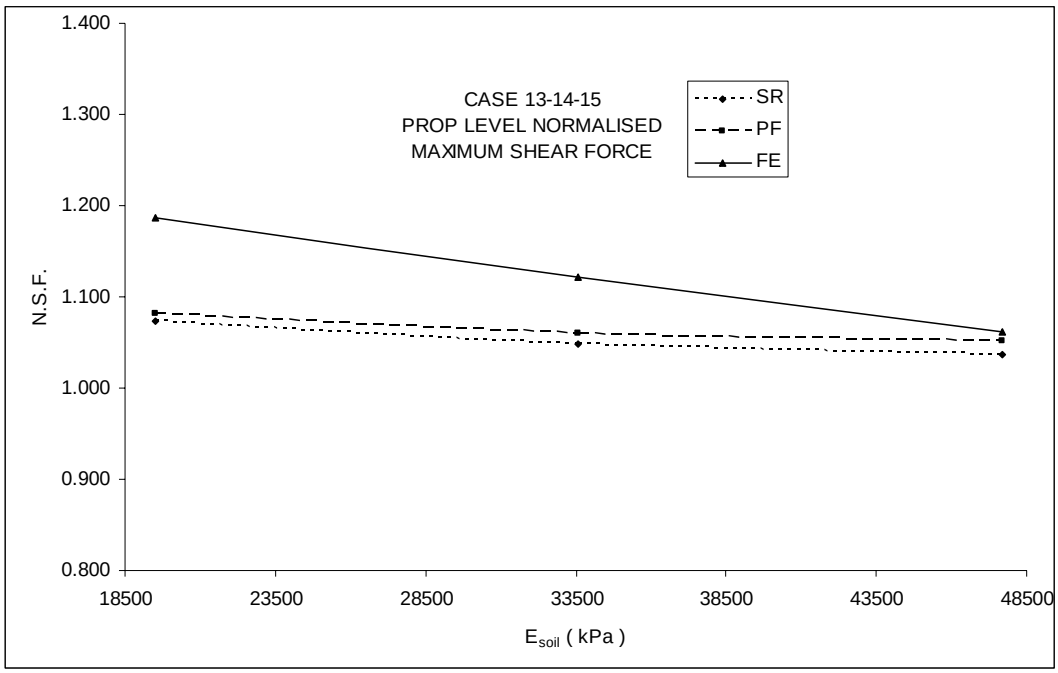

Figure 4.65 Prop level normalised maximum shear force vs E_{soil}

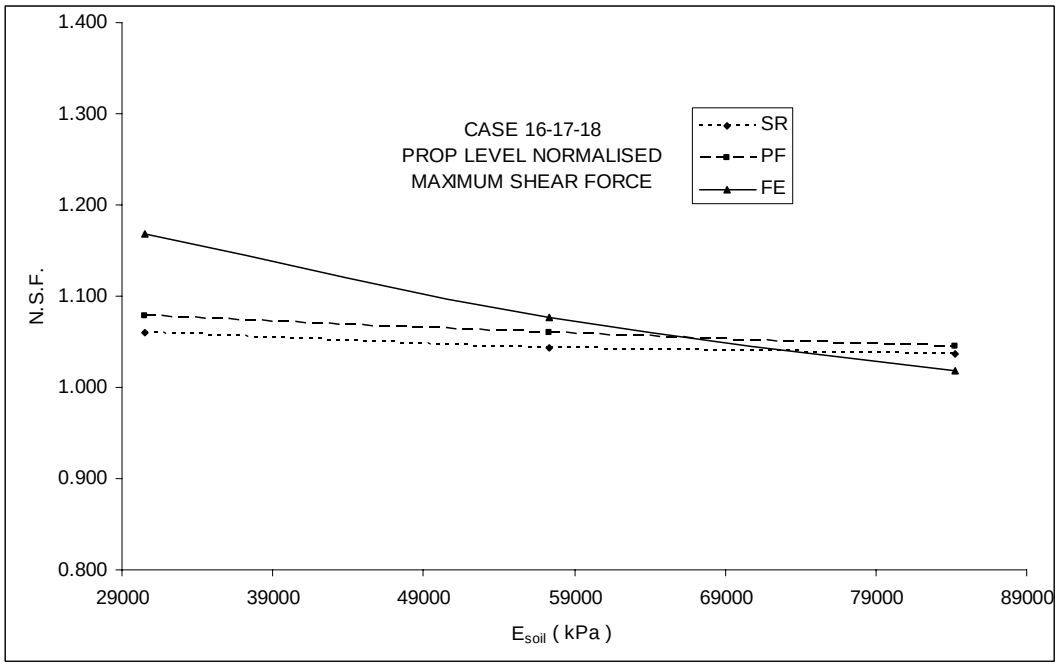

Figure 4.66 Prop level normalised maximum shear force vs E_{soil}

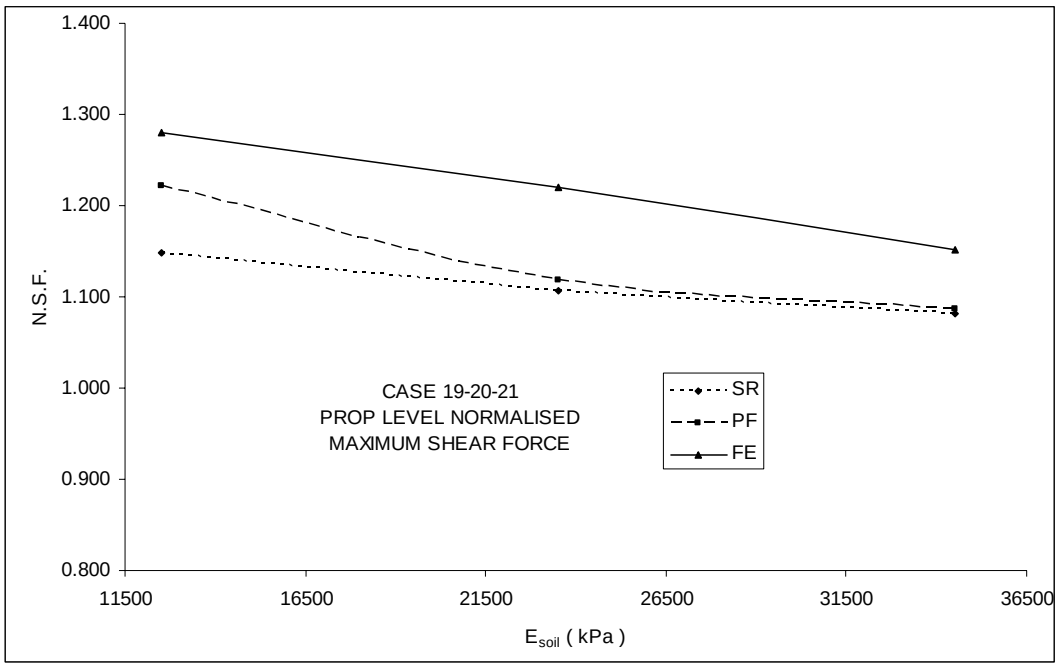

Figure 4.67 Prop level normalised maximum shear force vs E_{soil}

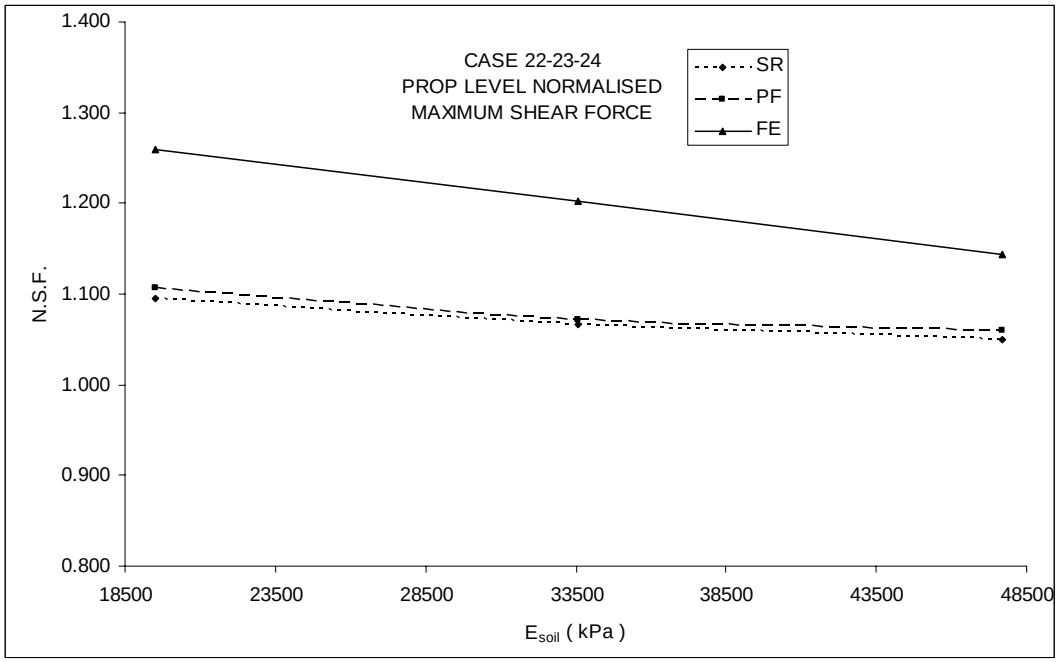

Figure 4.68 Prop level normalised maximum shear force vs E_{soil}

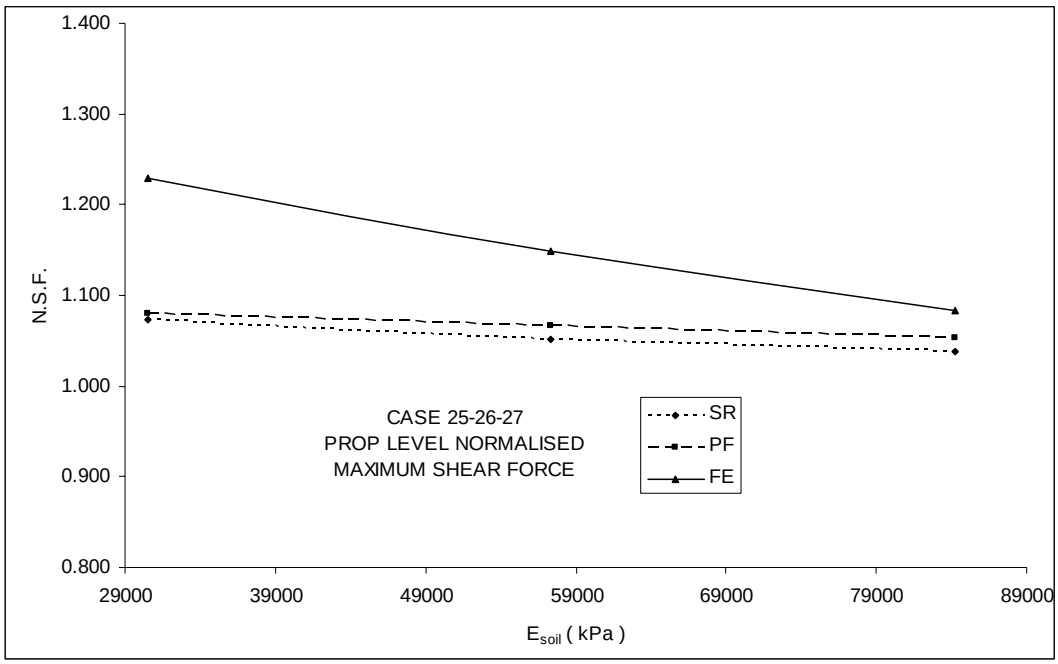

Figure 4.69 Prop level normalised maximum shear force vs E_{soil}

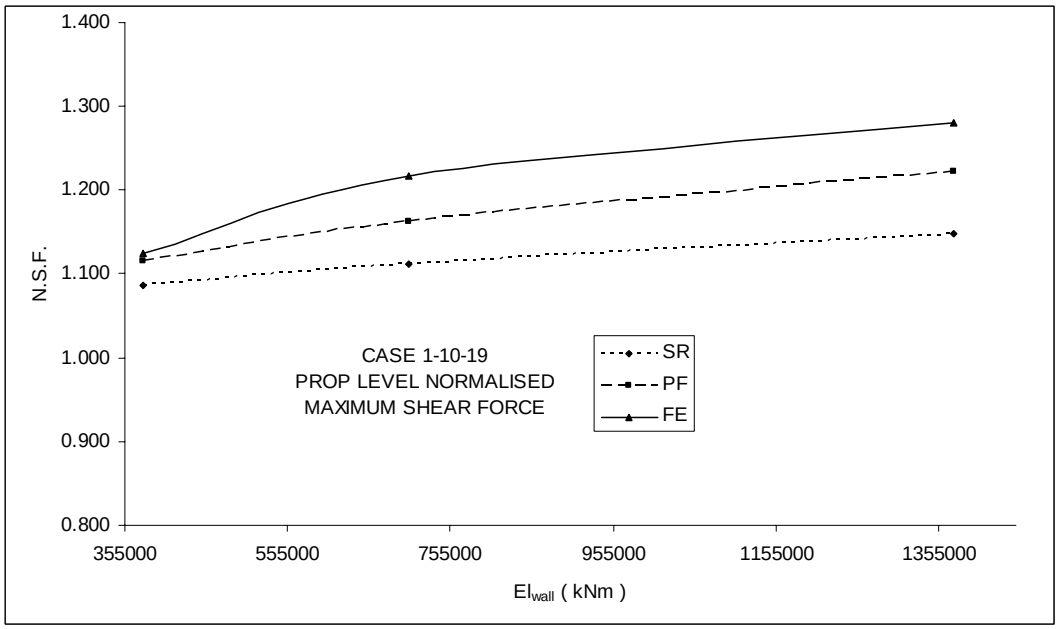

Figure 4.70 Prop level normalised maximum shear force vs EI_{wall}

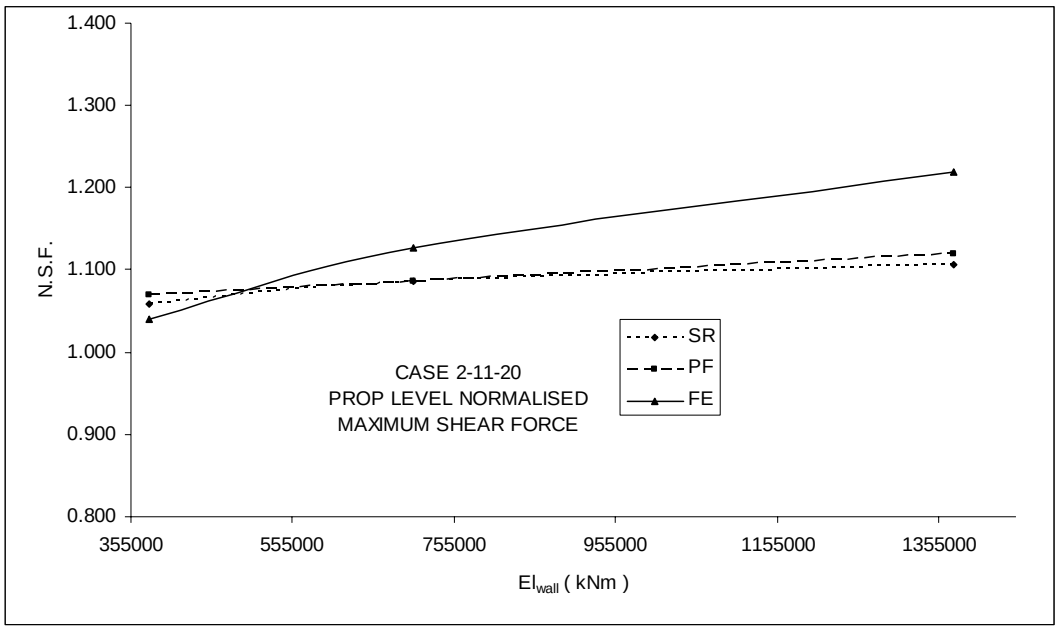

Figure 4.71 Prop level normalised maximum shear force vs EI_{wall}

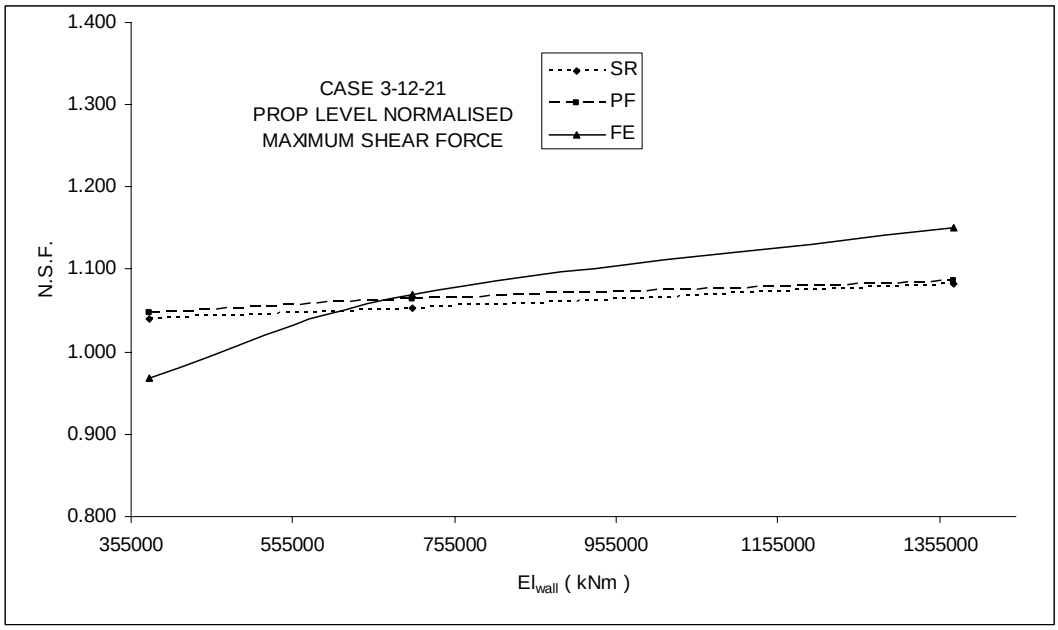

Figure 4.72 Prop level normalised maximum shear force vs EI_{wall}

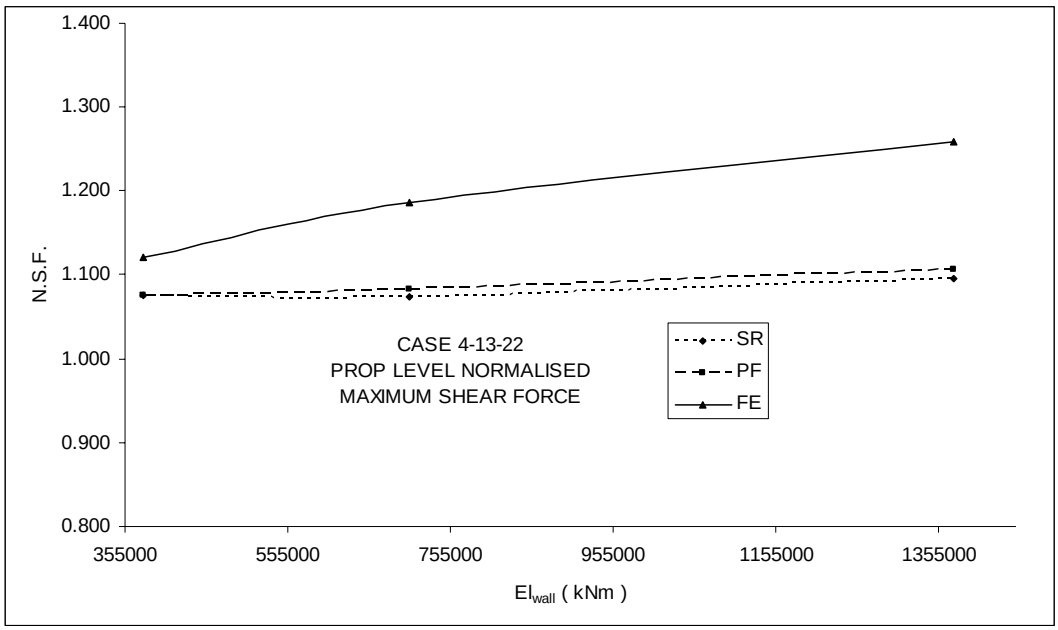

Figure 4.73 Prop level normalised maximum shear force vs EI_{wall}

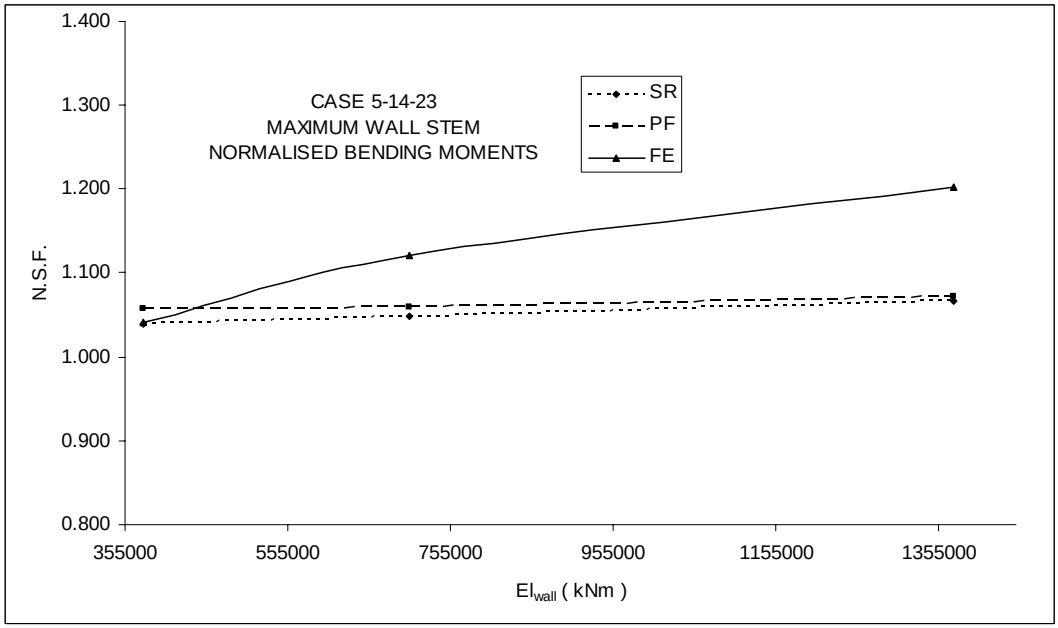

Figure 4.74 Prop level normalised maximum shear force vs EI_{wall}

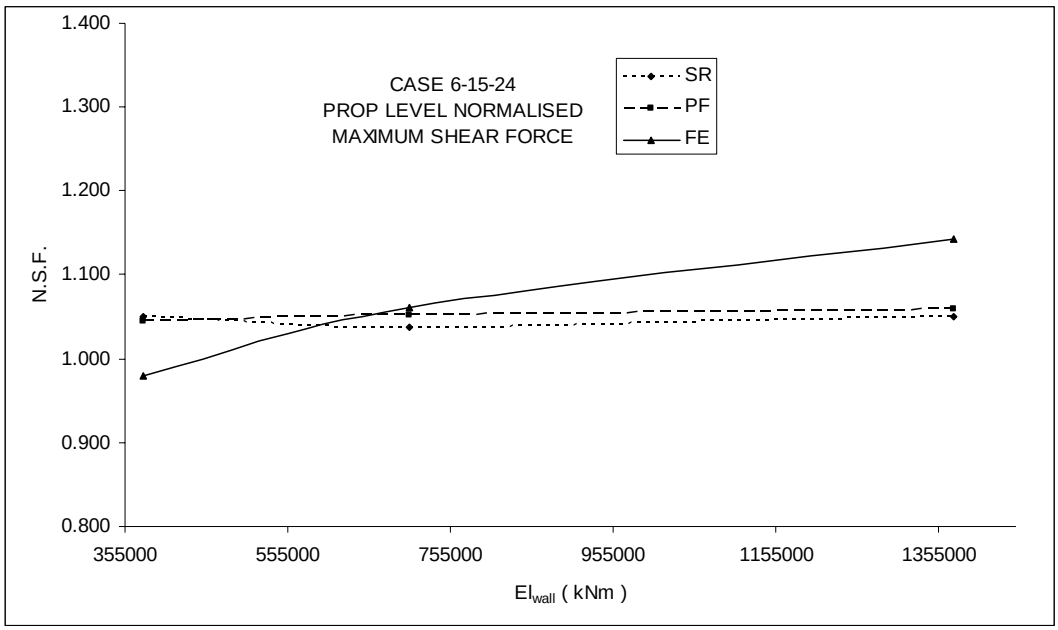

Figure 4.75 Prop level normalised maximum shear force vs EI_{wall}

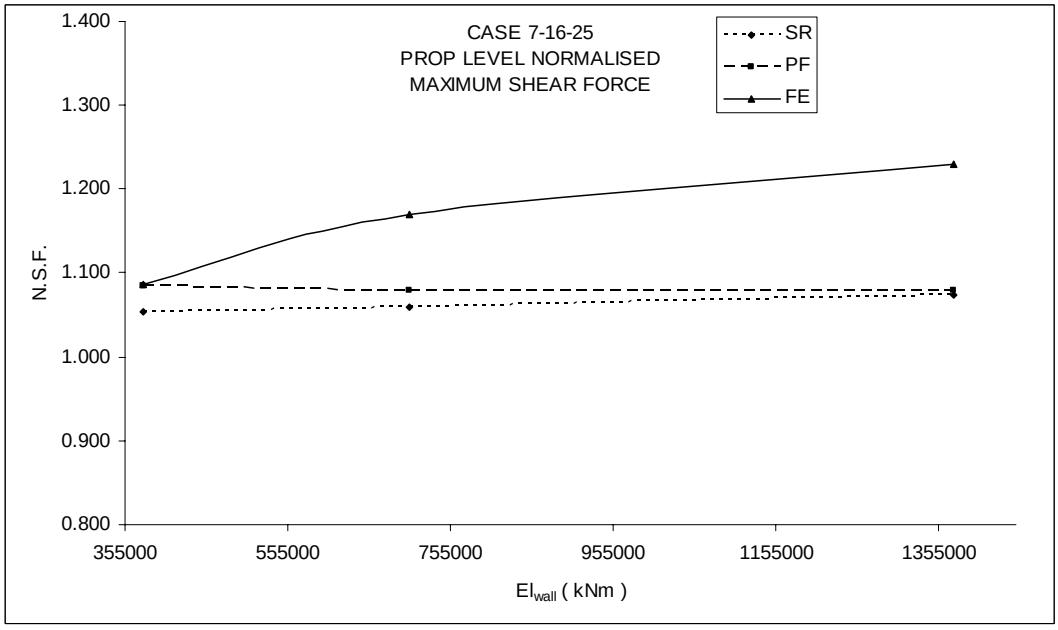

Figure 4.76 Prop level normalised maximum shear force vs EI_{wall}

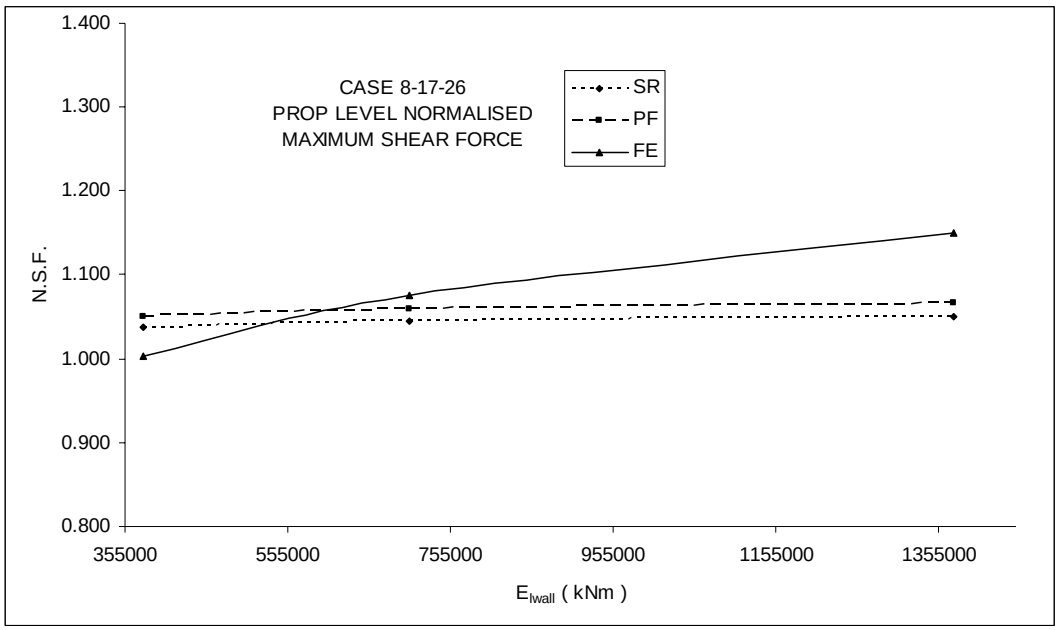

Figure 4.77 Prop level normalised maximum shear force vs EI_{wall}

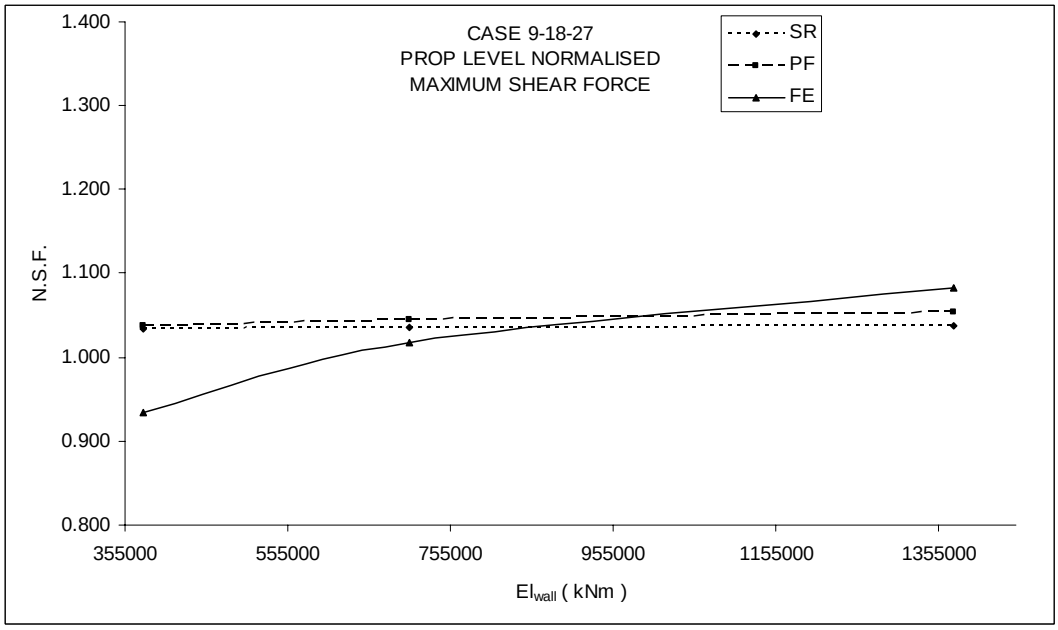

Figure 4.78 Prop level normalised maximum shear force vs EI_{wall}

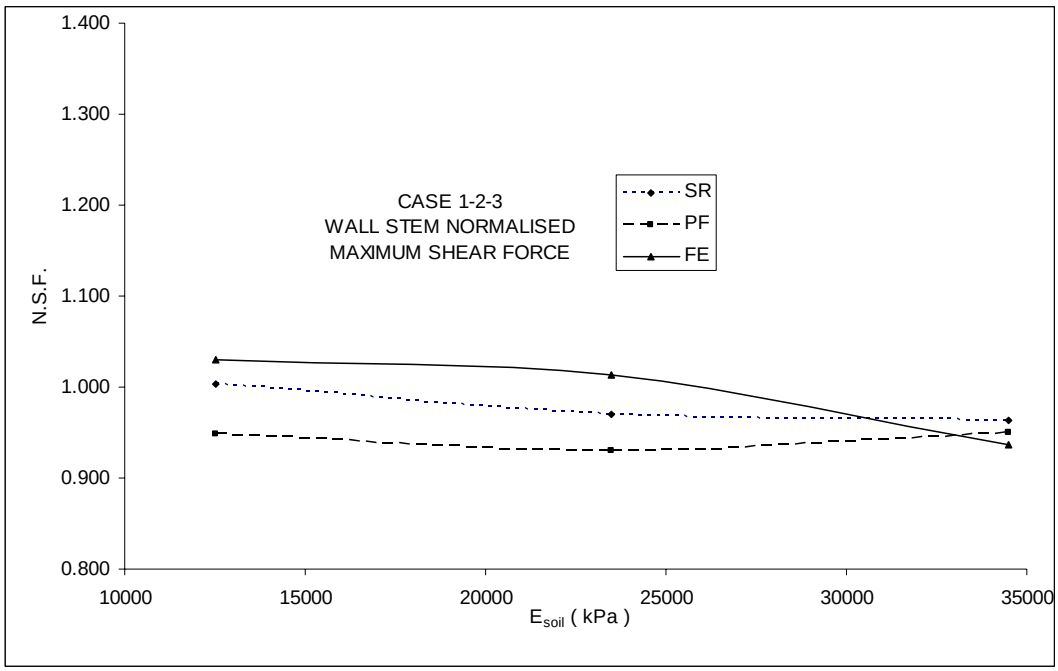

Figure 4.79 Wall stem normalised maximum shear force vs E_{soil}

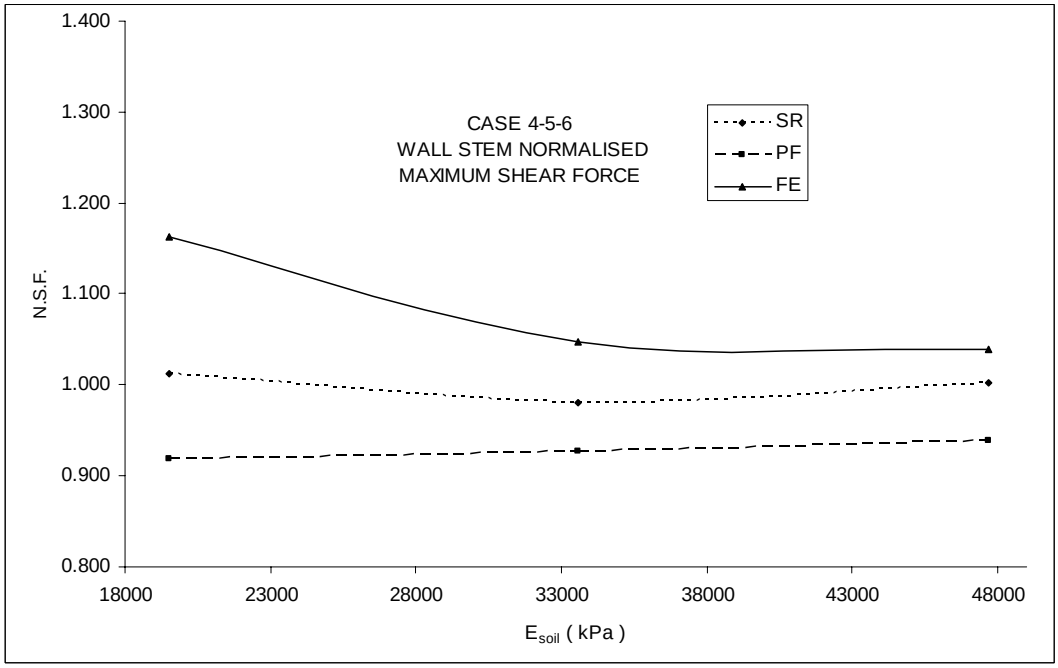

Figure 4.80 Wall stem normalised maximum shear force vs E_{soil}

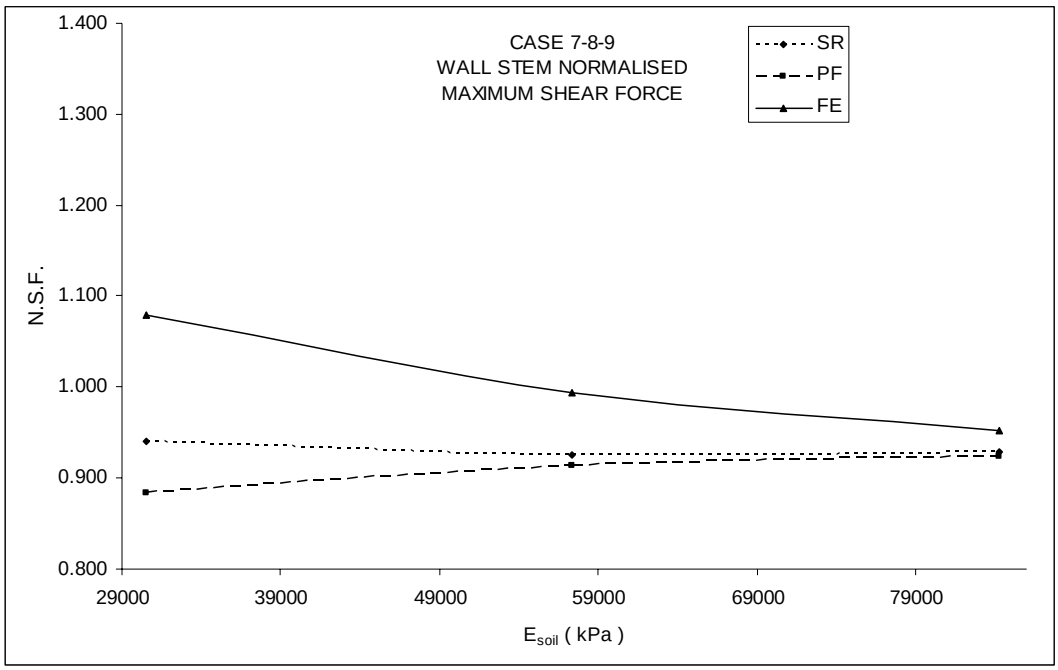

Figure 4.81 Wall stem normalised maximum shear force vs E_{soil}

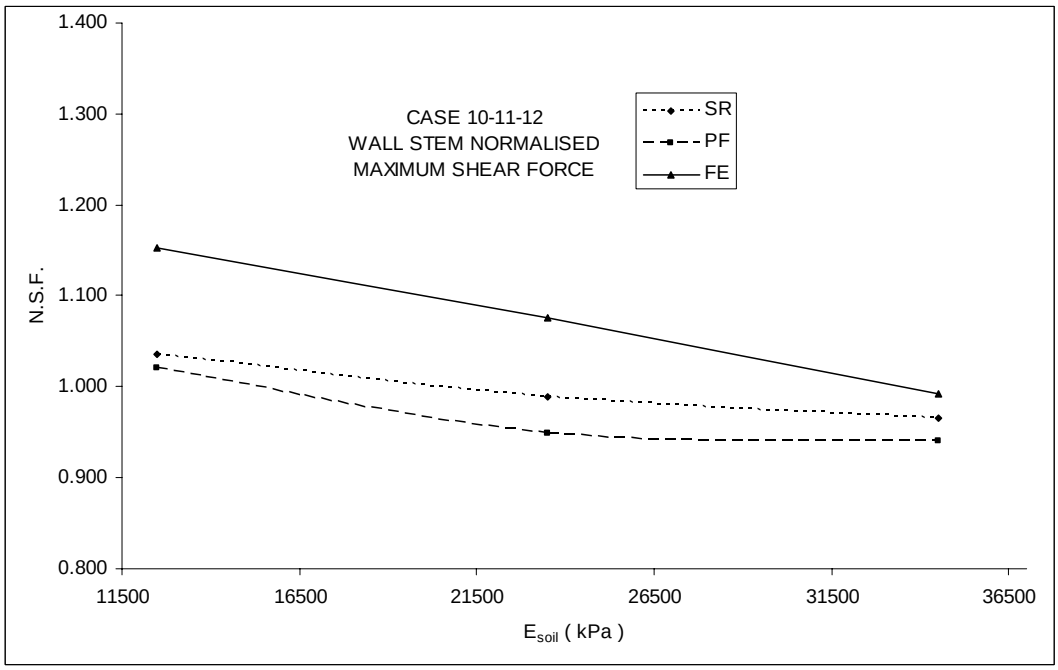

Figure 4.82 Wall stem normalised maximum shear force vs E_{soil}

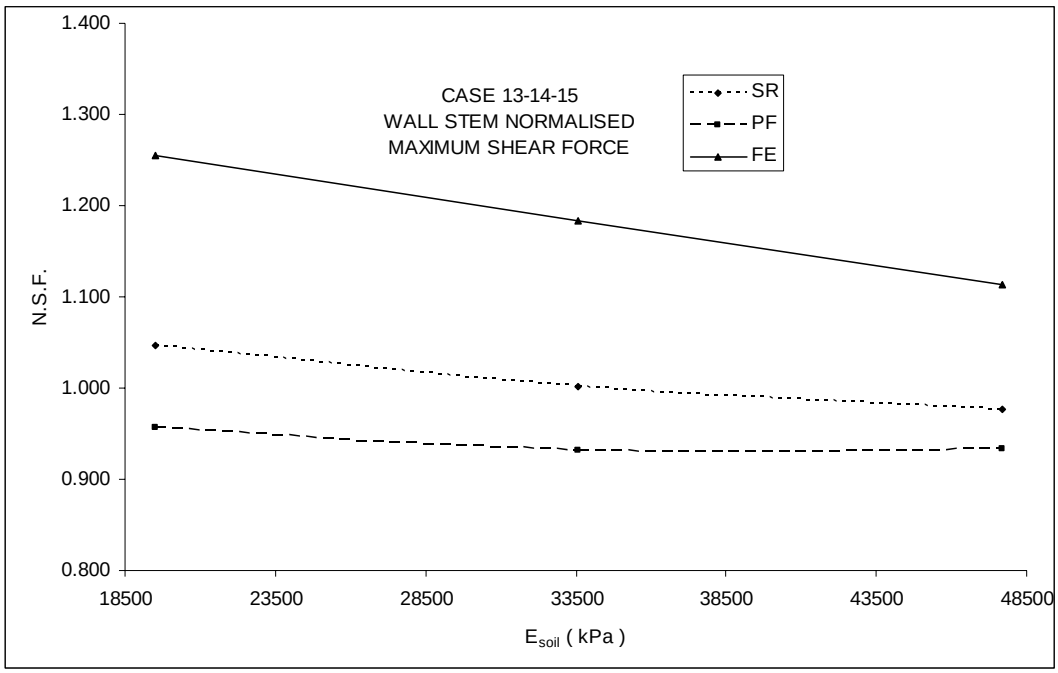

Figure 4.83 Wall stem normalised maximum shear force vs E_{soil}

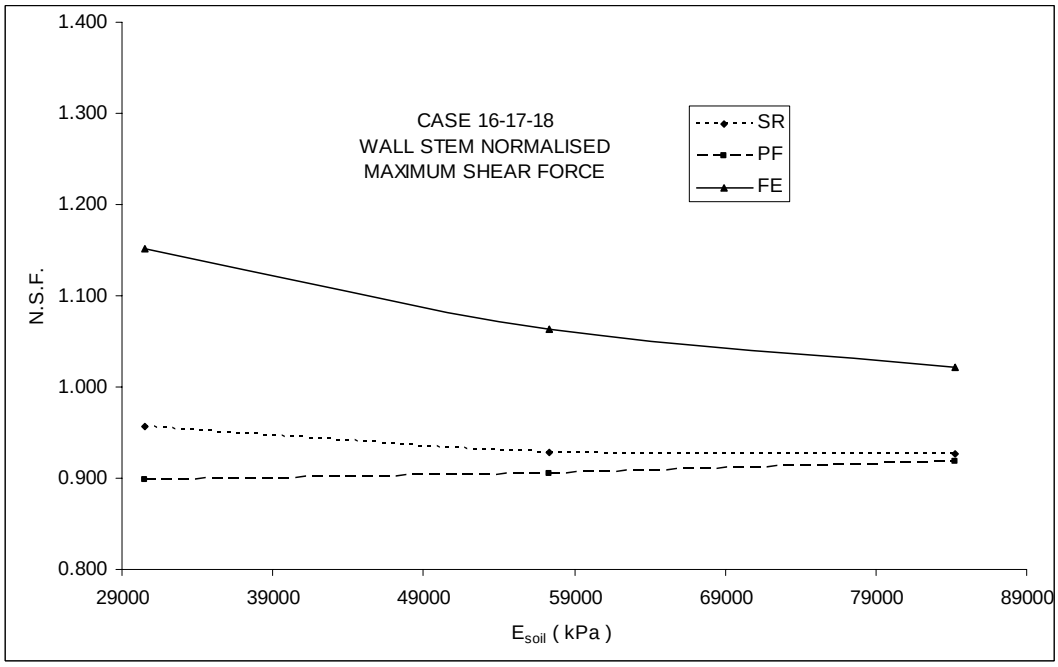

Figure 4.84 Wall stem normalised maximum shear force vs E_{soil}

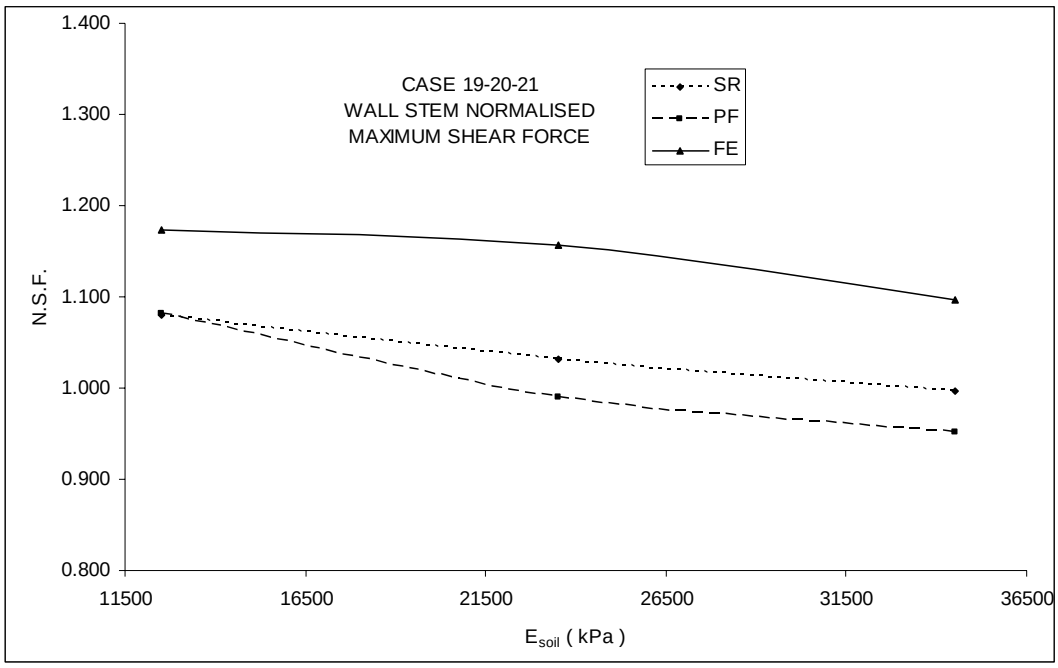

Figure 4.85 Wall stem normalised maximum shear force vs E_{soil}

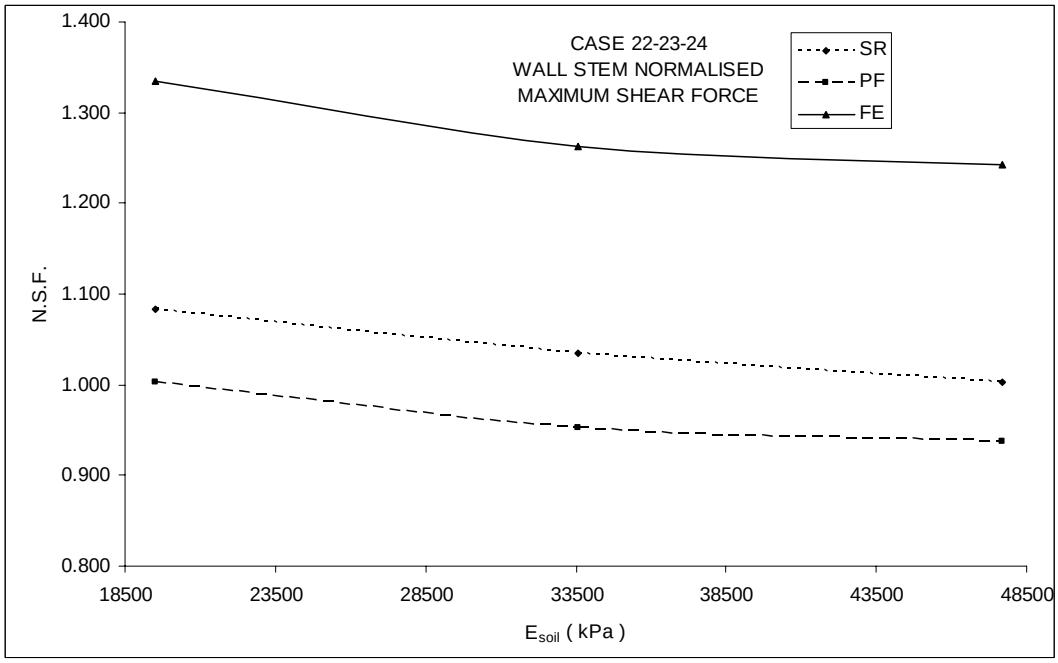

Figure 4.86 Wall stem normalised maximum shear force vs E_{soil}

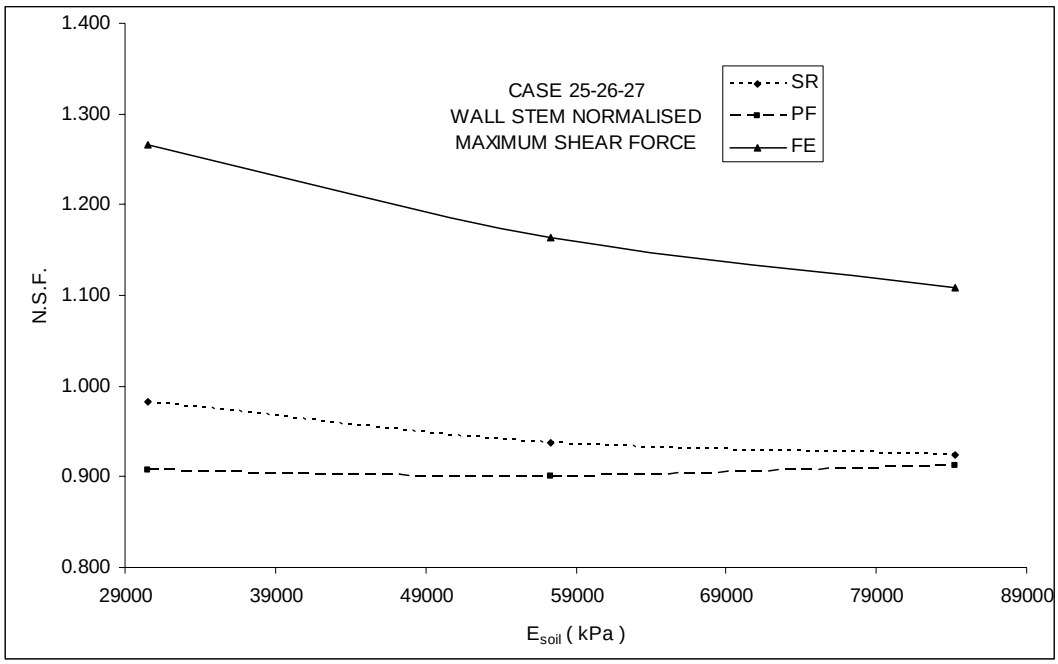

Figure 4.87 Wall stem normalised maximum shear force vs E_{soil}

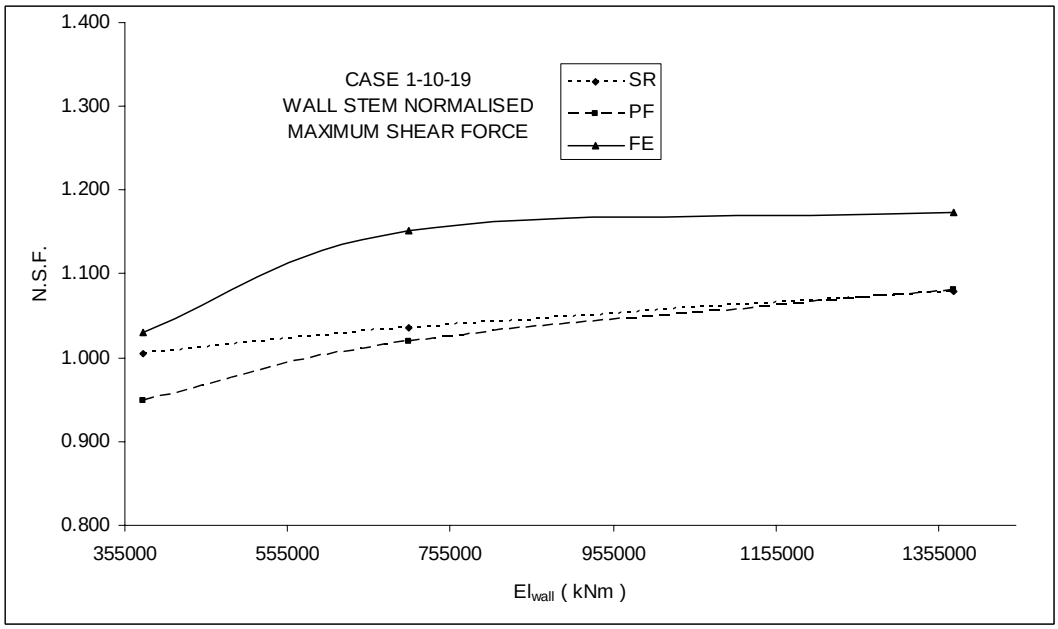

Figure 4.88 Wall stem normalised maximum shear force vs EI_{wall}

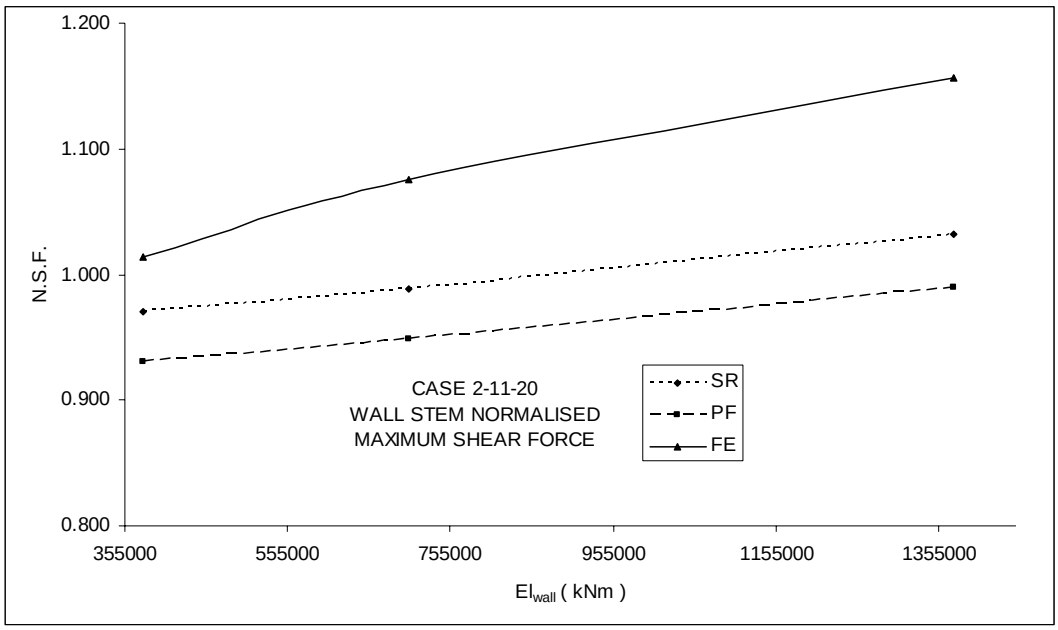

Figure 4.89 Wall stem normalised maximum shear force vs EI_{wall}

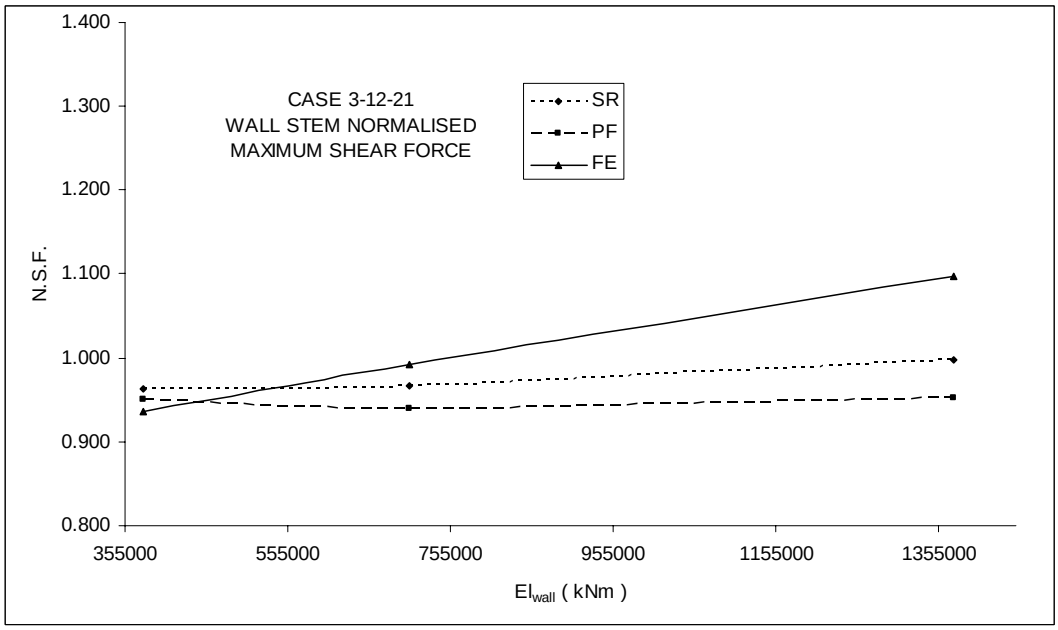

Figure 4.90 Wall stem normalised maximum shear force vs EI_{wall}

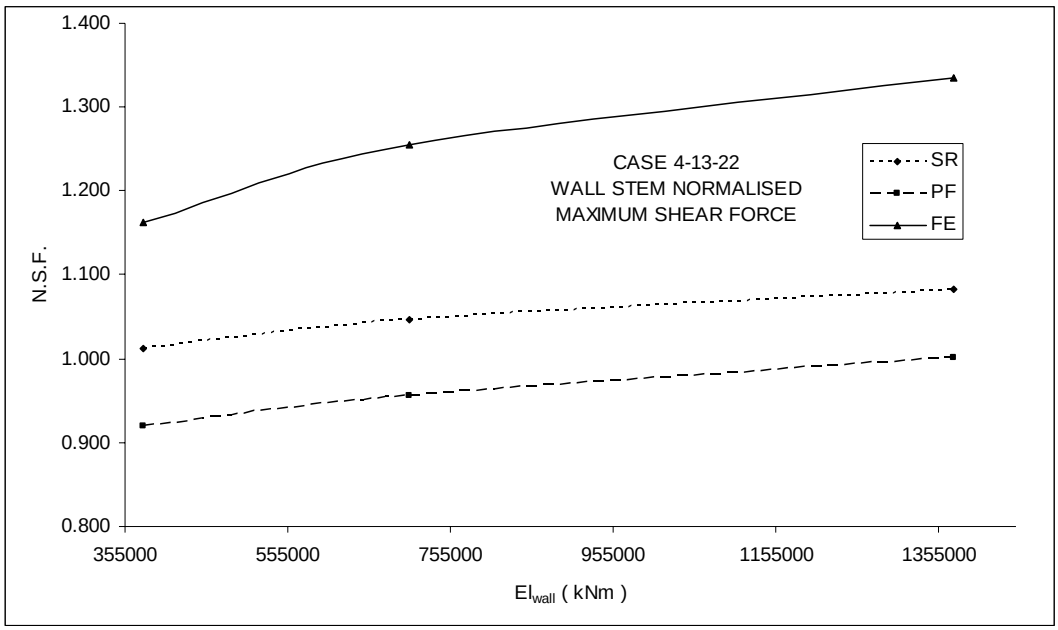

Figure 4.91 Wall stem normalised maximum shear force vs EI_{wall}

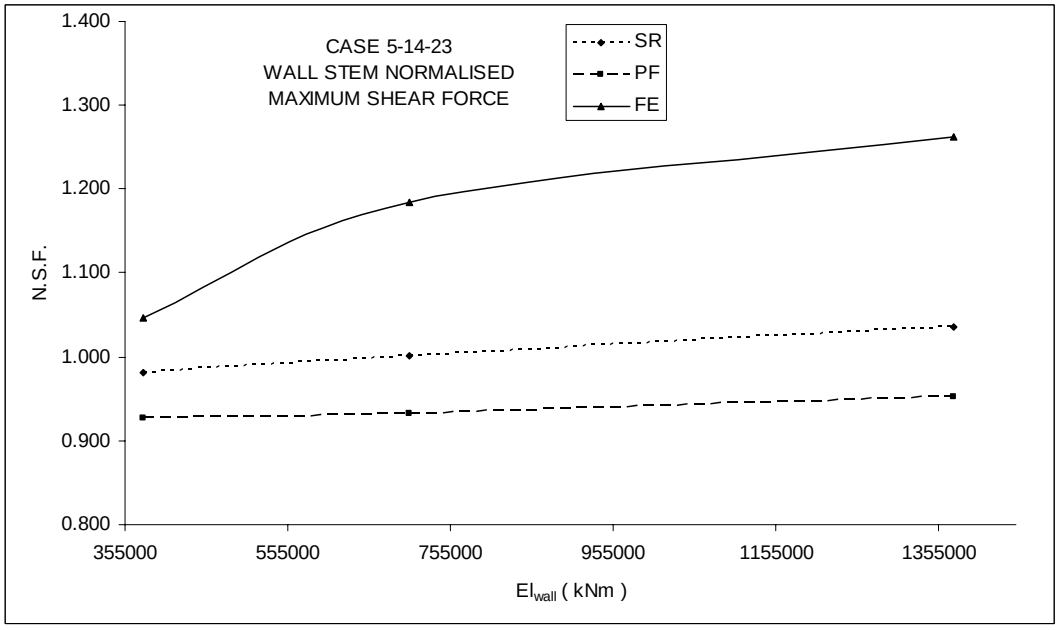

Figure 4.92 Wall stem normalised maximum shear force vs EI_{wall}

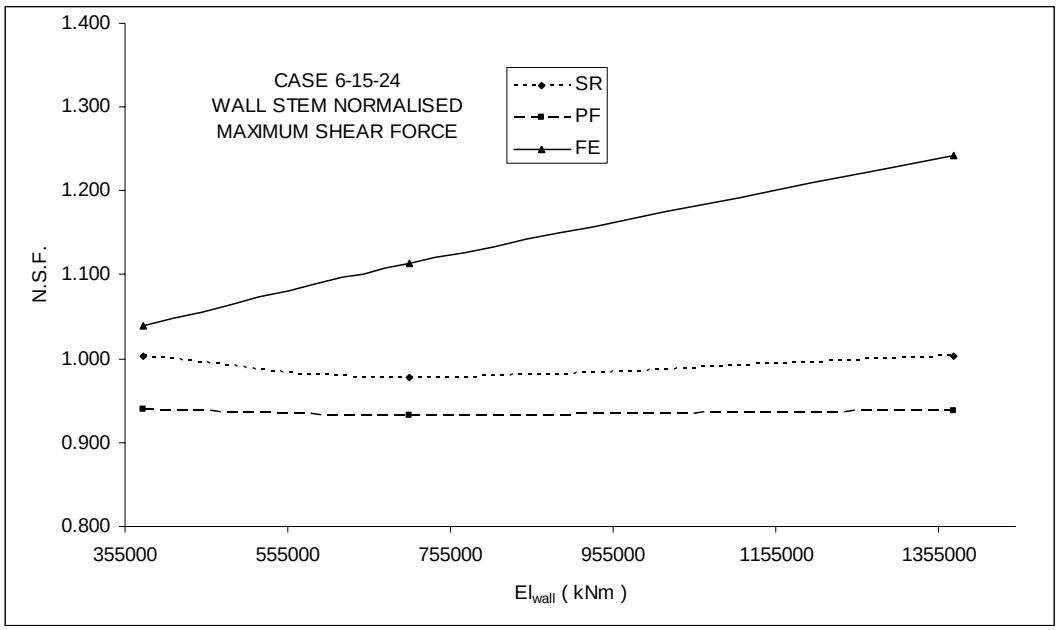

Figure 4.93 Wall stem normalised maximum shear force vs EI_{wall}

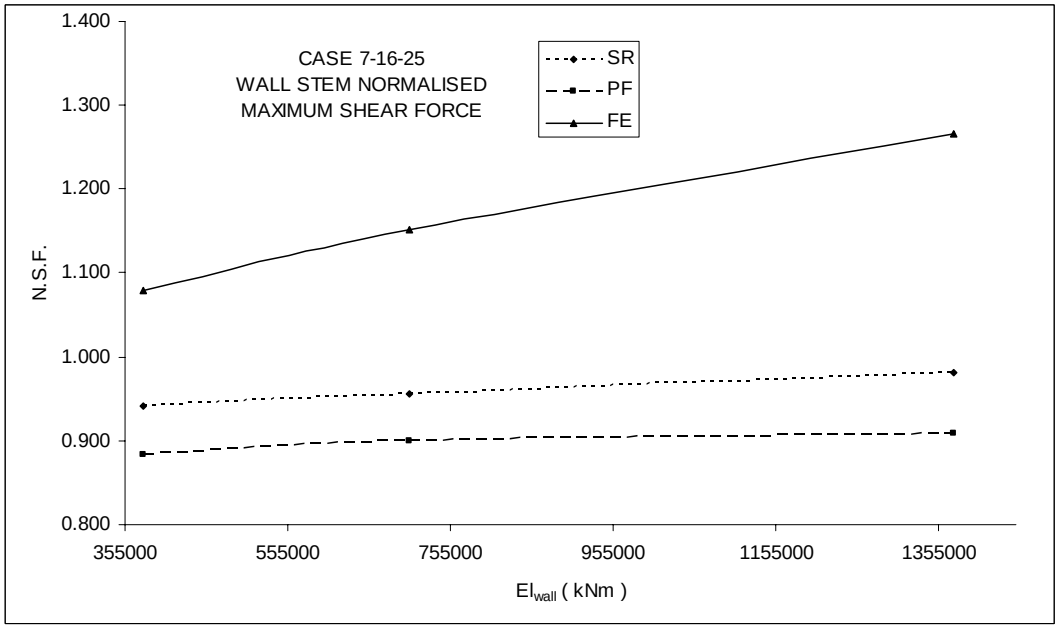

Figure 4.94 Wall stem normalised maximum shear force vs EI_{wall}

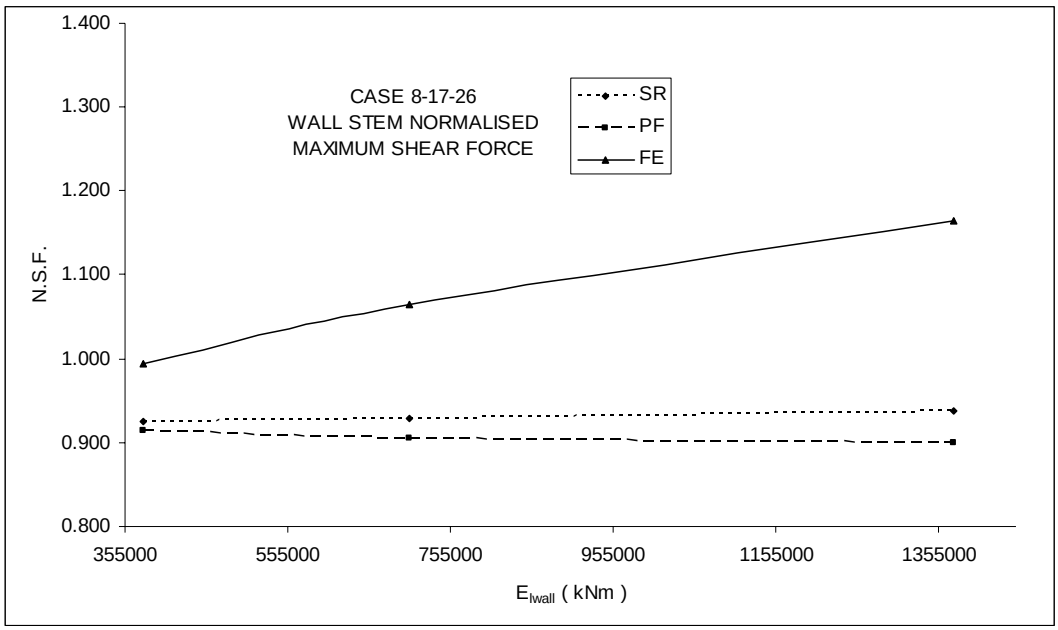

Figure 4.95 Wall stem normalised maximum shear force vs EI_{wall}

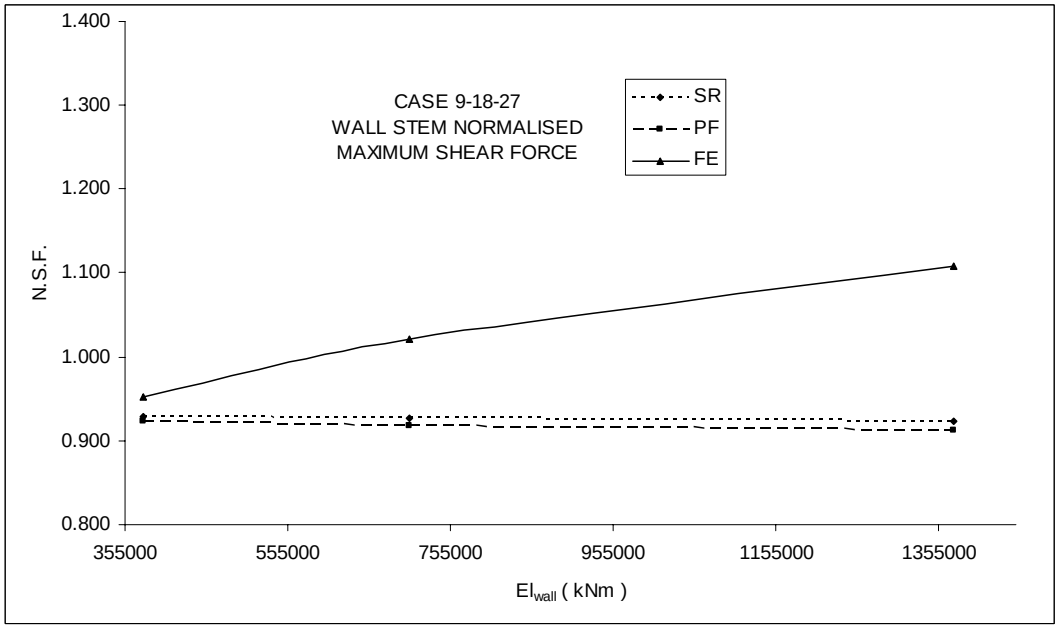

Figure 4.96 Wall stem normalised maximum shear force vs EI_{wall}

CHAPTER 5

CONCLUSIONS

A parametric study is carried out in order to asses the effect of wall rigidity, soil stiffness, soil friction angle on structural forces for single-propped embedded retaining walls. Analyses are made by utilizing subgrade reaction method, pseudo-finite element method, finite element method and limit equilibrium method.

A single propped tangent pile embedded wall (Figure 3.1) in a deep normally consolidated cohesionless sand deposit is considered. The excavation width is taken as 12 m and retained height h as 8 m. The wall is supported by a single strut at 2 m below the top (-2.00 level) with a center to center spacing of 5 m in horizontal direction. Soil friction angles are taken as 30^o, 35^o, and 40^o. Three different values of soil stiffness are taken into account for each value of soil friction angle, ϕ.

Following conlusions are drawn as a result of the study:

- For all of the analysis cases and internal friction angle values of 30^o, 35^o, and 40^o normalized strut loads decrease as Young's modulus of the backfill increases.

- For all wall configurations and soil friction angle values, normalised strut loads increase as the wall flexural rigidity, EI_{wall}, increases.

- Maximum strut load in each case is obtained by finite element method while the minimum strut load is obtained in subgrade reaction method.

- Normalised wall bending moment at strut level decreases with increasing wall rigidity in finite element and pseudo-finite element methods, for all the wall configurations studied and backfill internal friction angles of 30^0, 35^0, and 40^0. However, in subgrade reaction method normalized bending moment at strut level is not affected by a change in wall rigidity.

- The subgrade reaction method yields almost the same wall bending moment at prop level with the limit equilibrium method. The finite element method yields greater bending moments as compared to the results obtained by limit equilibrium method. The pseudo finite element method yields values of bending moments at prop level between those of obtained by subgrade reaction and finite element methods.

- For all of the wall configurations and soil internal friction angle values of 30^0, 35^0, and 40^0, the normalized shear force at prop level decreases by increasing soil stiffness. It is also observed that for all of the cases normalised maximum shear force at wall stem increases by increasing soil stiffness in finite element analyses.

- For all of the wall configurations and soil internal friction angle values of 30^0, 35^0, and 40^0 the normalized shear force at prop level increases by increasing wall stiffness. It is also observed that, normalised maximum shear force at wall stem increases by increasing wall stiffness in finite element analyses.

REFERENCES

Bica, A.V.D. and Clayton C.R.I. (1998). Experimental study of the behaviour of embedded lengths of cantilever walls.Geotechnique, vol 48, no 6, pp 731-745

Bolton,M.D. and Powrie, W. (1987). Collapse of diaphragm walls retaining clay. Geotechnique, vol 37, no 3, pp 335-353

Bowles, J.E. (1988).Foundation analysis and design.USA, The McGraw-Hill Companies,Inc.

British Steel (1997). Piling handbook 7th edn., British Steel, Scunthorpe

Burland,J.B. , Potts, D.M. and Walsh, N.M. (1981).“The overall stability of free and propped embedded cantilever retaining walls, Ground Engineering, 14(5), pp 28- 38

Dawkins, W.P. (1994a). User’s guide: computer programs for winkler soil-structure interaction analysis of sheet-pile walls (CWALLSSI), Instruction Report ITL-94-5, U.S. Army Engineer Waterways Experiment Station, Vicksburg, MS.

Dawkins, W.P. (1994b). User’s guide: computer programs for analysis of beam-column structures with non-linear supports (CBEAMC), Instruction Report ITL-94-6, U.S. Army Engineer Waterways Experiment Station, Vicksburg, MS

Haliburton, T.A. (1987). Soil structure interaction: numerical analysis of beams and beam-columns, Technical Publication No.14, School of Civil Engineering, Oklahoma State University, Stillwater, Oklahoma

Peck, R.B. and Davisson, M.T. (1962). Discussion of design and stability considerations for unique pier, by J.Michalos and D.P. Billington , Transactions of the ASCE 127, 413-24

Potts, D.M., Burland,J.B. (1983). A parametric study of the stability of embedded earth retaining structures , Transport and Road Research Labarotary Supplementary Report 813

Padfield, C.J., Mair, R.J. (1991). Design of retaining walls embedded in stiff clays, London, Great Britain, Construction Industry and Information Association

Pfister, P., Evers, G., Guillaud, M., and Davidson, R.(1982). Permanent ground anchors-Soletanche design criteria, Report FHWA-RD-81-150, Federal Highway Adminstration, McLean, VA.

Potts, D. M. and Zdravkovic, L. (1999). Finite element analysis in geotechnical engineering – theory. London, Great Britain: Thomas Telford

Powrie,W. (1996). Limit equilibrium analysis of embedded retaining walls, Geotechnique, vol 46, no 4, pp 709-723

Powrie, W. , Gaba, A.R., Simpson, B. and Beadman, B. (2003). Embedded retaining walls – guidance for economic design, London, Great Britain, Construction Industry and Information Association

Strom,R.W., Ebeling, R.M. (2001). State of the practice in the design of tall,stiff and flexible tieback retaining walls,Washington, U.S. Army Corps of Engineers

Terzaghi, K. (1955). Evaluation of coefficient of subgrade reaction, Geotechnique 5, pp 297-326

Weatherby, D.E. , Chung, M., Kim, N.K., and Briaud, J.L. (1998). Summary report of research on permanent ground anchor walls; II, full-scale wall tests and a soil-structure interaction model, Report FHWA-RD-98-066, Federal Highway Adminstration, McLean, VA.

Williams,B.P. and Waite,D. (1993) The design and construction of sheet piled cofferdams, London Great Britain, Construction Industry and Information Association